Applications and Industry®

March 1960

Transactions Papers

NUMBER 47

Published Bimonthly by

AMERICAN INSTITUTE OF ELECTRICAL ENGINEERS

Communication and Electronics—March 1960

Science and Electronics Division

Communication Division

(*See inside back cover*)

Note to Librarians. The six bimonthly issues of "Applications and Industry," March 1960–January 1961, will also be available in a single volume (no. 79) entitled "AIEE Transactions—Part II. Applications and Industry," which includes all technical papers on that subject presented during 1960. Bibliographic references to Applications and Industry and to Part II of the Transactions are therefore equivalent.

Applications and Industry. Published bimonthly by the American Institute of Electrical Engineers, from 20th and Northampton Streets, Easton, Pa. AIEE Headquarters: 33 West 39th Street, New York 18, N. Y. Address changes must be received at AIEE Headquarters by the first of the month to be effective with the succeeding issue. Copies undelivered because of incorrect address cannot be replaced without charge. Editorial and Advertising offices: 33 West 39th Street, New York 18, N. Y. Nonmember subscription $8.00 per year (plus 75 cents extra for foreign postage payable in advance in New York exchange). Member subscriptions: one subscription at $5.00 per year to any one of three divisional publications: Communication and Electronics, Applications and Industry, or Power Apparatus and Systems: additional annual subscriptions $8.00 each. Single copies when available $1.50 each. Second-class mail privileges authorized at Easton, Pa. This publication is authorized to be mailed at the special rates of postage prescribed by Section 132.122.

Printed in United States of America

Number of copies of this issue 5,400

Lead-Acid Storage Batteries in Telephone Service

R. C. SHAIR
NONMEMBER AIEE

WHILE THE PRIME SOURCE of power for the Bell System communication network is alternating current purchased from utilities, almost all service is backed up by a storage battery reserve which at all times stands ready to take over the load for limited periods of time. Rarely is telephone service interrupted during periods of failure of commercial power.

About one third of the yearly Bell System expenditure for power equipment is for storage batteries. This large investment necessitates exacting requirements for the batteries themselves and well defined operating procedures to maximize their life and usefulness. A basic understanding of the characteristics of batteries is desirable in order to formulate these requirements and operating procedures.

The most common battery in use today for telephone service is the lead-sulfuric acid storage battery. The advantages of this battery are its low cost, the availability of the raw materials, and the fact that this is the battery about which most manufacturing and performance information is known. The disadvantages of the lead-acid battery are its poor low-temperature charging characteristics, its low power-to-weight ratio, and its maintenance requirements. The most common method of operation in the Bell System is "full float." In this type of operation the battery is connected directly across the output of the rectifier or motor generator in parallel with the load in such a manner that enough current flows through the battery in a charge direction to overcome its internal losses. During most of its life the battery is being slightly overcharged, and it is deeply discharged only when commercial power fails.

Paper 60-51, recommended by the AIEE Chemical Industry Committee and approved by the AIEE Technical Operations Department for presentation at the AIEE Winter General Meeting, New York, N. Y., January 31–February 5, 1960. Manuscript submitted March 25, 1958; made available for printing November 20, 1959.

R. C. SHAIR, formerly with Bell Telephone Laboratories, New York, N. Y., is now with Gulton Industries, Inc., Metuchen, N. J.

The author gratefully acknowledges his many communications with Mr. U. B. Thomas who has for many years been observing the characteristics and explaining the behavior of storage batteries in Bell System telephone service.

The Lead-Acid Storage Battery

Briefly, a lead-acid telephone cell consists of two lead electrodes kept apart by a battery separator and retainers between them, with the whole assembly immersed in 1.210 specific gravity sulfuric acid contained in a glass, ceramic, rubber, or plastic jar.[1] A battery is made up of one or more cells connected in series.

The positive electrode controls battery life. It is a thick plate consisting of a lead alloy grid which supports and provides electric contact to a positive active paste material consisting primarily of lead dioxide. The negative electrode controls self-discharge but its grid is not appreciably oxidized and can therefore be considerably thinner; it consists of a lead alloy grid and a negative active paste material consisting primarily of sponge lead. The main chemical reaction of the whole battery is, on discharge

$$Pb + PbO_2 + 2H_2SO_4 \rightarrow 2PbSO_4 + 2H_2O$$

for which the open-circuit voltage is 2.06 volts, at 77 F (degrees Farenheit), with 1.210 sulfuric acid.

Batteries used for telephone service are stationary batteries and therefore do not have to be particularly rugged or spillproof.[2] Compactness, lightness, and ruggedness are sacrificed in order to give long life, low self-discharge rates, and stable characteristics. The life of a lead-acid battery used in float service is a function of the mass and cross section of the positive grid material; the battery will fail when this grid has corroded sufficiently to collapse and short circuit the electrodes, or when the grids have separated in such a manner as to isolate portions of active material which will sulfate, thus reducing battery capacity. (This type of failure will be first noticed by loss of high rate performance.) Fig. 1 shows a positive plate of a lead-calcium storage battery after about 10 years of float service. A piece of the grid frame, *A–B*, was cut out and potted in Wood's metal contained in a brass tube. A section *CC* was smoothly cut and polished and observed under the microscope. The intact lead grid metal is shown at *D*; the lead dioxide corrosion product formed from the grid metal is shown at *E* and is about 3 mils thick; Wood's metal and brass tube are *F* and *G*, respectively. When the corrosion product has grown and consumed a considerable portion of the underlying grid the grid will begin to fall apart and any pieces which short the positive plates to the negative plates will cause failure of that cell.

The rate of grid corrosion is dependent, among other things, on the anodic corrosion current passing through the cell. Pure lead is resistant to the corrosion process, but it is too ductile to fabricate, and for many years batteries have utilized grids of lead alloyed with about 12% antimony for increased strength and facility of fabrication. Their life has been 14 years in float operation. A new development uses calcium as the alloying material, rather than antimony, which reduces the corrosion current, and has extended float service life to an estimated 25 years.[3] The use of calcium has had other effects on battery characteristics which will be discussed later (and investigated by J. F. Rittenhouse and H. E. Jensen in an unpublished conference paper).

Functions of Storage Batteries in Telephone Service

In telephone installations batteries have two important functions.[4] They supply an ampere-hour reserve in case of

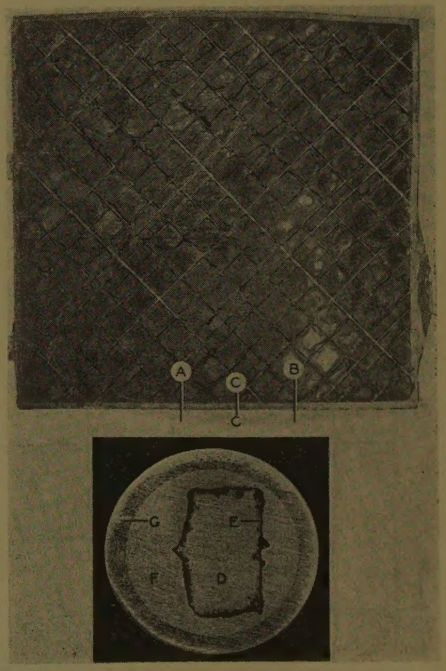

Fig. 1. Corrosion of a positive plate grid

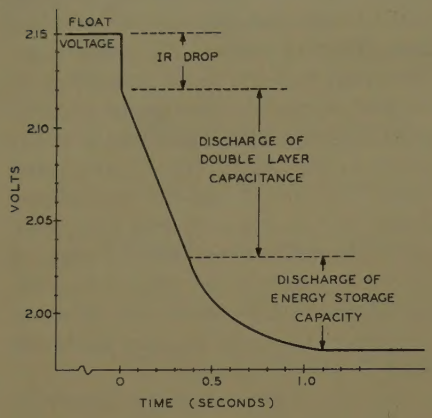

Fig. 2. Transient capacitance of a 300-ampere-hour cell

the transient capacitance just indicated, a battery has a pseudo capacitance which can be used to express its energy storage capacity. An equivalent capacitor for a 300-ampere-hour cell would have the fantastically high value of 3.48×10^5 farads.

Fig. 2 shows the transient characteristic of a cell from which its capacitance was determined. The cell was initially at steady state, floating at 2.15 volts. At time zero a load of 30 amperes was connected across the cell terminals causing the voltage to drop in three distinct steps. In the first step the internal resistance of the cell caused an instantaneous 0.03-volt drop in terminal voltage, equal to *IR*. During the next step, the terminal voltage decreased practically linearly in a manner controlled by the discharge of the double layer at the negative electrode interface with the electrolyte. During the third step the rate of change of voltage with time decreased as the pseudo capacitance, or true energy storage capacity, of the cell was discharged. The second step is of interest in calculating transient capacitance. In 0.36 second the cell voltage decayed 0.09 volt. Using the relationship $i=Cdv/dt$, an approximation can be made because of the linearity of the decay, yielding

$$C=\frac{i}{\Delta v/\Delta t}=\frac{30}{0.09/0.36}=120 \text{ farads}$$

$$i=C\frac{dv}{dt}\quad C=\frac{i}{\Delta v/\Delta t}=\frac{30}{0.09/0.36}=120 \text{ farads}$$

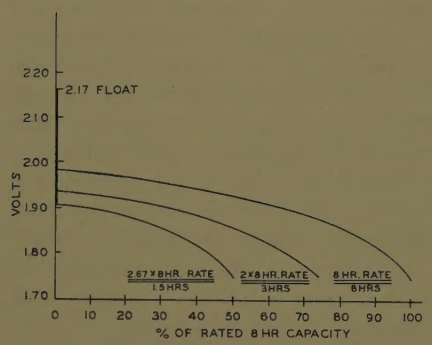

Fig. 3. Constant current discharge characteristics

Cycle Characteristics

Fig. 3 shows the terminal voltage of a lead-acid cell as a function of time at various discharge rates. These curves are constant current dischargd characteristics. Telephone batteries are designed for the 8-hour rate, and therefore at higher rates the available capacity when discharged

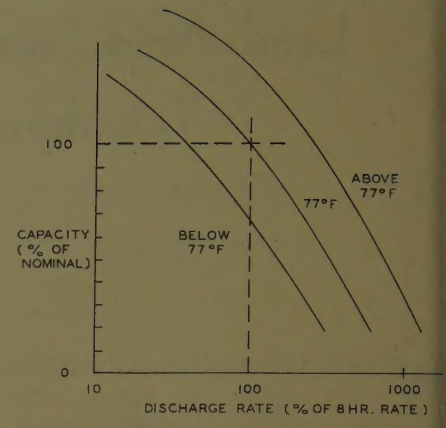

Fig. 4. Dependence of capacity on temperature and rate of discharge

to 1.75 volts per cell is significantly decreased.

Fig. 4 shows the dependence of discharge capacity on temperature and rate of discharge. The reference point is usually taken as 77 F at the 8-hour rate. At higher temperatures or lower rates the available capacity is increased. At the 8-hour rate, 100% capacity is attained at 77 F, 86% at 50 F, and 109% at 100 F.

Fig. 5 shows the current and voltage characteristics of a cell during constant current charge. Current is, of course, constant and should be kept at a value less than or equal to the finish rate specified by the manufacturer. Currents higher than the finish rate cause excessive gassing and can damage the cell. If the cell has been completely discharged to its end voltage of 1.75 volts, its open-circuit voltage will soon recover to about 2.0 volts. Within a short time after constant current recharge at the 8-hour rate has begun, the cell voltage will rise to about 2.1 volts. For a period of time thereafter

emergency and they act as a crosstalk or noise filter. As a filter the battery acts as a large capacitance in parallel with the load and the power supply. This large capacitance provides a low-impedance path to ground for the noise and transients generated by rectifiers and rotating d-c generators and also isolates simultaneous messages utilizing the common power supply. The value of this capacitance is amazingly high—120 farads for a 300-ampere-hour cell. In addition to having

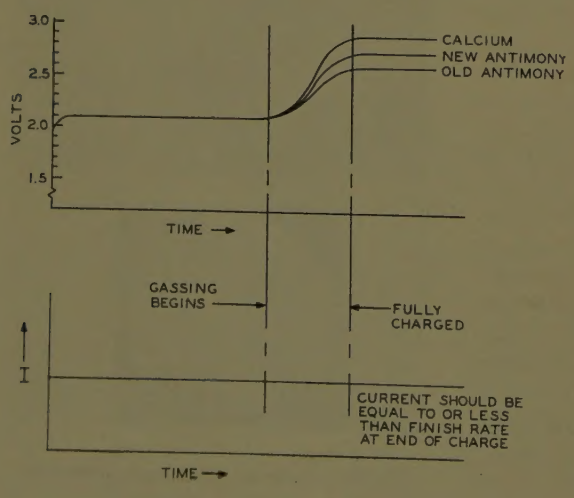

Fig. 5 (left). Constant current charge characteristics

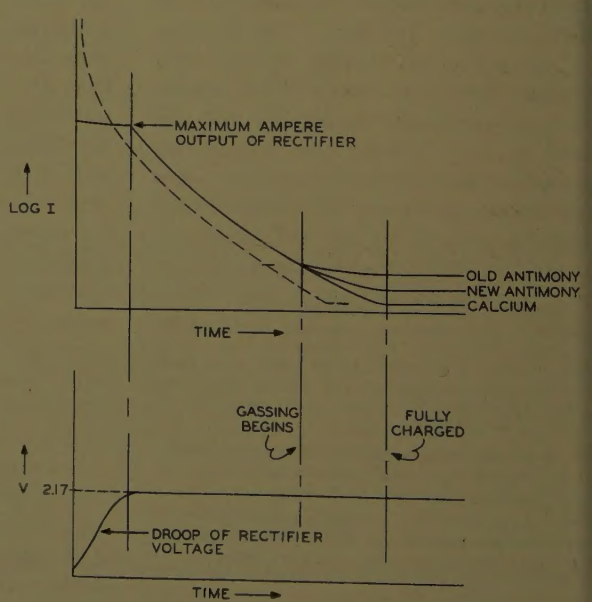

Fig. 6 (right). Constant voltage charge characteristics

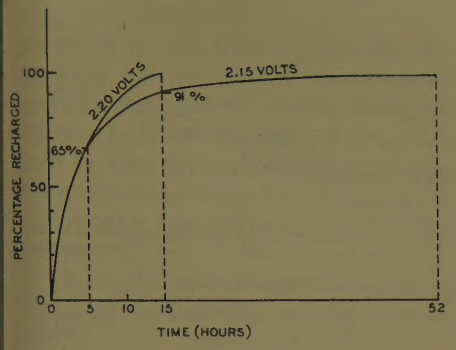

Fig. 7 (left). Recharge characteristics for several values of constant voltage

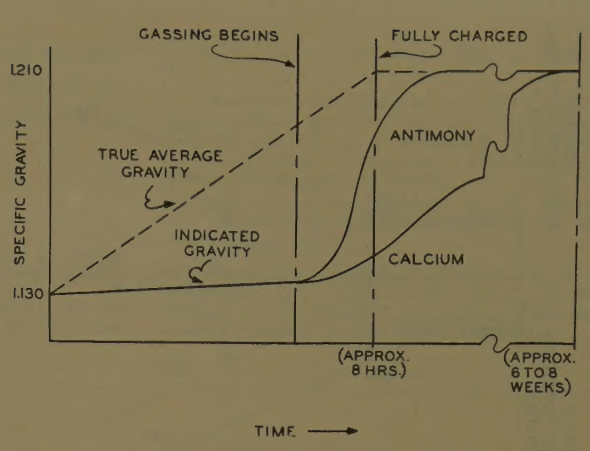

Fig. 8 (right). Increase of specific gravity during recharge at low final voltage

cell voltage will remain practically constant, until gassing begins. When the cell is gassing, its back electromotive force or polarization, has increased and a higher potential is required to pass the constant value of current through the cell. Voltage will continue to rise until the cell is completely charged at which time stable conditions are attained and most of the charge current is being wasted by gassing of the electrodes. The differences between antimony and calcium cells will be discussed later.

In the Bell System, constant-voltage operation of equipment predominates. Rectifiers and rotating power equipment provide a regulated constant voltage to their batteries and to the load. Fig. 6 shows constant-voltage battery charge characteristics for a practical case where in the initial stages of recharge the battery is capable of accepting larger currents than the rectifier can deliver and as a result the voltage of the rectifier droops while its current output remains approximately constant. The dashed line shows how the recharge characteristic would look if the battery were charged from a rectifier with enough excess capacity to deliver very high currents in the early stages. Gassing would begin sooner, and the cell would be fully charged in less time.

The operating voltage of telephone equipment is dictated by circuit requirements and is kept essentially constant at a value of 2.17 times the number of lead-acid storage cells used. After an emergency discharge this constant voltage is impressed across the discharged battery which then recharges at constant voltage. The question has often arisen as to whether a battery can recharge at a voltage as low as 1.17 volts per cell, and how long it would take to recharge. In Fig. 7 are shown the recharge characteristics at 2.20 volts per cell and 2.15 volts per cell. Note that within 5 hours, 65% of the battery's capacity has been returned to the battery at either voltage. The large excess of time required at 2.15 volts to reach 100% recharge actually elapses during the last 9% of capacity, when at the lower voltage, polarization inside the battery limits charge acceptance. These curves indicate very nicely that when the battery is low, such as right after an emergency discharge, it is then best able to accept charge and telephone operating reserve is returned to the battery very rapidly.

When only lead-antimony batteries were used in the Bell System, recharge was usually followed by a high-voltage overcharge during which the cells gassed sufficiently to mix the electrolyte thoroughly, and immediately thereafter measurement of the specific gravity of the electrolyte at the top of the cell was a true indication of the state of charge. With low-voltage overcharges, however, mixing of the electrolyte is reduced and there is a lag between the apparent and true specific gravity indications at the top of the cell. This lag is significantly long for lead-calcium cells for which the overcharge or gassing (and hence mixing) current is only about one tenth that of lead-antimony cells. Fig. 8 illustrates how the aparent specific gravity (at the top of the cell where it is measured) changes during recharge at low final voltage, and also indicates the true specific gravity of the electrolyte. It is seen that about 6 weeks is required for the apparent specific gravity of calcium cells to approach the true value. In cases where the battery is regularly subjected to slight discharges, the time required to attain the true specific gravity reading may be extended to 10 weeks.

Float Characteristics

The mechanism of float operation is quite different from that of cycle operation. Several reactions tend to occur:

Grid Corrosion: (at positive electrode)

$$Pb + 2H_2O \rightarrow PbO_2 + 4H^+ + 4e$$

where the four electrons, 4e, represent a portion of the float current. This same float current causes hydrogen to be released at the negative electrode in accordance with the reaction

$$4H^+ + 4e \rightarrow 2H_2 \uparrow$$

Gassing: (at both electrodes)

$$2H_2O \rightarrow 2H_2 + O_2 \uparrow$$

Self-Discharge: (at negative electrode)

$$Pb + H_2SO_4 \rightarrow PbSO_4 + H_2 \uparrow$$

The voltage of a battery at float is maintained slightly higher than the equilibrium open-circuit voltage so that enough current flows through the battery in the charge direction to overcome its self-discharge losses. This higher voltage is caused by the polarization developed on the electrodes as the result of the electrolytic formation and liberation of hydrogen and oxygen gas. The relationship between float voltage and current is depicted by a polarization curves which is known as a modified form of Tafel curve. For this curve the voltage of a cell or single electrode is plotted as ordinate against the logarithm of the overcharge current as abscissa and yields a straight line, which relationship was described by J. Tafel in 1905. Typical float characteristics are shown in Figs. 9 and 10. Fig. 9 is the Tafel curve of a complete cell, and Fig. 10 shows the

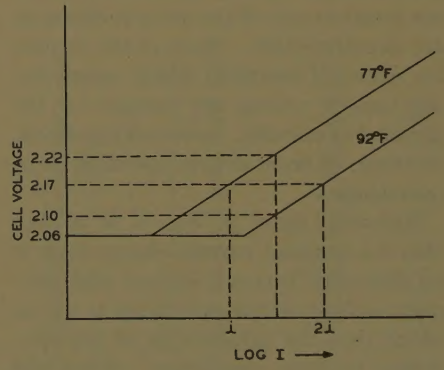

Fig. 9. Tafel curves for a cell, showing effect of temperature

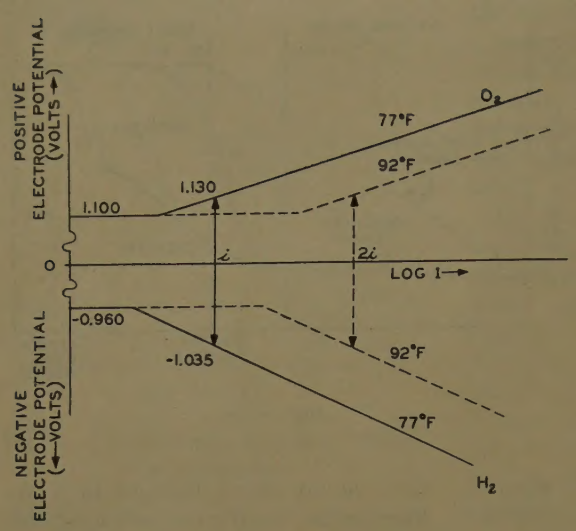

Fig. 10 (left). Tafel curves for individual electrodes

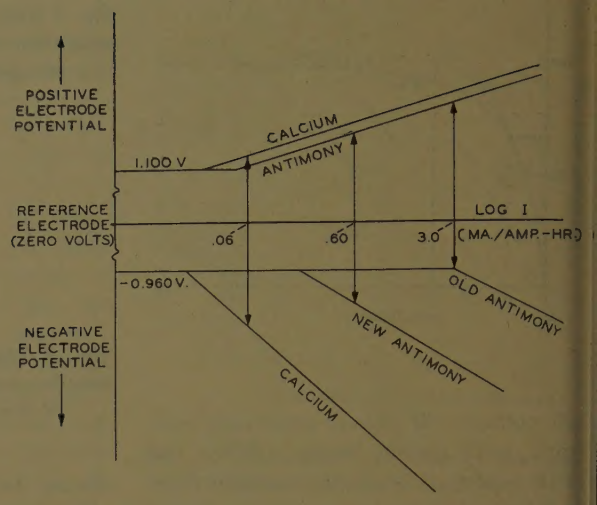

Fig. 11 (right). Tafel curves showing differences between calcium and antimony cells

Tafel curve of each individual electrode; cell voltage is the sum of the two electrode potentials. These two curves show the effect of operating temperature on float voltage and current. For every increase of 15 F the float current doubles if the cell voltage is maintained constant. It can be seen from Fig. 9 that when several cells are connected in series to form a battery, each receives the same series float current, but cells at different temperatures will be at different float voltages. Some may be at such a low voltage that they are self-discharging, or sulfating.

Earlier in the paper references have been made to the use of calcium as a grid alloying constituent in place of antimony. Both antimony and calcium harden pure lead so that it can be handled and fabricated into grids. Antimony, however, dissolves from the positive electrodes during the normal corrosion process which occurs during battery operation and migrates across to the negative plate where it depresses the electrode's voltage. In the early 1930's it was found at Bell Laboratories[5] that a little less than 0.1% calcium in place of 12% antimony imparted the necessary properties to pure lead to facilitate its fabrication, but did not result in any of the adverse effects at the negative plate. None of the reversible chemical reactions which occur during battery cycling are changed by the presence of calcium; most striking effects, however, do occur in float operation or on overcharge.

Referring again to Fig. 5, it is seen that for constant current charge there is no difference between calcium and antimony cells until the cells begin to gas at which time the polarization of the electrodes becomes significant. When the cells are fully charged the calcium cells will be at higher voltage for a given value of current. Old antimony cells will be the lowest voltage cells since the voltage depression is a function of the amount of antimony which has migrated to the negative plate. Fig. 6 shows that for constant voltage charge the characteristics of calcium and antimony cells are identical until gassing begins, but when the cells are fully charged the calcium cells will take a smaller float current than will antimony cells. In Fig. 11 are shown the Tafel curves of calcium and antimony cells.

Potential is plotted as a function of the logarithm of the overcharge current. Individual electrode potentials are measured with respect to a mercurous sulphate electrode immersed in the cell electrolyte. The cell potential is the absolute sum of the individual electrode potentials. For very low values of overcharge current both the positive and negative electrode potentials are constant at the open-circuit values indicated. At the point where the break in each of the curves occurs gassing of the electrode begins. Oxygen is evolved from the positive electrode while hydrogen is evolved from the negative electrode. As the current is increased the electrodes polarize and their potentials rise. At the positive electrode there is only a slight potential difference between electrodes having calcium alloy grids and antimony alloy grids. The more significant differences between these two types of batteries occur at the negative plate. To maintain a cell voltage of 2.17 a calcium cell requires approximately one tenth of the float current required by a new antimony cell. As antimony cells age, metallic antimony continues to deposit on the negative plate and its voltage depressing effect increases. In fact, for very old antimony cells the float current will be so high that all of the cell polarization will occur on the positive plate. The negative plate, no longer polarized, will self-discharge and sulfate, and frequent raised voltage boosting becomes necessary to keep the negative plate in a healthy full-charge condition.

Several advantages have been realized by using calcium alloyed grids rather than antimony alloyed grids:

1. Lower float current (approximately 1/10–1/50 of the current used in antimony batteries) causes less water loss because of gassing and therefore less maintenance is required.

2. As a result of the lower self-discharge rate (1/5–1/10 that of antimony) fewer boost charges and correspondingly less maintenance are required.

3. Examination has shown that the rate of grid corrosion for calcium cells at float voltages is approximately 1/2 the rate of grid corrosion for antimony cells, which results in longer battery life.

There are also some disadvantages associated with the use of calcium cells:

1. They are more difficult to manufacture. In the early days of manufacture these difficulties were not recognized, and differences between cells resulted in disturbing voltage variations of the cells in a telephone battery.

2. The end of life is harder to predict since the available capacity just before end of life is greater than 100% of the battery's nominal capacity and there is no change of float characteristics with age.

3. Because of the low gassing currents, mixing of the electrolyte is not readily effected and specific gravity readings commonly used in battery maintenance tend to be erroneous until the electrolyte has had a chance to mix by diffusion.

Summary

Some of the chemistry, physics, and engineering aspects of lead-acid storage batteries were discussed.

In telephone service storage batteries serve as an emergency reserve and as a

crosstalk or noise filter. While the more common charge-discharge characteristics govern their behavior during emergency cycling, telephone batteries for the greater part of their life are maintained in float-type operation when the overcharge or polarization characteristics govern their behavior.

The use of calcium alloy for grids instead of antimony alloy has brought about significant improvements in lead-acid storage batteries. The effect of calcium alloy grids on battery characteristics was described.

References

1. Storage Batteries (book), G. W. Vinal. John Wiley & Sons, Inc., New York, N. Y., 1955.

2. Lead-Acid Stationary Batteries, U. B. Thomas. Journal, Electrochemical Society, New York, N. Y., vol. 99, Sept. 1952, pp. 238C–41C.

3. Corrosion and Growth of Lead-Calcium Alloy Storage Battery Grids as a Function of Calcium Content, U. B. Thomas, F. T. Forster, H. E. Haring. *Transactions*, Electrochemical Society, vol. 92, 1947, pp. 313–25.

4. Why Storage Batteries? R. D. deKay. *Bell Laboratories Record*, New York, N. Y., vol. 33, Dec. 1955, pp. 458–60.

5. Electrochemical Behavior of Lead, Lead-Antimony and Lead-Calcium Cells, H. E. Haring, U. B. Thomas. *Transactions*, Electrochemical Society, vol. 68, 1935, pp. 293–307.

The Effect of Electrical Grounding Systems on Underground Corrosion and Cathodic Protection

B. HUSOCK
MEMBER AIEE

THE essential purpose of most electrical grounds is protection. The National Electrical Code states that: "Circuits are grounded for the purpose of limiting the voltage upon the circuit which might otherwise occur through exposure to lightning or other voltages higher than that for which the circuit is designed: or to limit the maximum potential to ground due to normal voltage."[1] It states further that exposed metal enclosing electric conductors or enclosing electric equipment are grounded for the purpose of preventing a potential above ground on those enclosures. While there are other purposes for electrical ground, such as those which are required in the communication field, most grounding is done for protection either of equipment or of personnel. Even static grounding at oil or gasoline unloading facilities is a protective device.

Although the purposes for electrical grounds are not of particular concern in this paper, it is obvious that the increased use of electricity, especially electricity which is distributed at a higher voltage, necessitates the use of more extensive grounding systems. While the use of water pipes, and in some instances gas pipes, is recommended for grounding by the National Electrical Code, and while that type of grounding is sufficient for homes and lower voltage distribution, it is not adequate for industrial plants and power plants. In most plants, grounding is accomplished by means of made grounds and the material which is almost invariably used for those grounds is copper. It is not unusual to find all metallic structures within a plant connected to a copper grounding system. These structures would include underground pipelines, lead sheath cables, buried tanks, building steel, etc. Because copper is a noble metal, it can have serious corrosion effects on the underground structures which are made of iron or steel, and which are connected to the copper. It is the purpose of this paper to discuss some of those effects as well as to indicate methods which can be used to mitigate them. Those effects are worthy of deepest consideration because the problem of corrosion resulting from the use of copper grounds is a serious one which promises to grow more serious unless it receives greater attention and treatment.

It should be noted that a-c grounding to an underground pipe does not in itself cause corrosion of that pipe. It has been shown that corrosion is a phenomenon involving d-c electricity and that alternating current has very little or no effect. There has been some discussion in regard to the effect of rectified alternating current, particularly in regard to the rectifying properties of a copper-oxide film on a copper ground rod. However, this observer has never encountered a corrosion problem which can be entirely attributed to this effect, and it is doubtful whether it plays any major role in the over-all corrosion problem on underground pipes. Thus, it is our conclusion that the corrosion produced on underground structures by electrical grounds is strictly galvanic in nature and results from bimetallic activity between the underground structure and the copper grounding system.

Paper 60-4, recommended by the AIEE Chemical Industry Committee and approved by the AIEE Technical Operations Department for presentation at the AIEE Winter General Meeting, New York, N. Y., January 31–February 5, 1960. Manuscript submitted April 23, 1959; made available for printing September 23, 1959.

B. Husock is with the Harco Corporation, Cleveland, Ohio.

Copper Grounds and Corrosion

While the fact that a bimetallic corrosion effect between copper and less noble metals exists is well known, the exact nature of that effect is often not fully appreciated. It is obvious that different structures in different environments are affected differently. Therefore, it is worth while to discuss some of the different ways in which underground structures can be affected.

There are four basic considerations which determine the seriousness of the corrosion on an underground structure

Table I. Pipe-to-Soil Potential Measurements for Copper–Copper-Sulfate Reference Electrode on 8-Inch-Diameter Coated-Steel Pipeline Insulated from Other Structures

Reading No.	Location of Reference Electrode, Station No.	Pipe-to-Soil Potential, Millivolts: Over Line	Pipe-to-Soil Potential, Millivolts: 20 Feet from Line
1	0 + 00	−635	
2	0 + 65	−655	
3	1 + 65	−652	
4	2 + 63	−665	−677
5	3 + 65	−665	−672
6	4 + 65	−670	−680
7	5 + 65	−660	−635
8	6 + 65	−695	
9	7 + 65	−650	−640
10	8 + 65	−650	−652
11	9 + 65	−680	−670
12	10 + 65	−680	−670
13	11 + 65	−690	−695
14	12 + 65	−685	−688
15	13 + 65	−700	−695
16	14 + 65	−685	−685
17	15 + 65	−675	−662
18	16 + 65	−665	−650
19	17 + 65	−690	−660
20	18 + 65	−670	−670
21	19 + 65	−652	−655
22	20 + 65	−655	−648

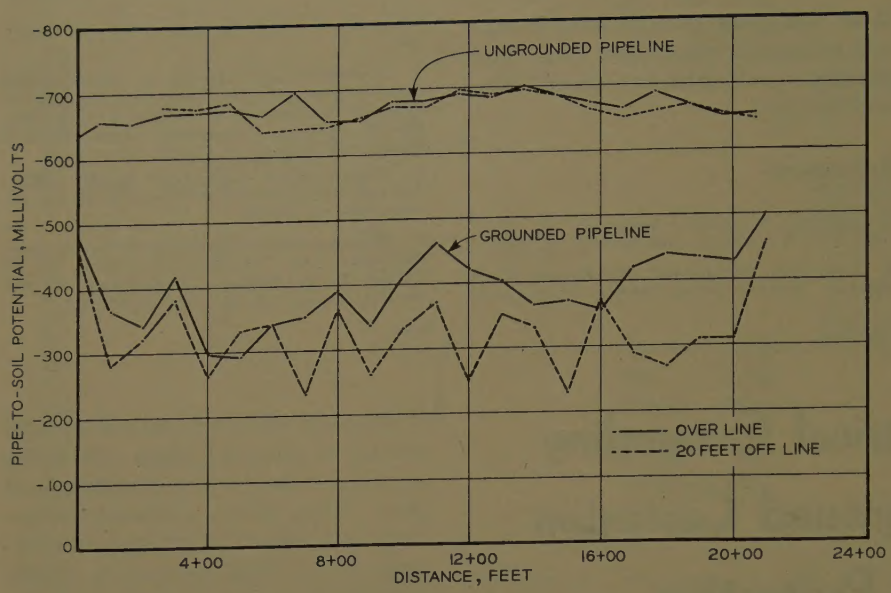

Fig. 1. Effect of copper ground on coated pipeline

resulting from a copper grounding system. These considerations are the ones which govern the magnitude and intensity of the corrosion current generated and can be briefly summarized as follows:

1. The potential between the structure and the copper ground.
2. The ratio of the exposed area of the structure to that of the copper ground.
3. The electrical resistance between the structure and the copper ground.
4. The electrical continuity of the underground structure.

It is realized that this listing is an oversimplification, and that the considerations given are not independent of one another. It is also realized that other considerations such as polarization characteristics and film formation enter into the corrosion mechanism. However, the considerations outlined can be used to describe most of the situations encountered in the field.

Table II. Pipe-to-Soil Potential Measurements for Copper–Copper-Sulfate Reference Electrode on 72-Inch-Diameter Coated-Steel Pipe Connected to Copper Grounding System

Reading No.	Reference Electrode Location, Distance from Start, Feet	Pipe-to-Soil Potential, Millivolts: Over Line	Pipe-to-Soil Potential, Millivolts: 25 Feet from Line
1	0	−480	−460
2	100	−365	−280
3	200	−340	−320
4	300	−415	−380
5	400	−295	−200
6	500	−290	−330
7	600	−340	−340
8	700	−350	−230
9	800	−390	−360
10	900	−335	−260
11	1,000	−410	−330
12	1,100	−460	−370
13	1,200	−420	−250
14	1,300	−400	−350
15	1,400	−365	−330
16	1,500	−370	−230
17	1,600	−355	−370
18	1,700	−420	−290
19	1,800	−440	−270
20	1,900	−435	−310
21	2,000	−430	−310
22	2,100	−500	−460

Potential

The current which is generated by a bimetallic couple is a function of the "open-circuit" potential between the two metals involved. In underground corrosion, the couple almost always concerned is an iron-copper couple. Owners of underground lead sheath cables are, of course, concerned with a lead-copper couple. While the potential of an iron-copper couple and of a lead-copper couple can vary depending on conditions, it can be assumed that in most instances the open-circuit potential of both of these couples will be approximately 0.50 volt. It is true in some instances that the potential of iron to copper can be as little as 0.20 volt or as great as 0.75 volt, but in most instances the potential will be in the range of 0.40 to 0.60 volt. This potential relationship is also true of most lead-copper couples. Thus, the driving potential of the couple is inherent in materials which are used, and once these have been selected, the open-circuit potential is a relatively fixed characteristic of the particular couple. The magnitude of the corrosion current generated by the couple and the intensity of the attack is then dependent upon the other consideration listed.

It is well to note at this point that a copper grounding system can have a considerable effect on the pipe-to-soil potential of an underground pipeline. Table I lists the pipe-to-soil potentials taken along a portion of an 8-inch-diameter coated-steel pipeline which is not connected to a grounding system, and Table II lists the pipe-to-soil potential measurements taken along a 72-inch coated-steel pipeline which is connected to an extensive grounding system in which ground mats are installed at 50-foot intervals along that pipeline. It can be seen that the 72-inch line is at a potential which is considerably less negative than that of the 8-inch line. It can also be seen that the relationship of the "over-the-pipe" readings to the "off-the-pipe" readings is different in the two examples. Thus, in the case of the 8-inch pipeline, the off-the-pipe readings are almost equal to the over-the-pipe readings, whereas in the case of the 72-inch line the off-the-pipe readings are considerably less negative than the over-the-pipe readings. These relationships are apparent from the graphs in Fig. 1, in which the values of potential listed in Tables I and II are plotted against distance along the pipelines.

The manner in which the copper grounding system can affect an underground structure can be further illustrated by comparing the potential of a pipe before it is connected to the copper ground with the potential after it is connected to the copper ground. The example used to illustrate this is one in which measurements were taken on hydrants along a fire line which was a nonmetallic line. An interesting sidelight is that the fire line was originally a coated-steel pipe and the rate at which leaks occurred necessitated the replacement of that entire line within 2 years. It is true that the soil itself was a very corrosive one (the average resistivity was 500 ohm-centimeters) but the very rapid failure must be attributed mainly to the effect of the copper grounding system. Table III lists the values of potential taken on three of the hydrants both before and after connection to the grounding system. It can be seen that at each

Table III. Potential Measurements on Fire Hydrants Before and After Connection to a Copper Ground

Hydrant No.	Pipe-to-Soil Potential, Millivolts: Before Connection	Pipe-to-Soil Potential, Millivolts: After Connection	Short-Circuit Current, Milliamperes
1	−688	−390	110
2	−700	−360	64
3	−580	−410	70

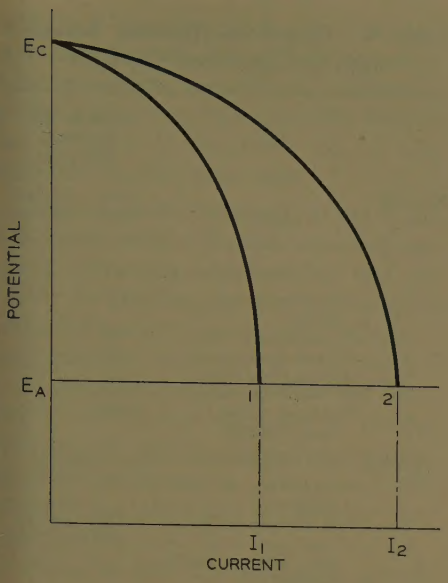

Fig. 2. Bimetal-couple cathodic control

hydrant the potential was less negative after grounding than before grounding, and that the changes in potential were substantial, ranging from 160 to 340 millivolts. The magnitude of the current derived from this bimetallic couple is also substantial when it is considered that over 2 pounds of iron are consumed by 100 milliamperes of current per year. It is obvious that, if all of the current leaving a particular pipeline is concentrated at only a few locations, such as at flaws in a coating, the penetration of that pipeline can be extremely rapid.

Ratio of Exposed Areas

The damage which is done by a particular bimetallic couple is not only governed by the total corrosion current generated, but is also a function of the intensity of the current at the anodes. While the total corrosion current is dependent upon the potential difference between the two metals as well as the resistance between them, the intensity of the anode current is primarily a function of the ratio of the areas of the anodes and cathodes. One of the basic principles of corrosion engineering is to maintain a high ratio of anode area to cathode area. In other words, never couple a small anode to a large cathode. Although this is a rather obvious principle and one which is widely recognized in the corrosion field, many of the corrosion difficulties which result from the use of copper grounds are attributable to the fact that this principle was disregarded in the design of a particular facility.

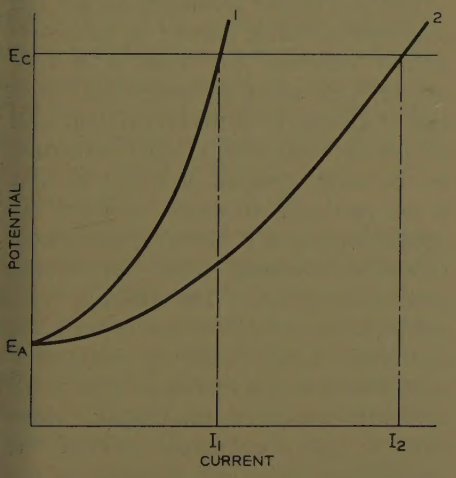

Fig. 3. Bimetal-couple anodic control

It is worthwhile at this point to discuss briefly how area relationships affect the behavior of bimetallic couples. These relationships can be categorized into three basic relationships: (1) the cathode area is very small with respect to the anode area, (2) the anode area is very small with respect to the cathode area, and (3) the two areas do not differ appreciably.

In the first case, where the cathode area is very small, the coupling of the two metals results in little change in the potential of the anode, whereas the cathode polarizes to nearly the open-circuit potential of the anode. The behavior of this couple is shown in Fig. 2, and is one which is said to be under cathodic control. Thus, the corrosion current generated is governed almost entirely by the polarization characteristics of the cathode. The smaller the cathode the more quickly it will polarize, and the smaller will be the magnitude of the corrosion current. Although this particular area relationship is one which usually can be tolerated, it is interesting to note that in a system under cathodic control, the corrosion current is in direct proportion to the cathode area. If the anode area remains unchanged, the intensity of the anode current (which is a measure of the corrosion attack) also increases in direct proportion to the cathode area.

In the second case, where the anode area is very small, the coupling of the two metals results in little change in the potential of the cathode, whereas the anode polarizes to nearly the open-circuit potential of the cathode. The behavior of this couple is shown in Fig. 3, and is one which is said to be under anodic control. The corrosion current generated is governed almost entirely by the polarization characteristics of the anode and is in direct proportion to the area of the anode. While this area relationship is one which usually cannot be tolerated, it is interesting to note that an increase in anode area, while resulting in an increase in the total corrosion current, does not necessarily result in an increase in the intensity of the anode current.

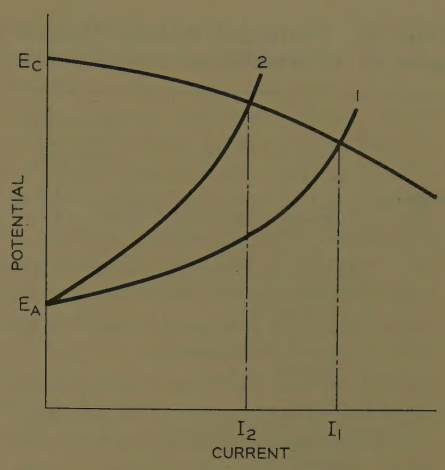

Fig. 4. Bimetal-couple mixed control

The third case, where the anode and cathode areas do not differ greatly, is the one which is more commonly encountered than the first two cases. The behavior of this couple is said to be under mixed control and is shown in Fig. 4. While it is obvious that an increase in cathode area, assuming that the anode area remains unchanged, results in an increase in the intensity of the corrosion current at the anode, the effect of a change in anode area should be noted. It is interesting to note that while a decrease in anode area decreases the total corrosion current, the intensity of the current at the anode increases. It is this condition which accounts for many of the corrosion difficulties which result from the use of copper grounding systems.

As an example, it is common knowledge that coupling of a steel pipeline to a copper grounding system will generate corrosion on the pipeline. In acknowledging this condition, it is often decided to install coated pipe in an attempt to mitigate the corrosion. The principles described above indicate that although the coating reduces the total corrosion current generated, the intensity of the corrosion current at any flaws in the coating will be increased. Therefore, unless the coating is perfect, a condition which has probably never been obtained in practice, penetration of the pipe can be more rapid than if the pipe were installed without coating. Similarly, on grounded lead-sheath cables installed in ducts which are filled with ground water, measures to eliminate the water from the ducts can increase the intensity of attack at any location where water remains.

These examples are rather obvious in light of the principles governing area relationships. However, the practices used in combatting underground corrosion all

Table IV. Pipe-to-Soil Potential Measurements for 16-Inch-Diameter Blowdown Line

Reading No.	Location of Reading	Pipe-to-Soil Potential, Millivolts: Over Line	Pipe-to-Soil Potential, Millivolts: 25 Feet off Line
1	Air valve at 3+20	−640	−610
2	Air valve at Pike and 15th Streets	−650	−680
3	South side of building (connected to copper ground)	−315	−285
4	Air valve at Scioto Street	−620	−550
5	50 feet east of fence	−525	−525
6	Air vent west of Perimeter Road	−650	−635
7	300 feet west of highway	−570	−575
8	Station no. 125+02	−695	−685

too often run counter to the practices indicated by these principles. It is not uncommon to find that a corrosion problem is tackled by treating the symptoms at the anode areas rather than by treating the entire corrosion mechanism.

Resistance

The current generated by any galvanic cell is governed by Ohm's Law and is, therefore, inversely related to the resistance between the anode and the cathode. The resistance between two underground structures of given areas is a function of the resistivity of the soil as well as of the distance between the two structures. Thus, if a steel pipeline is installed in low-resistivity soil and in close proximity to a copper grounding system, the corrosion current generated will be of larger magnitude than the magnitude of current generated in high-resistivity soil where there is a considerable distance between the pipe and the copper ground. However, the relationship of resistivity and distances is rarely as clear cut as this. Thus, for a given electric system which is to be grounded, it is the usual procedure to design a ground with a given resistance, irrespective of the soil resistivity. Therefore, the cathode resistance is usually fixed by the electrical requirements and is independent of the soil resistivity. Therefore, in high-resistivity soils, the amount of copper required for obtaining a given resistance will be greater than in lower resistivity soils.

Similarly, the effect of physical separation is not a direct relationship. While very close proximity between two structures is to be avoided, increasing this separation when the distance is greater than 100 feet usually has very little effect.

Therefore, in most instances, increased soil resistivity only increases the anode resistance. While this increased resistivity will reduce the total corrosion current, it is possible for the intensity of the current at any low-resistivity areas along the pipe to be greater than would be the case if the entire length were in a low-resistivity environment. For example, it is a common practice at industrial plants to backfill the pipelines with a high-resistivity material such as sand. The sand backfill, of course, increases the anode resistance, but at any location where native soil comes in contact with the pipe, the corrosion attack can be more severe than if the entire pipe were backfilled with native soil.

Electrical Continuity

In determining how a given pipeline will be affected by connection to a copper ground, the electrical continuity of the pipe, or more exactly, the continuity of the pipe joints, must be considered. Thus, in determining the area relationship between the pipeline and the copper, it is very easy to fall into the error of considering the entire length of the line. While an electrically continuous line, such as a welded line, is affected throughout its length, this is not the case on a line which is coupled with pipe joints which are electrically discontinuous.

For example, the coupling of more than 12,000 feet of 16-inch bare pipeline to a small copper ground rod does not appear to be a dangerous procedure. However, if the line is coupled with mechanical joints which are insulating, the effect of the ground rod will be concentrated only on the particular length of pipe which is connected to that ground rod. This effect is illustrated by the example in Table IV. It can be seen that all of the readings are in the normal range for iron or steel pipe with the exception of Reading no. 3 where the potential was considerably less negative than that at other locations along the line. It was at this point that the connection to the copper ground rod had been made. Potential measurements indicate that the effect of that ground rod is concentrated only on one pipe length.

One common practice which can result in concentrating the corrosion activity is the use of insulating flanges to isolate and sectionalize a line. This is illustrated by the potentials measured along a gas line which runs between various buildings at a plant as given in Table V. In this particular case, insulating joints were not purposefully used to sectionalize the pipe, but plastic pipe was inserted at locations where the pipe had been repaired and this plastic pipe served to sectionalize

Table V. Pipe-to-Soil Potential Measurements for Coated-Steel Gas Lines

Reading No.	Location	Pipe to Soil Potential, Millivolts: Over Line	Pipe to Soil Potential, Millivolts: 25 Feet off Line
	Section No. 1		
1	Northeast corner of garage	−665	−625
2	50 feet from garage	−615	−615
3	100 feet from garage	−585	−615
4	150 feet from garage	−615	−625
5	200 feet from garage	−685	−645
6	Northeast corner of main building	−690	−655
	Section No. 2 (Connected to Copper Ground)		
7	At entrance to main building	−270	−95
8	East of main building	−320	−140
9	50 feet east of tee on east side of main building	−390	−180
10	100 feet east of tee on east side of main building	−375	−175
11	140 feet east of tee on east side of main building	−285	−150
	Section No. 3		
12	200 feet east of tee	−740	−770
13	250 feet east of tee	−725	−760
14	300 feet east of tee	−725	−747
15	350 feet east of tee	−735	−747
16	400 feet east of tee	−730	−745
17	450 feet east of tee	−720	−745
18	Gas well building	−700	−702

the pipe. It also served to concentrate all of the effect of an extensive copper grounding system on section 2 because that was the only section which remained electrically connected to that copper grounding system. It can be seen that the potentials on that section are of considerably lower negative value than the potentials on the other sections of the line and that all of the off-the-pipe readings on that section were less negative than the over-the-pipe readings.

Copper Grounds and Cathodic Protection

Just as a copper grounding system can affect the corrosion pattern on an underground structure to which it is connected, it can affect the design and operation of a cathodic protection system used to prevent corrosion of that structure. In the ideal situation, it would be best if the particular structure on which cathodic protection is to be applied, were completely isolated from any copper grounding system. The isolating procedure would not only reduce the cathodic protection requirements but would eliminate the bimetallic corrosion of the structure with respect to the copper. However, in many instances, isolating the structure is either not desirable or not practical. For example, on pipe-type

able it is necessary to maintain a low-esistance ground connected to the pipe o accommodate fault currents. Whereas n the ordinary pipeline insulating flanges an be used at the ends, this is not esirable for pipe-type cable.

Let us examine the results achieved on 3.5-mile section of cable on which ca-hodic protection was installed and on vhich the grounding system at both ends emained connected to the pipe. The sys-em installed made use of two rectifier nits installed near the ends of the pipe, ne of which was energized to deliver 9.5 amperes and the other was energized o deliver 9.5 amperes. The pipe in this xample is a new 6-inch line which is very vell coated.

Table VI lists the values of pipe-to-oil potential measured along the line fter the system was energized. It hould be noted that the magnitude of cur-ent required is extremely large relative o that which would be required on an solated pipe of this type. A total cur-ent requirement of 1.0 ampere would be onsidered as excessive if this pipe were n isolated one. It can be noted further hat the lowest values of potential were btained at the ends of the pipe, near the opper ground, despite the fact that the rain points of the cathodic protection ystem are near the ends of the line. Thus, it is apparent that almost all of the athodic protection current is being rained by the copper grounding system. This condition obtains because it is neces-ary to bring the potential of the copper round up to the open-circuit potential of he steel before any protective current lows to the steel.

It is true that the drain points in this xample are close to the copper, and it nay well be asked why the cathodic rotection system did not make use of one ectifier unit installed near the mid-point f the line rather than the system which vas used. This was not done because ests prior to the installation indicated hat if a rectifier unit were installed near he mid-point, it would be necessary to aise the potential along the middle of the ine to an excessive value before the ends f the line could be brought up to a pro-ective level.

In the application of cathodic protection o pipe-type cable, success has been re-orted with devices which isolate the pipe rom the station grounds, and yet provide low-resistance path for fault currents.[2] This type of device would, of course, re-uce the cathodic protection requirements onsiderably. However, in many cases, is preferable to install the additional athodic protection equipment rather than attempt to maintain the insulating device in proper operating condition.

Table VI. Pipe-to-Soil Potential Measurements Before and After Cathodic Protection on 3.5 Miles of 6-Inch Pipe-Type Cable

Reading No.	Location, Manhole No.	Pipe to Soil Potential, Millivolts System "Off"	System "On"
1	7	−540	−950
2	6	−575	−940
3	5	−520	−1,020
4	4	−660	−1,260
5	3	−700	−1,420
6	2	−625	−1,450
7	1 (at 40th Street)	−570	−1,360
8	19 (at 40th Street)	−550	−830

In the above example, although it is not desirable, it is possible to isolate the pipe from the grounding system. However, at many industrial plants and power plants, it is almost impossible to separate the pipes from the grounding grid. Therefore, a cathodic protection system for the underground pipe at those plants must be designed with sufficient current to overcome the iron-copper potential as well as to deliver sufficient current to the pipes to overcome the corrosion activity produced by the soil alone.

Other Considerations

The items which have been discussed lead to some questions concerning present grounding practices. The first question is: Why copper? Perhaps the use of copper for grounding systems arises out of habit. While it is true that copper has the best conductivity of the economical metals, the resistance of an electrical ground to earth depends only negligibly upon the grounding material which is used. For instance, in cathodic protection work, very low-resistance ground beds are installed using graphite rods, a material which is far less conductive than copper. This does not mean that graphite should be used for electrical grounds instead of copper (graphite is also cathodic with respect to iron), but it does indicate that, as concerns the electrical characteristics of a ground, other materials such as steel or zinc can be used. It is, of course, true that copper is more resistant to underground corrosion than is steel, but it is possible to install a grounding system using steel rods, and then to provide cathodic protection systems for those steel rods. This type of installation is reported to have been installed at the Fairless Works of the Steel Corporation,[3] and the results reported indicate that the installation was successful as well as economical.

The second question which arises concerning present grounding practices is one which questions the practice of connecting underground pipes to the grounding system. There is good reason for grounding the pipe where it comes up above ground, but this does not mean that the underground portion of a particular line need be connected to the grounding system. There is no apparent reason why insulated joints cannot be installed at the points where the underground pipes come up above ground. If this were done, the above-ground portions of the lines could be grounded without having any effect on the underground portions of the lines.

There are, no doubt, other questions which can be raised concerning existing grounding practices, and other suggestions made on how those practices can be altered in mitigating underground corrosion. However, in the design of many plants, the electrical and the mechanical portions are often designed separately and the co-ordination in regard to corrosion problems is often neglected. Therefore, many plants are constructed with built-in underground corrosion problems. In order to avoid many of these built-in problems, new ideas and methods for grounding, such as those used at the Fairless Works, may be necessary instead of many of the currently employed practices.

Summary

Many electrical grounding systems using copper produce corrosion on underground structures because of the bimetallic activity generated when those underground structures are electrically connected to the grounding system. The corrosion current generated and the intensity of the corrosion attack are dependent upon the usual principles governing the behavior of bimetallic couples. In the case of underground pipelines, the corrosion attack depends primarily upon (1) the potential between the structures and the copper ground, (2) the ratio of the exposed area, (3) the resistance between the two structures, and (4) the electrical continuity of the structure. These principles must be observed in order to avoid the serious corrosion problems which can result from the use of copper grounding systems.

In providing cathodic protection for an underground structure which is connected to a copper grounding system, it is

often necessary to use considerably more current than in providing protection for isolated underground structures. While it would be best to isolate the underground structure from the copper grounding system, in many instances this is either not desirable or not practical. Thus, in designing a cathodic protection system for a given structure, it is often necessary to provide sufficient current not only to overcome the normal corrosion activity on that structure, but to overcome the potential between the structure and the electrical ground.

Because of the serious corrosion problems which can arise from the use of electrical grounds, existing grounding practices should be reviewed, and new ideas and methods for grounding be investigated.

References

1. National Electrical Code. National Fire Protection Association, Boston, Mass., 1946, article 250.

2. Corrosion Protection for Pipe Type Electric Transmission Lines in the Chicago Area, W. T. Rose. *Corrosion*, Houston, Tex., Oct. 1958.

3. Electrical Grounding and Cathodic Protection at the Fairless Works, W. E. Coleman, H. G. Frostick. *AIEE Transactions*, pt. II (*Applications and Industry*), vol. 74, Mar. 1955, pp. 19–24.

Modified Optimum Nonlinear Control

T. MITSUMAKI
NONMEMBER AIEE

Synopsis: Recently, many papers have been published concerning optimum nonlinear control systems. It seems that the controllers which utilize this control method have become more complex than conventional controllers. In this paper, the author proposes a new type of control action, "modified optimum nonlinear control," which not only reduces the complexities of the controller but also gives a nearly optimum control, i.e., control action, which is a compromise between theory and practice. The analog computer study of this control method and its comparison with the discrete compensation techniques in sampled-data control systems are also shown.

AT PRESENT, proportional plus integral plus derivative control action is widely used as the best available in the field of automatic control. However when an experienced operator controls a process his control action is not a simple linear action but includes a number of complex nonlinear terms.

In practice, the amount of the manipulated variable which is applied to the controlled systems as a corrective action is limited with saturation. An optimum nonlinear control which utilizes this available maximum power effectively was proposed by D. McDonald[1] and A. M. Hopkin[2] around 1950, and though much progress has been seen since then in theoretical approach, this method has not realized extensive use in the field of automatic control because of its complexity.

From this point of view, the author proposes a control action-modified optimum nonlinear control, not only to reduce the complexities of the controller but also to obtain a nearly optimum control action.[3]

Paper 59-837, recommended by the AIEE Feedback Control Systems Committee and approved by the AIEE Technical Operations Department for presentation at the AIEE Winter General Meeting, New York, N. Y., January 31–February 5, 1960. Manuscript submitted October 30, 1958; made available for printing October 8, 1959.

T. Mitsumaki is with Hitachi, Ltd., Tokyo, Japan.

The author wishes to acknowledge the valuable suggestions of Prof. Y. Takahashi, and the constructive criticisms of Dr. S. Akiyama, Dr. T. Sudo, and A. Kamoi.

Modified Optimum Nonlinear Control Systems

The optimum nonlinear control system is shown in Fig. 1. At point a, error and error rate are positive, i.e., controlled variable is about to run away from the equilibrium value. Thus it is logical to apply the maximum available power $+A$ to the controlled system in order to pull back a controlled variable to the equilibrium. Then, m is reversed to $-A$ and the error decreases slowly as shown in Fig. 1. If the reversal time is favorable, it is possible to reach a state in which the error and the error rate become zero simultaneously. At this instant, keeping m to its equilibrium value, the controlled variable holds its value and the transient is completely finished. To determine this reversal time, it is convenient to discuss the switching curve in the phase-plane whose co-ordinates are error and error rate. The control action is determined whether the point in the phase-plane is in the right or left side of the switching curve. To realize this control method, it is necessary to solve this switching equation or to simulate the switching curve with an element such as a function fitter; however, this results in the increase of the complexities of the controller. This applies only to second-order control systems. In nth order systems, the optimum performance can be obtained by $(n-1)$ times reversals of manipulated variable. However, it is almost impossible to realize such a control action because of its complicated switching surface and noise due to higher order error derivatives.

On the other hand, an on-off control system is widely used for its simple mechanisms. The derivative action is added to prevent an overshoot and to stabilize the system. In this case, the switching curve is a simple straight line in the phase-plane as shown in Fig. 2. This problem is analyzed by Flügge-Lotz in detail.[4] It has been shown that the response comes to an end point at p in Fig. 2 and, due to the existence of the small transfer lags, jitters around the switching line and converges to the origin of the phase-plane.

The modified optimum nonlinear control takes into account the progress above mentioned and at the same time keeps the complexities of the controller to minimum. The switching curve of an ordinary optimum nonlinear control is uniquely defined by the transfer function of the system and maximum

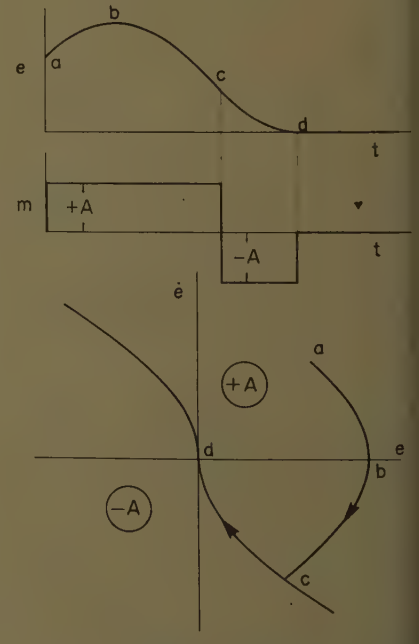

Fig. 1. Optimum nonlinear control

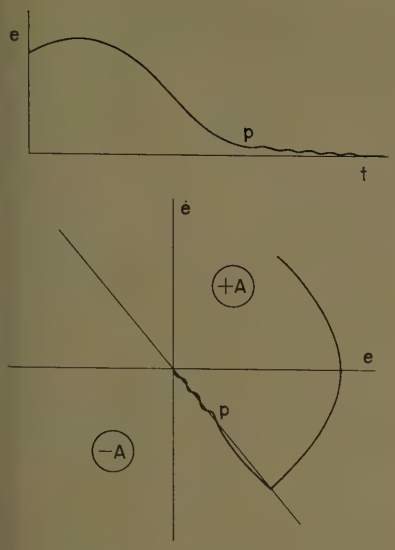

Fig. 2. End point phenomenon in relay control systems

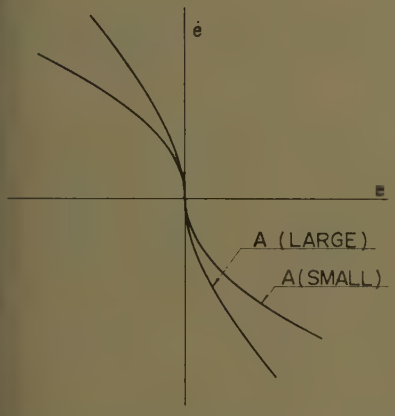

Fig. 3. Shape of switching curve for various values of A

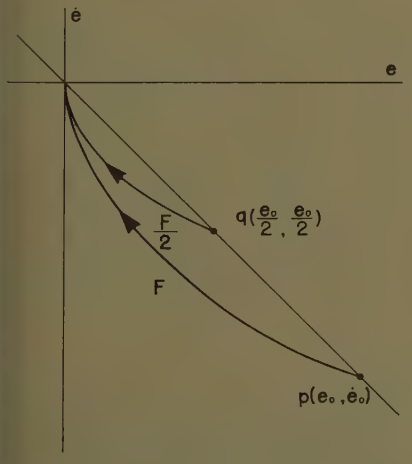

Fig. 4. Determination of modified value

vailable power. The switching curve lters its shape as shown in Fig. 3 by the ariation of maximum power A. The arger the A is, the closer the switching urve to the ordinate in the phase-plane. rom this fact, it is possible to make use f a moderate value of manipulated variable. If a phase trajectory returns from an initial point $p(e_o, \dot{e}_o)$ to the origin of the phase-plane with a corrective power F, another phase trajectory from $q(e_o/2, \dot{e}_o/2)$ can be pulled back to the origin with a corrective power $F/2$ as shown in Fig. 4, for the linear characteristics of the controlled systems.

In order to reduce the complexities of the controller, the switching curve is replaced with a straight line, whose equation is

$$e+k\dot{e}=0 \qquad (1)$$

Thus, the desired moderate value is determined by a simple equation

$$-A\frac{e_s}{a} \qquad (2)$$

where

e_s = the value of error when the phase trajectory crosses the switching line
a = the value of error at the crosspoint of the switching line and the switching curve

Consider the response from a point P in Fig. 5 where the manipulated variable is positive, i.e., $+A$, and the phase trajectory is PQ. In the optimum nonlinear control system, the m is reversed at point S and the trajectory falls into the origin of the phase-plane. In the case of a modified optimum control system, the sign of the manipulated variable is reversed at point R, the cross point of the switching line and the phase trajectory PQ. If the value of $-A$ is applied to the controlled system at this instant, the corrective action is great enough to cause the phenomenon of end point. However, if the moderate value of m is applied as a corrective action at point R, it is possible to obtain a response that falls precisely into the origin of the phase-plane.

The control action is expressed as follows: When the response curve crosses the switching line in the phase-plane, the sign of the corrective action is reversed, and the magnitude of the corrective action is modified proportional to the value of the error (or error rate) at the reversal point. This control method is called "modified optimum nonlinear control" and is applicable to any type of transfer function of second-order controlled systems except an oscillatory system. This technique may be extended to higher order controlled systems with the complexities of the controller kept to a minimum.

The response time of the system is calculated by integrating the reciprocal value of the error rate with respect to error. In regard to the response time, the optimum nonlinear control system is superior to the modified optimum system because the phase trajectory of the optimum system lies below the modified systems.

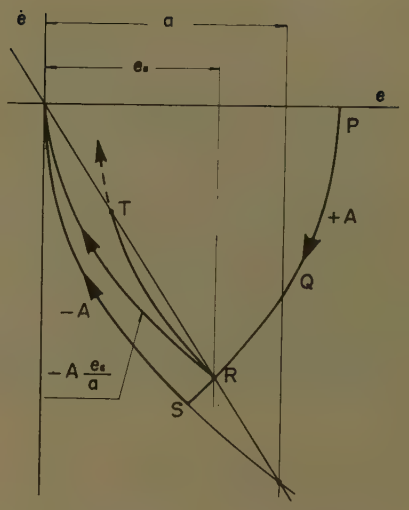

Fig. 5. Principle of modified optimum nonlinear control

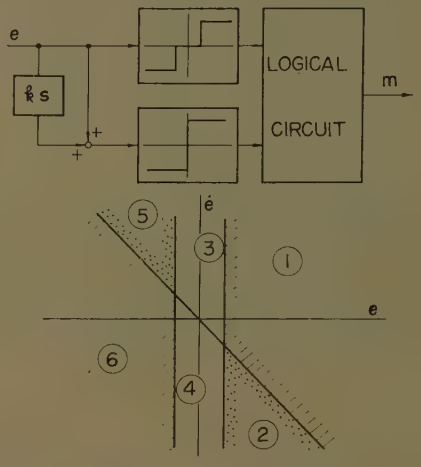

Fig. 6. Composition of controller; see Table I

The Composition of Modified Optimum Controller

To realize the control action mentioned, the composition of the controller is as shown in Fig. 6. The error values are divided into three parts by the 3-position element, and the error-plus-error rate values $(e+k\dot{e})$ are divided into two parts by the 2-position element. By combin-

Table I. Composition of Controller

Region	e	e+kė	Manipulated Variable
1	+	+	+maximum value
2	+	−	−modified value
3	0	+	linear action
4	0	−	linear action
5	−	+	+modified value
6	−	−	−maximum value

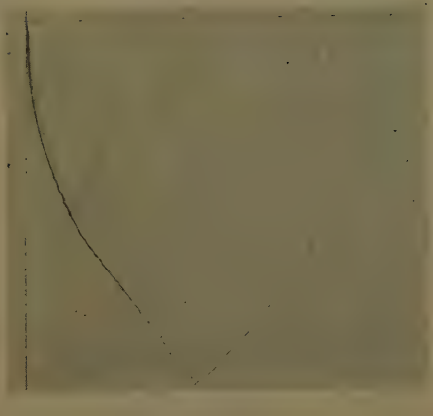

Fig. 7. Phase-plane plot of optimum nonlinear control

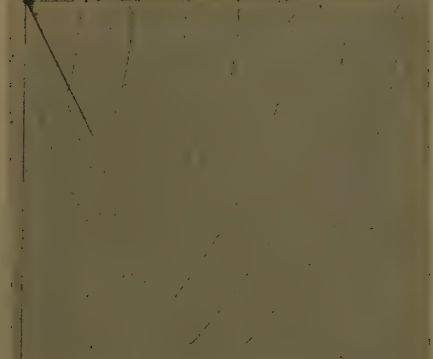

Fig. 8. Phase-plane plot of relay control system

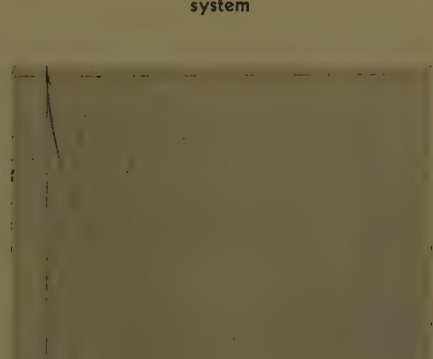

Fig. 9. Phase-plane plot of modified optimum nonlinear control

ing these two elements, the phase-plane is divided into six regions. According to the present value of error and error rate, the manipulated variable is assigned values as shown in Table I. In this table, maximum value means to apply a maximum available power of the manipulated variable to the controlled system and a moderate value means a linearly modified value of m according to the information of the switching instant. A linear control action is provided in the small error region to avoid a limit cycle due to the large corrective action. If the phase trajectory enters region 2 or 5 directly from the linear region, it is desirable to apply a maximum available power instead of moderate value. If this logical action is added, the controller becomes more complete.

Analog Computer Study

In this section, the result of the analog computer study of this control method is shown. The controller consists of polarized relays and high-speed relays. These relays are combined so that the phase-plane is divided into four regions instead of six for simplicity. An operational amplifier with capacitors as its input and output impedances is used as a holding circuit to modify the manipulated variable proportional to the switching error.

Adjustable values of this controller are the gradient k of the switching line and the constant K of the moderating circuit and they are adjusted by the following procedures. First, for the maximum magnitude of the step input e_{max}, k is adjusted so that the phase trajectory just falls into the origin of the phase-plane with plus and minus signs of full power. Next, with the same input, K is adjusted to obtain a minus full power using a moderating circuit in the latter half of the response. After these adjustments, all the responses precisely fall into the origin for any magnitude of step input less than e_{max}.

In the analog computer study, the controlled system is considered to be $1/(20_s s^2)$, the m_{max} is selected to be ± 50 volts, and the maximum magnitude of step input is assumed to be about 70 volts. The phase-plane plot of the optimum nonlinear control system is shown in Fig. 7, in which the transient response curves for seven different input magnitudes are traced. These curves are calculated by the analog computer made by Hitachi Ltd., and are plotted with Variplotter (Electronic Associates Inc.). The switching curve of optimum system is simulated with a function fitter.

The phase-plane plot of an ordinary relay control system is shown in Fig. 8. For maximum input, the response is the same as that of an optimum system, but for a smaller input, it is seen that the phenomenon of end point arises and the phase trajectory converges to the origin jittering closely around the switching line. As will be shown, the response time is large in these cases.

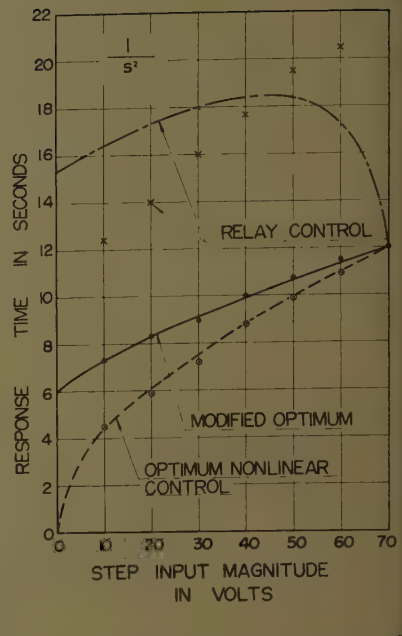

Fig. 10. Comparison of response time for various nonlinear systems (line: theoretical, plots: experimental)

The phase-plane plot of the modified optimum nonlinear control is shown in Fig. 9. In the latter half of the response, manipulated variable is modified according to the value of the error at switching instant and all the responses fall into the origin directly.

The comparison of the response times of these nonlinear systems is shown in Fig. 10. For maximum step input, all these responses are the same as those of these optimum control and have the same response time. For a smaller input, the response time of the optimum system is the shortest of the three. In relay control, the response from the end point is very slow and the response time for the minimum input does not become shorter than that for the maximum input. On the other hand, in the modified system, the response time becomes smaller according to the magnitude of the step input and from this result it seems to be very valuable to modify the magnitude of the manipulated variable.

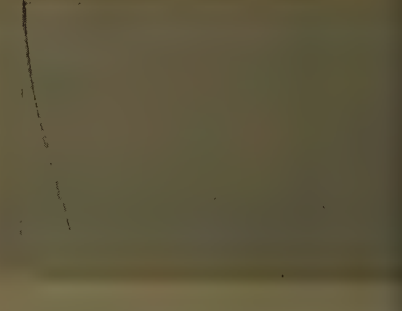

Fig. 11. Phase-plane plot of modified optimum nonlinear control ($1/s\ (1+Ts)$)

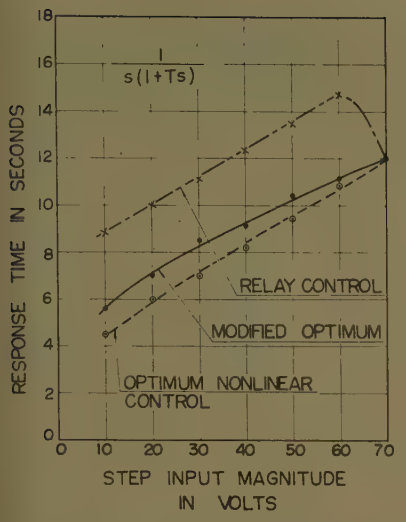

Fig. 12. Comparison of response time for various nonlinear systems

In the same figure, theoretical values are shown with the experimental data, but in the relay system, the experimental value does not coincide with the theoretical value. In calculating the response time of the relay system, it is assumed that (1) the response from the end point goes to the origin along the switching line, and (2) the response time is defined as the time from the start to the instant when the transient response enters 1% of the initial step magnitude (theoretical recovering time to the origin is infinite). However, in the experiment the response time is measured from the start to the time when the response falls into the vicinity of the origin of the phase-plane. Therefore, the larger the input magnitude is, the longer the measure of the response time is apt to be. If the result is compensated for by taking into account the aforementioned points the discrepancy of two curves will be diminished.

The phase-plane plot of the modified optimum nonlinear control applied to second-order systems with viscous damping is shown in Fig. 11. The comparison of the response time for the other nonlinear systems is shown in Fig. 12. In this case, there occurs a velocity limit and all the phase trajectories fall into the vicinity of a point in the phase-plane. Therefore, end point phenomenon gives fewer defects. But if the moderate value is applied, the response time decreases monotonously according to the decrease of input magnitude.

Comparison with the Discrete Compensation Techniques

In sampled-data control systems, there is a technique to obtain a finite settling time response which makes use of a delay-line-synthesizer as a controller.[5] This control method is nonlinear (discrete) in time domain, but linear in spacial domain. Therefore, if the input is too large or the sampling interval is too short, the manipulated variable cannot attain the calculated necessary value by saturation.

Assume that the controlled system is a second-order system having no damping and no dead time. The response can be settled within two sampling intervals as shown in Fig. 13. If manipulated variable is supposed to be a single pulse whose magnitude is m and duration is one sampling interval, the output sequence of controlled variable is given in equation 3:

$$c(n\Delta)=\frac{m}{2k}\Delta^2(0+1z^{-1}+3z^{-2}+5z^{-3}+7z^{-4}+9z^{-5}+\dots) \quad (3)$$

The manipulated variable is shown in Fig. 13 and the output sequence is

$$c(n\Delta)=\frac{\Delta^2}{2k}\begin{bmatrix} m_1(0+1z^{-1}+3z^{-2}+5z^{-3}+ \\ 7z^{-4}+9z^{-5}+\dots) \\ -m_2(0+0z^{-1}+1z^{-2}+ \\ 3z^{-3}+5z^{-4}+7z^{-5}+\dots) \end{bmatrix} \quad (4)$$

From a condition that c has the same value after $n=2$

$$m_1=m_2 \quad (5)$$

Suppose the maximum magnitude of the step input is r_{max}, then

$$m=m_1=m_2\frac{r_{max}K}{\Delta^2}\leqq A \quad (6)$$

Practically, the manipulated variable has a saturation value, therefore, the sampling interval must be chosen so that manipulated variable does not exceed this saturation value. The value of error when the sign of the manipulated variable is changed is

$$e(\Delta)=r-c(\Delta)=\frac{\Delta^2}{2K}m=\frac{r}{2} \quad (7)$$

From this, it is found that the discrete compensation control action in a second-order system without damping is the action to apply an equal reverse corrective power when the error becomes the half of the initial value.

The optimum nonlinear control is a control method to apply an equal maximum available power A and the modified optimum is the action to apply the manipulated variable of the maximum and the moderate value. On the other hand, the discrete compensation is a control method to apply values $\pm m$ $(m\leqq A)$ as shown in Fig. 14. As m is assumed to be less than or equal to its saturation

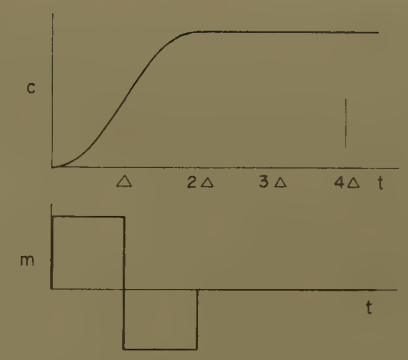

Fig. 13. Finite settling time response

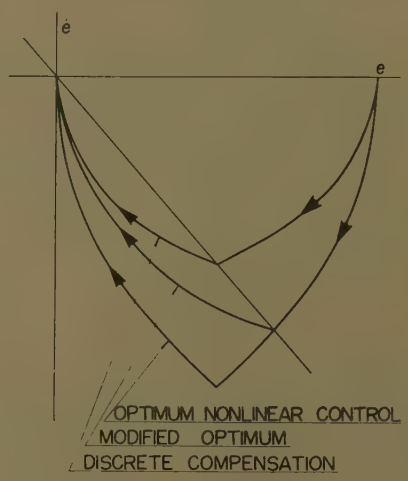

Fig. 14. Phase-plane plot of discrete compensation comparing with optimum and modified optimum control systems

value, the system is linear and the so-called switching curve in the phase-plane is nothing but a straight line like that of a relay control system.

From the phase trajectories shown in Fig. 14, the response time of each control method is compared in Table II. In this case, two sampling intervals are chosen for minimum response time, but it is possible to use a shorter sampling interval. However, the problem arises as to which program the controlled variable should be raised to follow the step input. So far this problem has not been studied in detail, but Table II holds completely well even in these cases.

The second-order system without damping is selected for the simplicity of calculation. However, the results shown here may be extended to any type of second-order control systems.

Table II. Comparison of Response Times

Control Action	Response Time
Optimum nonlinear	shorter
Modified optimum nonlinear	↕
Discrete compensation	longer

Conclusions

A technique for obtaining a nearly optimum control action without increasing the complexities of the controller by replacing a switching curve with a switching line and modifying a manipulated variable according to the value of the error at switching instant is presented.

It is shown from the analog computer study that the proposed nearly optimum control system is practicable and that the application of the modified manipulated variable is very effective in shortening the response time.

Comparisons of this control method with optimum nonlinear control systems, and relay control systems, as well as with discrete compensation in sampled-data control systems, are also included.

References

1. Nonlinear Techniques for Improving Servo Performance, D. C. McDonald. *Proceedings*, National Electronics Conference, Chicago, Ill., vol. 6, 1950, pp. 400–21.

2. A Phase-Plane Approach to the Compensation of Saturating Servomechanisms, A. M. Hopkin. *AIEE Transactions*, vol. 70, pt. I, 1951, pp. 631–39.

3. Modified Optimum Nonlinear Control (in Japanese), T. Mitsumaki. *Transactions*, Japan Society of Mechanical Engineers, Tokyo, Japan, vol. 24, no. 147, 1958.

4. Discontinuous Automatic Control (book), I. Flügge-Lotz. Princeton University Press, Princeton, N. J., 1953.

5. Sampled-Data Processing Techniques for Feedback Control Systems, A. R. Bergen, J. R. Ragazzini. *AIEE Transactions*, pt. II (*Applications and Industry*), vol. 73, Nov. 1954, pp. 236–47.

Report of Field Tests on Aluminum Potline Rectifier Systems

C. A. LANGLOIS, ASSOCIATE MEMBER AIEE
V. N. STEWART, MEMBER AIEE
R. P. STRATFORD, MEMBER AIEE

Synopsis: The test program on a large aluminum potline system was directed towards the investigation of some basic electrical characteristics of aluminum potlines and large d-c systems. The program consisted of three parts: impedance measurements, system and tie-line circuit-breaker tests, and anode circuit-breaker arc-back tests.

The impedance measurements tests gave an actual test value of the inductance and a-c resistance of a hot potline under operating conditions at different positions along the main bus. The resistance and inductance values were obtained for both the potline circuit and the rectifier circuits feeding the potline.

Under the system and tie-breaker tests, the decay time of the potline current was determined to be approximately 0.15 second. The energy stored in the potline was dissipated in the resistance of both the potline and the rectifier circuits. The rectifier circuits accounted for approximately 3 to 4% of the total stored energy. If the a-c source of a potline is lost when it is paralleled with another potline through a small capacity tie line, the tie breaker would be required to interrupt only the stored energy in the rectifier system. The duty imposed upon a tie breaker under these conditions is light compared with its normal ability and requirements as feeder or main circuit breakers. The mercury-arc rectifiers of the de-energized potline will pick up the potline current even after excitation has been removed.

The anode breaker performed a high-speed interrupting function with current-limiting action under maximum conditions that could exist with 900-volt system operation.

NUMEROUS PAPERS have been presented in the last several years on various aspects of the performance of the equipment applied to supply large blocks of d-c power. Nevertheless, many questions remain unresolved as to the characteristics of the system to which the equipment is applied, and as a result, the data for the service which is actually imposed upon the equipments are still needed. This paper deals with tests conducted to assess the performance under maximum service conditions. The high-speed anode circuit breakers performed interruptions of various controlled arc backs, and the semihigh-speed d-c breaker performed under some of the operating conditions to which it may be subjected when being used as a tie between large d-c loads supplied by mercury-arc rectifiers. In addition, data on the d-c characteristics of the system which would have a bearing upon the actual and evaluated performance were gathered wherever possible.

The Reynolds Metals Company system is shown in the complete one-line diagram, Fig. 1, for the three large potlines involved in various stages of the test. The 154-kv power is supplied from the nearby generation of the Tennessee Valley Authority power system. For the utilization of the power for the production of aluminum, the system is designed and arranged to achieve efficiency in the operation of each nominally rated potline of 80,000 amperes and 850 volts.

Test Arrangements and Facilities

The test series was conducted with the advantage of an unusual situation which allowed a much greater than normal flexibility in establishing operating conditions. At the test location in Reynolds' Lister Hill, Ala., plant, a large addition was being made in the power conversion equipment. All but one of the potlines, composed of 14 rectifier sections rated 6,000 amperes at 850 volts each, was operating at full load. The last line was still waiting to pick up its load. Short bus ties between the lines permitted a combination of circumstances between the unused line and an operating line which could be varied to suit the test. In the performance of the two major items of the test program, i.e., the system study when operating through a heavy-duty d-c tie breaker and rectifier arc-back conditions under simulated start-up, the arrangement was of considerable value.

System and Tie-Breaker Testing

Referring to Fig. 2, the circuit parts are identified and the instrumentation given for the system and bus-tie tests. The line with a connected load is potline *7* and the unloaded line is potline *8*. Current measurement for each of the a-c lines and the transformer nearest to the bus tie were measured along with the potline values from the DCCT (d-c current transformer). The a-c currents and the few tests which include a check on the 13.8-kv bus voltage were recorded from the output of a full-wave 3-phase rectifier circuit,

Paper 60-14, recommended by the AIEE Chemical Industry and Industrial Power Rectifiers Committees and approved by the AIEE Technical Operations Department for presentation at the AIEE Winter General Meeting, New York, N. Y., January 31–February 5, 1960. Manuscript submitted February 20, 1959; made available for printing October 2, 1959.

C. A. Langlois is with the Reynolds Metals Company, Richmond, Va. V. N. Stewart and R. P. Stratford are with the General Electric Company, the former in Philadelphia, Pa., and the latter in Schenectady, N. Y.

The authors acknowledge the contribution and assistance of R. B. Newman and N. F. Marty of the Reynolds Metals Company, and A. N. Greenwood, G. Hubbard, W. C. Kotheimer, T. Lee, T. J. Scully, and C. H. Titus of the General Electric Company, in carrying out the successful test program.

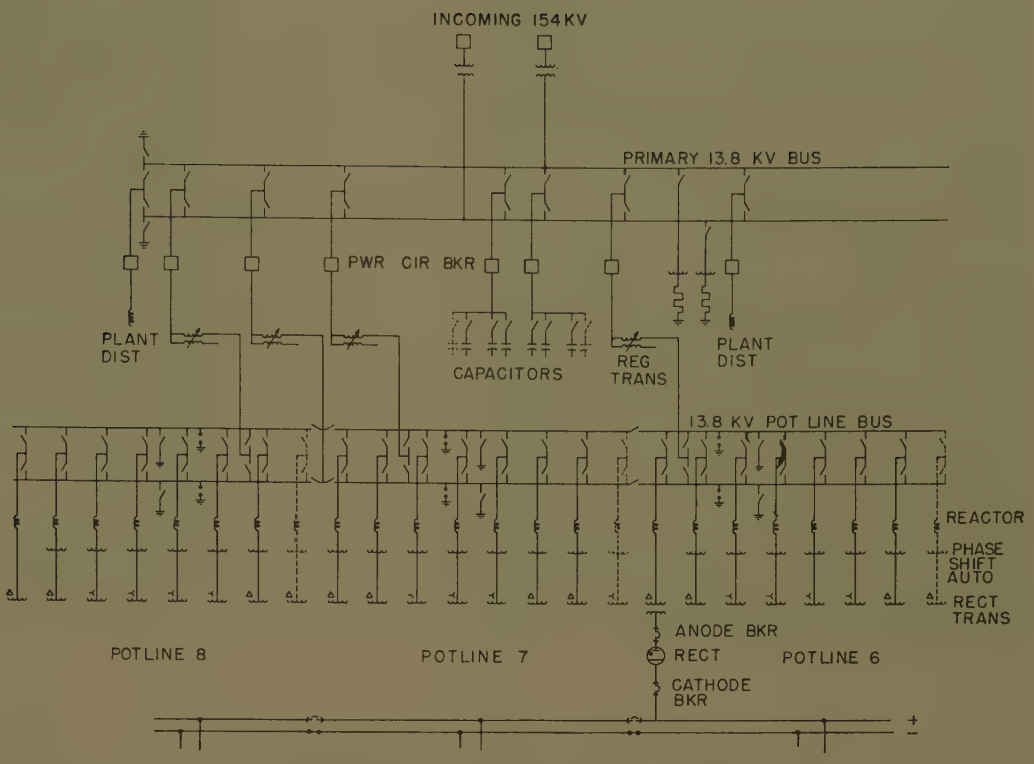

Fig. 1. One-line diagram of mercury-arc power rectifier system at Reynolds Metals Company, Lister Hill, Ala.

Fig. 3. This permitted a 3-phase record on one trace as indicated in trace *E* of Fig. 4 for potline current. This 3-phase measure requires the assumption of a sine wave to allow an evaluation to be made from the indicated peak currents.

The normal arrangement and mounting of the tie breaker for this rectifier system is shown in Fig. 5. The bus which normally supports the DCCT has been removed and in its place a 10,000-ampere instrument shunt has been connected with cables. This current measurement in the tie plus the breaker arc voltage and the two d-c bus voltages completed the instrumentation.

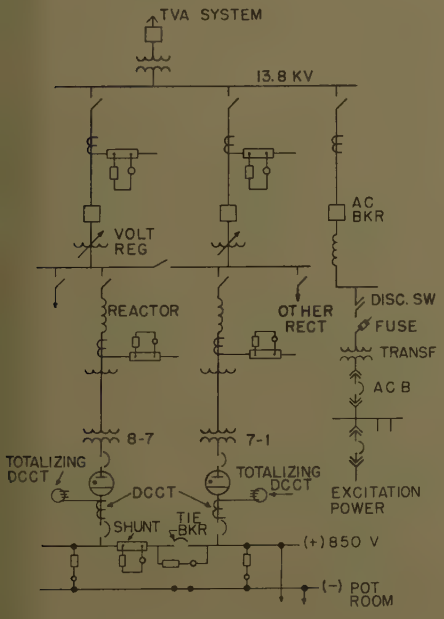

Fig. 2 (left). Instrumentation for system and tie-breaker tests

Realizing that one of the objectives was to obtain a maximum rate of transfer on the potline load from one line to the next the tests were run with 10,000 amperes being supplied through the tie. This represented a normal load for the breaker having a 12,000-ampere rating. The overcurrent trips were set at 15,000 amperes. However, the initial load current of the breaker had very little effect on the interrupting duty as the complete transfer was accomplished in slightly less than one-half cycle. Following the transfer of the load from line *7* to all rectifiers of line *8*, the current remained unchanged until the interruption by the tie breaker.

In these tests it was possible to observe the effect of the transfer of these large loads when switched to a weak or stiff system. These were represented in these tests by operating the unloaded line with one rectifier transformer or with six transformers.

Arc-Back and Anode-Breaker Testing

Controlled testing of arc backs was applied to the rectifier using methods employing a reverse-connected 16-inch-diameter pumpless rectifier tank. The connection diagram, Fig. 6, shows the tank associated with phase *2*. An alternate position of phase *4* was used to conduct tests with current paths which would give an opposite magnetic influence on the interrupters. Fig. 7 shows the special rectifier tank connections for tests being made with arc backs in phase *4*.

The firing of the test rectifier tank came from a full-phase control unit which was operated in conjunction with a Selsyn. This provided the necessary synchronous timing for the firing pulse of the ignitor.

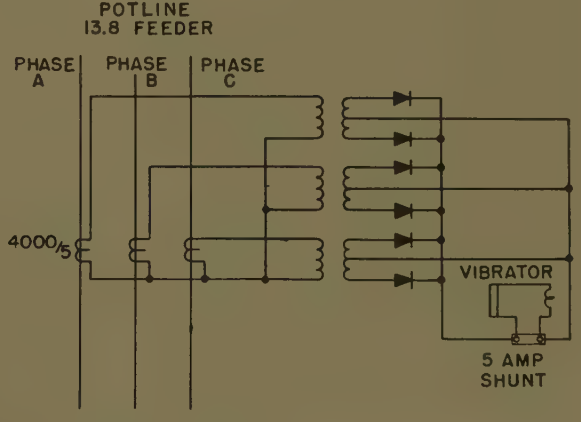

Fig. 3 (right). Instrumentation circuit used to record 3-phase line currents

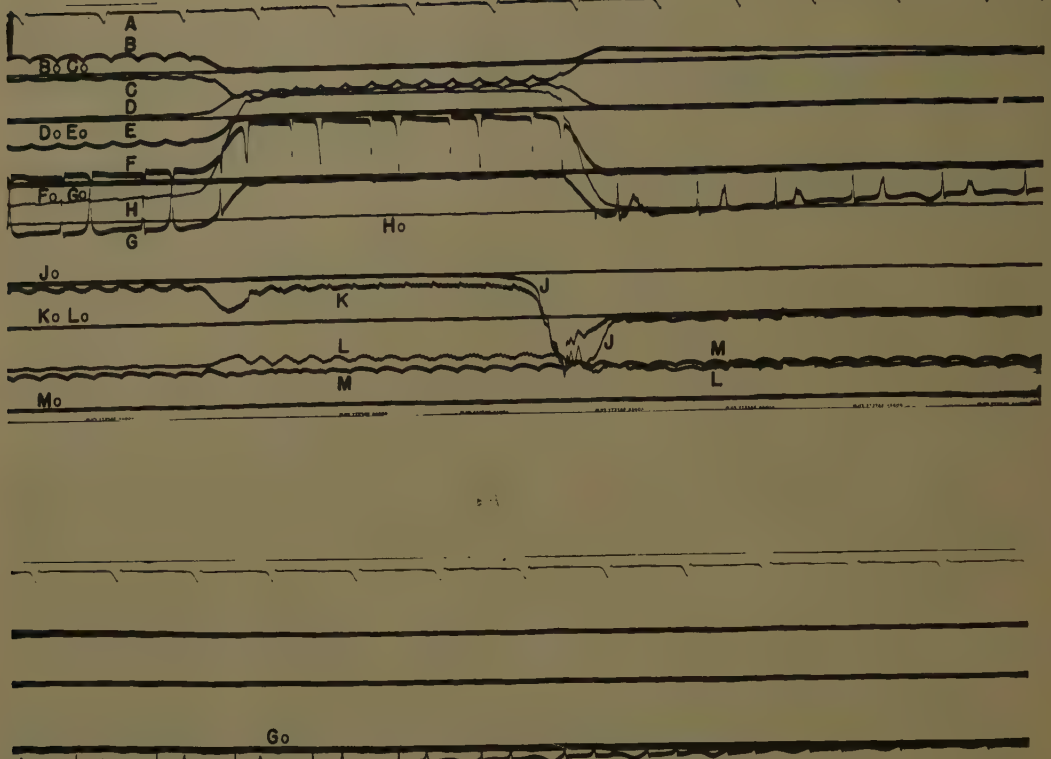

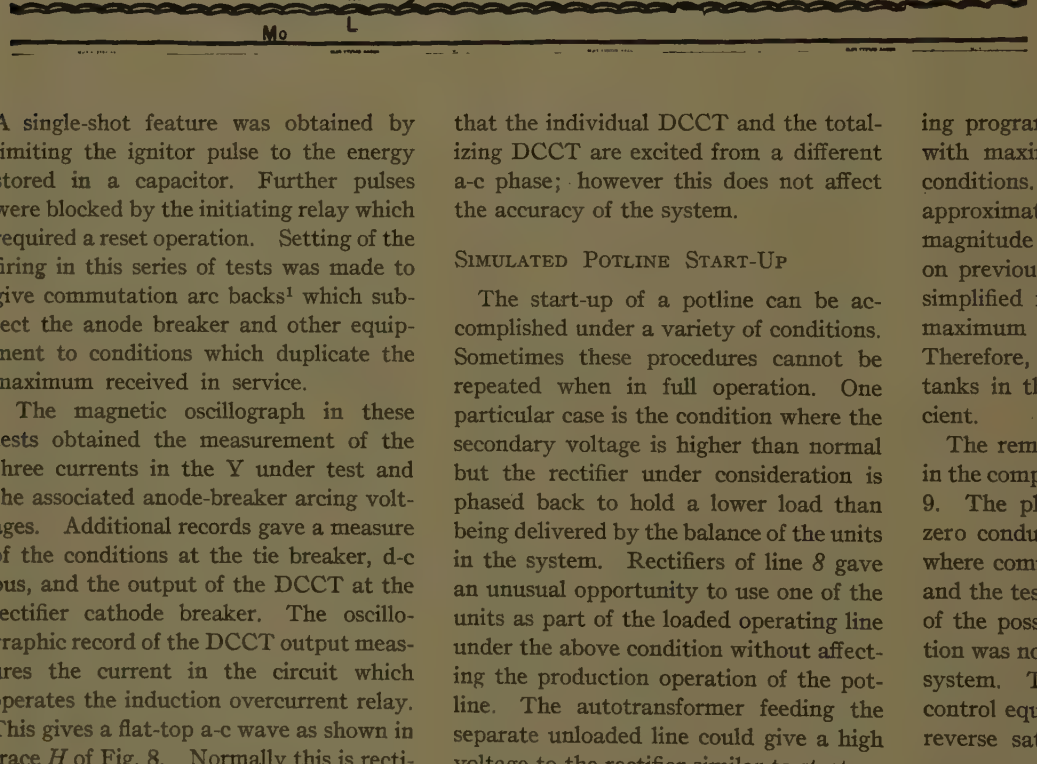

Fig. 4. Tie breaker and system conditions during loss of a-c power source

A—Time, 1/120 second
B—A-c rectifier 7-1
C—A-c rectifier 8-7
D—A-c pot-line 8
E—A-c pot-line 7
F—Totalizer current, potline 8
G—Totalizer current, potline 7
H—Tie-breaker current
J—Voltage across breaker
K—D-c volts, line 7
L—D-c volts, line 8
M—A-c volts, 13.8 kv

A single-shot feature was obtained by limiting the ignitor pulse to the energy stored in a capacitor. Further pulses were blocked by the initiating relay which required a reset operation. Setting of the firing in this series of tests was made to give commutation arc backs[1] which subject the anode breaker and other equipment to conditions which duplicate the maximum received in service.

The magnetic oscillograph in these tests obtained the measurement of the three currents in the Y under test and the associated anode-breaker arcing voltages. Additional records gave a measure of the conditions at the tie breaker, d-c bus, and the output of the DCCT at the rectifier cathode breaker. The oscillographic record of the DCCT output measures the current in the circuit which operates the induction overcurrent relay. This gives a flat-top a-c wave as shown in trace *H* of Fig. 8. Normally this is rectified for the recording instruments and appears as trace *G* in Fig. 4. The dip in the waveform which recurs every one-half cycle is from the a-c excitation wave. The additional dip indicated one-third of the way along the half-cycle wave shows that the individual DCCT and the totalizing DCCT are excited from a different a-c phase; however this does not affect the accuracy of the system.

Simulated Potline Start-Up

The start-up of a potline can be accomplished under a variety of conditions. Sometimes these procedures cannot be repeated when in full operation. One particular case is the condition where the secondary voltage is higher than normal but the rectifier under consideration is phased back to hold a lower load than being delivered by the balance of the units in the system. Rectifiers of line *8* gave an unusual opportunity to use one of the units as part of the loaded operating line under the above condition without affecting the production operation of the potline. The autotransformer feeding the separate unloaded line could give a high voltage to the rectifier similar to start-up and the loading determined through its phase control.

Interphase Transformer Saturation

Control of the interphase transformer saturation is essential in an arc-back testing program to assure consistent results with maximum severity for all service conditions. This item could give an approximate variation of 20% in the magnitude of the arc-back fault.[1] Based on previous experience, the method was simplified for this program as only the maximum fixed situation was needed. Therefore, the removal of firing from the tanks in the phase under test was sufficient.

The removal of the current is evident in the comparison of trace *B* in Figs. 8 and 9. The phase-*2* current trace indicates zero conduction until the timing instant where commutation arc back would occur and the test tank is fired. A comparison of the possible current magnitude variation was not attempted for this particular system. This would require additional control equipment for the unsaturated or reverse saturated conditions.

Sympathetic Arc Backs

The high-capacity system which places the duty in the forward conducting tanks at or near its maximum limit of performance during an arc back will frequently cause a sympathetic arc back on the fol-

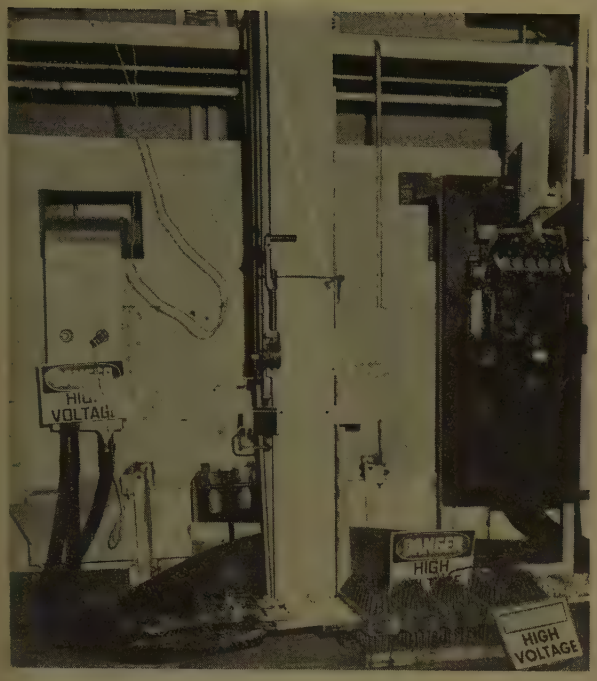

Fig. 5 (left). Type MC-5 tie breaker, 12,000 amperes, with temporary instrument shunt connected for tests

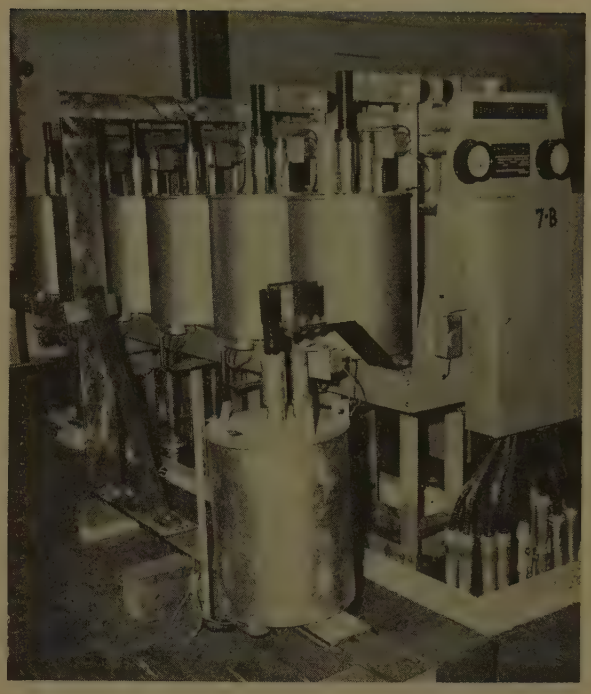

Fig. 7 (right). Reverse - connected 16-inch pumpless rectifier tank for arc-back tests

lowing phase of the same Y. Here, the system conditions have been altered from that of the initial arc back which opened one pole of the anode breaker. The new circumstances represent an increased duty on the interrupting device and this has to be considered in an evaluation of the complete operation.

In order to have a measurable value of the performances, it is desirable to have these sympathetic arc backs occur at a controlled instant of time. Further, it is necessary to keep the available power of the system at its normal maximum level. It was attempted to increase the incidence of sympathetic arc backs by forcing higher currents in one tank. It was found that this was not especially successful in this particular system, but may have some future benefit on one with different characteristics. The rectifier section used two tanks in parallel on each leg of the Y and by removal of the firing from one tank in the phase following the initial arc back, the double overload should contribute to a further arc back. Although the characteristics of this particular tank withheld this action in some cases, the frequency of occurrence was sufficient to provide a good demonstration of adequate performance under the sympathetic arc-back condition.

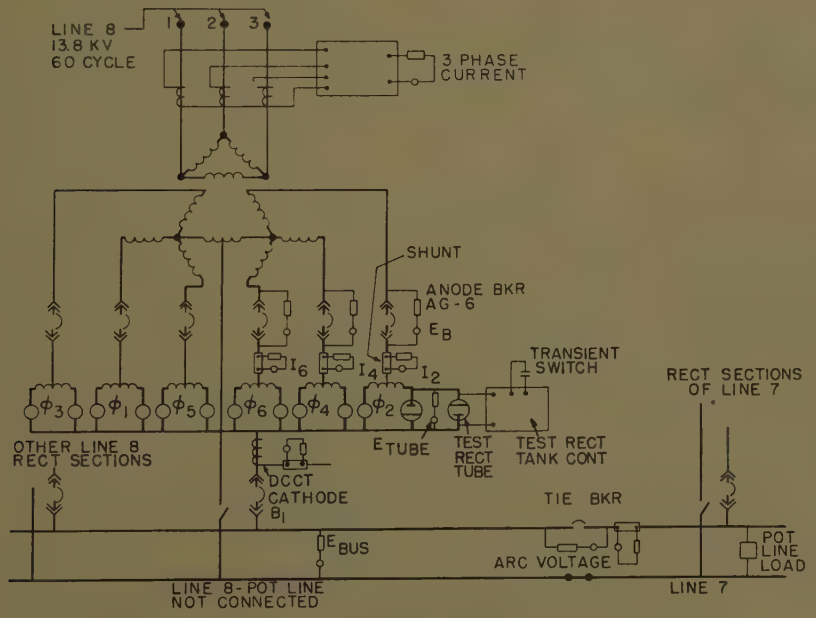

Fig. 6. Anode breaker and rectifier arc-back test connections and instrumentation

Tie-Breaker Field-Test Performance

The field tests were conducted with the normal installed tie breaker of the system which is a semihigh-speed single-pole heavy-duty type. It is a completely open unit of stationary mounting as shown in the test setup of Fig. 5 and has a continuous current rating of 12,000 amperes. Silver main contacts for current carrying are used in the circuit breaker along with sintered intermediate and arcing contacts for the interrupting function. The closing function of the breaker is accomplished by the d-c solenoid and operates through a trip-free mechanism. The combined opening time which is associated with the tripping device, mechanism, and contacts was determined to be less than 0.050 second.

The first test was made with 80,000-ampere load in potline *7* of which 10,000 amperes were being furnished through the tie breaker. This came from two adjacent rectifier sections operating from one rectifier transformer of potline *8*. The plan was to initiate the test by tripping the a-c power circuit breaker feeding line *7* and let the one rectifier unit pick up the total potline load through the tie breaker. The transfer of the large load would trip the tie breaker by overcurrent with a trip device setting of 15,000 amperes. The test was carried out with very little duty placed on the tie breaker. The opening of the tie breaker transferred the current back to the rectifiers on potline *7* which had continued to receive excitation even though the main a-c power

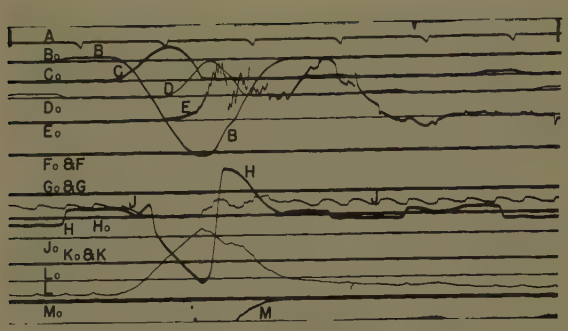

Fig. 8. Rectifier arc-back current with full-phase control and commutation arc backs

A—Time, 1/120 second
B—Current, phase 2
C—Current, phase 4
D—Current, phase 6
E—Anode-breaker arc volts, phase 2
F—Anode-breaker arc volts, phase 4
G—Anode-breaker arc volts, phase 6
H—Cathode-breaker current
J—D-c bus volts, pot line 8
K—Tie-breaker arc volts
L—Tie-breaker current
M—Arc-runner current

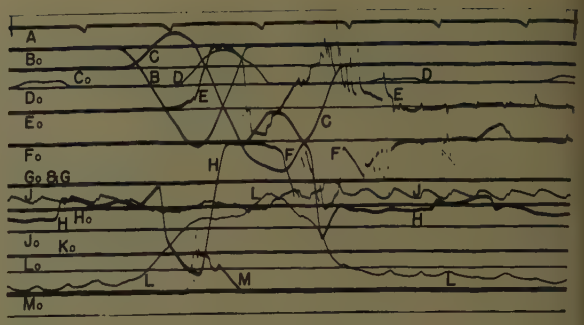

Fig. 9 (right). Rectifier arc-back current with interphase transformer saturated and having sympathetic arc back. See subcaption, Fig. 8, for trace identification

source was off. Once a rectifier is conducting it will carry this current until it decays to substantially zero value.

As a result of the test, the a-c power circuit breaker for potline *8* tripped from d-c overcurrent. However, the breaker takes approximately 5 cycles to open and did not interfere with the tests. Two arc backs occurred as a result of the high transient overload and the voltage on the d-c bus oscillated from 0 to 80%. This is a condition which results from the mutual inductance of the interphase winding when one rectifier is carrying a heavy overload.

Another test, shown in Fig. 4, was made with 12 rectifier sections on potline *8*. These rectifiers fed 10,000 amperes to the load through the tie breaker prior to the test. The results were similar to the above tests except that there were no arc backs and the bus voltage was sustained at rated level during the transfer of power from potline *8*. The tie breaker transferred the current easily and represented only a slight interrupting duty.

In the previously mentioned tests, the rectifiers were receiving their excitation from an a-c source which was independent of the line supplying the potline load. It was desirous to have the excitation removed from the rectifiers of potline *7* at the same time the main power was lost, the intent being to check the response of the rectifiers to pick up the current after the tie breaker opened.

In the first attempt, the timing sequence in the test removed the excitation before the a-c power circuit breaker had interrupted the main power. The rectifiers continued to carry almost normal currents for 0.025 second before an arc back occurred as shown in Fig. 10. Several arc backs occurred before the a-c power circuit breaker opened approximately 0.130 second (8 cycles) later. The potline current started to slowly transfer through the tie breaker before the arc backs started and continued to make the transfer until the tie breaker tripped. Here again, the breaker interrupted with little effort. The rectifiers continued to arc back until the a-c power was removed.

On the second attempt to remove excitation, the firing ceased at the same time the tie breaker opened. The rectifiers of potline *7* picked up the transferring current as expected.

It seemed evident from the test that the rectifiers of potline *7* would pick up the load when the tie breaker opened even with no excitation applied to the rectifiers. The characteristics of the rectifier tanks and the voltage on the bus will establish the potline circuit. The stored energy of the potline is dissipated in the circuit resistance. The tie breaker was only required to dissipate the energy stored in the equivalent d-c inductances of the a-c system which was feeding through the tie breaker. Therefore, the duty on the breaker was light as compared with other feeder and main breaker applications.

System Characteristics

Impedance Measurements

One of the important quantities used in calculations of short circuit and arc backs is the impedance of the potline and system. An investigation to obtain measurements of these values was made during the test. The method which was used gives a means of obtaining this information on a hot, operating line.

The method employed a resonant circuit set up as shown in Fig. 11 in which the

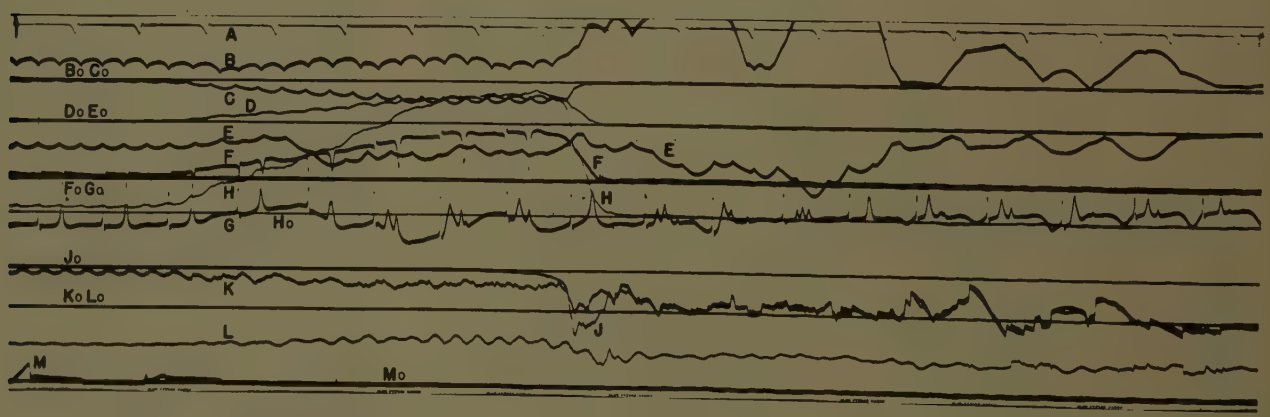

Fig. 10 Tie breaker and system conditions during loss of excitation and followed by loss of a-c power. See subcaption, Fig. 4, for trace identification, except M is holding anode voltage

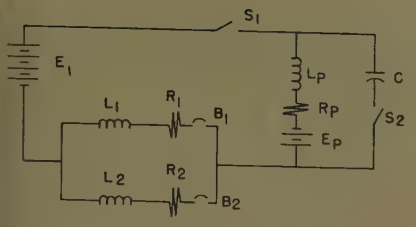

Fig. 11. Basic circuit representing system during impedance measurements

L_P = Potline inductance
L_1 = System inductance
L_2 = Closest rectifier inductance
R_P = Potline resistance
R_1 = System resistance
R_2 = Closest rectifier resistance
E_P = Potline counter electromotive force
E_3 = System voltage
C = Test capacitance

cathode-ray oscilloscope was used to make the measurement across the capacitor C through a voltage divider. In relation to the actual system, the breaker B_2 represents the single cathode breaker associated with the nearest rectifier, and B_1 represents all other cathode breakers. The switch S_1 represents all the negative disconnects of the system, and S_2 is the special closing switch to apply the capacitance across the hot, operating bus.

The switch S_2 was closed on different values of capacitance and a picture of the capacitor charging revealed an oscillatory voltage wave that resonated at a frequency equal to the resonant point of the circuit. A cathode-ray oscilloscope with Polaroid camera was used to record the voltage. A typical record is shown in Fig. 12 which is taken at the center of the d-c bus with the entire system connected. The capacitor value was 175 μf (microfarads). The following equations were used for the determination of inductance, capacitance, and frequency:

$$L = \frac{1}{C\left[\omega^2 + \left(\frac{\ln P_1 - \ln P_2}{\Delta t}\right)^2\right]}$$

$$R = 2\left(\frac{\ln P_1 - \ln P_2}{\Delta t}\right)L$$

$$f = \frac{1}{2(\Delta t)}$$

The values of capacitance were varied to see if the results checked at different resonant frequencies. The results are given in Table I. Tests were taken at the end of the bus and at the center of the bus with the adjacent rectifier either operating or disconnected. Tests were also taken with the rectifier system disconnected from the potline bus to give the inductance of the aluminum reduction potline (tests *96*, *97*, and *98* in Table I).

The tests were used to get the different values of inductance seen by the rectifier during arc back and short-circuit conditions. The results of this type of measurement can be used to confirm the calculated values and improve the analytical studies of these large systems. The value of the measured potline inductance will help to determine the rate of decay of the potline current and to apply circuit breakers and semiconductor rectifiers for potline service.

Potline Characteristics

The potline electrical characteristics were measured from some of the system and tie breaker tests. Fig. 4 is typical of some of the tests that were taken. The test was set up with potline *7* operating at 80,000-ampere load and receiving 10,000 amperes through the tie breaker from six rectifier units of potline *8*. The 13.8-kv power circuit breaker of potline *7* was tripped to initiate the test. The potline load transferred to potline *8* during the opening of the a-c breaker and made the major transition during approximately 0.005 second. In approximately 0.033 second (2 cycles) the tie breaker begins to open and completes the transfer back in an approximate total of 0.050 second to potline *7*. After the transfer, the current then decays to zero in approximately 0.130 second (8 cycles).

The stored energy of the potline when calculated from the measured inductances values and using the line current of 80,000 amperes will be as follows:

$$1/2LI^2 = 1/2(585\times10^{-6})(8\times10^4)^2$$

$$= 1.875\times10^6 \text{ joules}$$

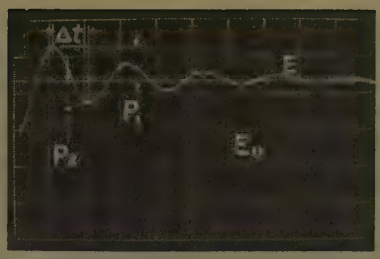

Fig. 12. Typical record of voltage transient measured during impedance measurements

After the tie breaker opened, the current in the pot line was 64,000 amperes, or an energy corresponding to 1.195×10^6 joules.

A major portion of the difference of 680,000 joules can be attributed to the normal decay rate. The transient effect of the breaker prevents a simple analysis of the decay rate but the amount handled by the breaker can be determined from Fig. 4. The breaker interrupter handled only 53,000 joules and represents rather light duty. The breaker duty is the stored energy of the equivalent d-c inductance of the source and these tests indicate that this is the part it must handle for this type of switching duty, which differs from the beliefs that have been associated with this kind of operation. Further, the duty is light by comparison to the field tests[2] reported on identical equipment where the breaker interrupter handled approximately 1,400,000 joules at the 220,000-ampere level.

Potline Current Decay

The decay time of the potline current can be found by writing the equation for the current at any time in the circuit represented by resistance, inductance, and

Table I. Test Results of Impedance Measurements of Aluminum Potline with Ignitron-Power Rectifiers

Test	Location and Switch or Breaker, Open in Test*	Test, Volts†	Test Capacitance, μf	Frequency of Oscillations, Cps	Measured Inductance, μhenrys‡	A-c Resistance, Ohms
96	7-1A (S1, B1, B2)	182	175	498	562	0.326
97	7-1A (S1, B1, B2)	178	100	670	565	0.339
98	7-1A (S1, B1, B2)	172	25	1,380	545	1.21
110	7-1A	822	175	2,240	28.6	0.121
111	7-1A	822	25	6,270	25.4	0.242
112	7-1A (B2)	826	25	5,880	33.9	0.303
113	7-1A (B2)	826	175	2,130	31.6	0.080
114	7-4A	822	175	2,370	25.4	0.077
115	7-4A	822	25	6,670	22.4	0.217
116	7-4A (B2)	818	25	6,540	23.4	0.245
117	7-4A (B2)	818	175	2,350	25.7	0.118
118	Tie Breaker (Near line 6)	825	175	2,270	27.4	0.076
119	Tie Breaker (Near line 6)	823	25	5,530	32.1	0.377

* See Fig. 11.
† D-c bus voltage.
‡ Includes approximately 5.5 μhenrys in test loop.

Fig. 13. Six-pole type AG-6 anode breaker with drawout equipment

back emf and then solving the equation for zero current. The current is of the form:

$$I_t = \epsilon^{\frac{-R_t}{L}} \left[I_o + \frac{E_o}{R} \right] - \frac{E_o}{R}$$

where

R = potline resistance
L = potline inductance
I_o = initial potline current
E_o = initial potline back emf
I_t = the current at any time

The oscillograms taken during the test showed the decay time varied from 0.142 second to 0.152 second (approximately 9.0 cycles). The decay time for the potline without any energy dissipating during breaker opening would be 0.152 second as shown in the film of Fig. 4. Using this decay time and the above equation, the potline resistance was calculated as 0.003 ohm.

Another approach to the potline resistance is obtained from:

$$R = \frac{E_{fl} - E_o}{I_{fl}} = \frac{823 - 200}{80{,}000} = 0.0078 \text{ ohm}$$

where

E_{fl} = full-load voltage
I_{fl} = full-load current

When using this value for R, the decay time of the potline current is 0.11 second (6.6 cycles). The difference in the resistance calculated from the decay times cannot be attributed to temperature difference or electrolyte concentration in the potlines over this short time. More information is needed before these differences are resolved. Certainly, the tests and measurements do demonstrate that the potline operating load resistance is in the order of 0.008 ohm and the decay of this line takes approximately 9.0 cycles.

Anode-Breaker Arc-Back Tests

A high-speed anode breaker, one which was a normal part of the rectifier installation, was used in this test program. It was constructed of six poles using a common base, Fig. 13, and equipped with drawout mounting. The drawout feature allowed an easy removal of the breaker to give rapid inspection of the parts being subjected to the repeated high duty.

This portion of the program was composed of two test sections. In the first section nearly all tests were made with full phasing and with interphase transformer saturation controlled to determine performance at maximum peak currents. The values in Table II for controlled interphase saturation show that the average peak currents and clearing time are a little higher than those obtained with random conditions under the same voltage. This does not represent the maximum number of variations that can occur from interphase saturation as indicated by reference 1. A typical film with unbalanced currents to give saturation is shown in Fig. 9.

Although it was attempted to induce sympathetic arc backs by forcing higher forward currents through one of the parallel rectifier tanks, the incidence of sympathetic arc backs was not increased in the tests. Therefore, it cannot be concluded that this would aid appreciably in any other test program. A number of sympathetic arc-back tests were recorded during the test program and indicated higher duty on the anode breaker in some cases as represented by the higher peak currents and longer clearing times.

A second section of tests was conducted, under conditions to simulate the operation experienced in potline start-up, in which high system voltage and phased back firing were used. This type of test had been planned to accomplish two purposes. First, the normal operation under arc backs was being checked for possible difference in performance, and second, the system was being checked for the existence of high surge voltage associated with this operating condition. The latter objective failed to be achieved due to limitations of instrumentation and testing time.

The level of phasing was established in the field tests by adjusting the excitation to reduce the current from the unit to 40%. Then the autotransformer was adjusted up to regain an approximate 5,000-ampere output. This was the equivalent of a 10% phase control.

In general, the performance was considered identical to those tests where the full phasing was used. In one instance, the duration of the current was longer during a sympathetic arc back but the time and magnitude of the peak current was unchanged from those of shorter duration. Therefore, the duty to the system was not considered greater than that of any other arc back.

Table II. Anode Breaker Arc-Back Performance Tests*

Testing Variation	No. of Tests	D-c Bus, Volts	Peak Arc-Back Current, Kiloamperes	Total Clearing Time, Milliseconds	Peak of Sympathetic Arc Back, Kiloamperes	Sympathetic Total Clearing Time, Milliseconds
System voltage	1	690	53.2	13.0		
	4	800	58.4–59.0	12.6–13.9		
	2	825	59.8–62.1	12.4–15.4		
	2	850	61.6–63.2	12.3–14.3		
	6	900	63.0–65.7	12.5–15.4		
Controlled interphase saturation	3	900	63.8–67.3	13.1–15.5		
Sympathetic arc backs	3	800	56.8–59.0	12.0–12.6	33.7†–66.0	10.5–21.8†
	2	850	60.9–63.2	11.3–11.6	61.2–61.3	10.4–12.0
Phase back of firing	1	825	63.0	13.9		
	2	900	63.0–66.5	12.9–14.0		
Phase back of firing and controlled interphase saturation	5	825	62.1–64.4	12.8–14.1		
Sympathetic arc back under phase back in firing	5	825	60.4–64.4	11.4–12.5	59.8–63.5	12.7–27.4

* Lister Hill, Ala., 1958.
† Arc back delayed approximately 90 degrees from commutation.

Analytical Study

An analytical study was made using the methods given in an earlier Institute paper.[3] Through a study of another system on which controlled tests were performed, the methods of calculation could be compared for agreement with varied system conditions. In this particular case, this system gave higher available currents and higher d-c bus voltages as well as variations in bus and equipment arrangement than was shown in the system study of an earlier report.[4]

With the potline operating at 900 volts, d-c arc-back tests were made on the end rectifier and the current peaks measured in the three phases of the transformer under test. With high-speed anode breakers in the system, the actual current values were dependent on the interrupter characteristic. Therefore the accuracy in duplicating the interrupter characteristic determined the degree by which the test and calculated values check. Applying a general interrupter characteristic for the breaker during the calculations, the following results were obtained:

Rectifier Phase	Peak Current, Amperes	
	Calculation	Tested
2	72,900	67,300
4	20,000	18,000
6	18,900	17,250

The difference between the calculated and test current in the arc back on phase is only 8%.

This difference is not considered excessive when following calculating procedures which determine bus inductance and resistance from system layouts and using a general interrupter characteristic for the anode breaker.

Conclusions

The extensive testing program conducted on the new Lister Hill mercury-arc rectifier system of the Reynolds Metals Company has provided additional information about the system and the breaker performance. These conclusions can be made:

1. The time constant of the potline tested at Lister Hill is 0.075 second, and the current decayed to substantially zero value in 0.15 second. The decay time is controlled by the resistance of both the potline and rectifier circuits but the major portion is associated with the potline cells.

2. Measurement of system and load inductances can be easily made with the capacitor test method applied in this program. Such measurements will greatly aid in the evaluation of system performance through application and analytical studies.

3. The resistance measurements that can be resolved from the capacitor tests are still lacking a satisfactory accuracy when trying to relate the high-frequency values to the d-c condition.

4. The tie-breaker application between the two mercury-arc rectifier systems is satisfactory for transmitting of power between lines within the rating of the breaker even though the a-c source for either load may be lost.

5. The duty imposed on the tie breaker in a large electrochemical rectifier system is generally small compared with one serving as a main on an equally large system. This results from the fact that the major portion of the energy continues to be absorbed in the potline cells and rectifiers even though the a-c line is disconnected.

6. The tie-breaker duty was exhibited in the tests as being equal to the stored energy of the source being disconnected from the potline by the tie breaker. Under the operating conditions of the system tested, this is only 3 to 4% of the potline stored energy when carrying full load.

7. The anode breaker during the test series performed a high-speed interrupting function with current limiting under maximum conditions which existed with the 900-volt system operation.

8. The comparison of test and calculated arc-back currents checked within 8% which is considered very satisfactory. This includes such considerations as the use of a general interrupter characteristic for the particular high-speed anode breaker tested.

References

1. Anode Breaker Testing with a High-Capacity Rectifier System, L. J. Harris, T. J. Scully, V. N. Stewart. *AIEE Transactions*, pt. II (*Applications and Industry*), vol. 78, Mar. 1959, pp. 43–48.

2. Field Testing D-C Air Circuit Breakers on a High-Capacity System, P. L. Hartsock, T. J. Scully, V. N. Stewart. *Ibid.*, vol. 77, 1958 (Jan. 1959 section), pp. 559–63.

3. A Mathematical Model and Procedure for Arc-Back Current Calculations for Power Rectifiers, H. P. Fullerton, J. Teno. *Ibid.*, Nov., pp. 456–64.

4. Comparison of Calculated and Measured Arc-Back Currents in Large Power Rectifier Systems, J. Teno, C. H. Titus, R. N. Wagner. *Ibid.* (Jan. 1959 section), pp. 585–89.

Discussion

V. Fraser (Aluminum Laboratories Ltd., Arvida, Que., Canada): The information obtained from the tests described in this paper will no doubt prove valuable in designing future installations.

A similar method of obtaining the values of L and R of a single cell was used some years ago. However, in this case, a capacitor was discharged across the cell, but it was found that the errors introduced by the inherent resistance of the capacitor and its connections gave far from accurate values of L. With a line of cells the accuracy would be greater because the difference between the resistance of the line and that of the capacitor and leads would be less.

The difference in resistance when calculated from the decay time is no doubt due to the use of a simple equivalent potline circuit containing only resistance, inductance, and a source. An equivalent circuit for a single cell suggested by W. E. Haupin of the Aluminum Company of America[1] contained in addition to this, two R-C circuits. Although the R-C circuits represent polarization voltages the values were not stated by Haupin, but measurements on production cells give the values shown in Fig. 14. These are approximate values and further measurements will have to be made. The R-C circuit with the long-time constant seems to be only a close approximation to the polarization since the rate of decay differs slightly from a true exponential curve. The voltages 0.25 and 0.28 exist at full-line current on cells ranging from 50,000 amperes to 100,000-ampere capacity.

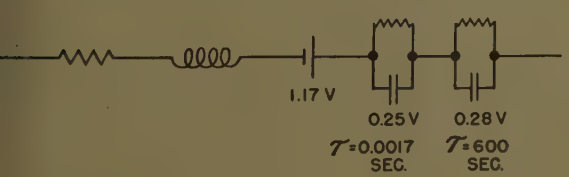

Fig. 14. Values for measurements on production cells

Reference

1. Polarization of an Aluminum Reduction Cell, W. E. Haupin. *Journal*, Electrochemical Society, Baltimore, Md., vol. 103, no. 3, Mar. 1956, p. 174.

R. P. Stratford: Mr. Fraser's discussion of the paper and additional information about aluminum pots is most welcome.

Using this additional information, the resistance calculation will change to: $(1.17+0.25+0.28)168=286$ volts.

$$R=\frac{823-286}{80{,}000}=0.00671 \text{ ohms}$$

Then the time constant is equal to:

$$T=L/R=\frac{0.00056}{0.00671}=0.0835 \text{ second}$$

If this is considered 63.2% of the time, the total time would be approximately 0.135 second or close to that observed in the tests.

This value of resistance checks other observed and calculated data.

Analysis of Load Transfer Oscillations in Parallel Aircraft A-C Electric Power Systems

H. A. KAHLE
ASSOCIATE MEMBER AIEE

THE PURPOSE of this paper is to investigate a method by which the performance of parallel aircraft a-c generator systems may be predicted, and to define boundaries for the characteristics of generator, regulator, constant-speed drive, and real and reactive load division circuit (LDC) which will guarantee satisfactory parallel operation. The method will be restricted to the analysis of load transfer oscillations in parallel generator systems. Its advantage is that only one generator system need be considered in order to investigate parallel operation and load transfer oscillations; this is because a parallel electric power system is symmetrical with respect to the voltage bus connecting the parallel generators.

Different problems arise in the operation of parallel a-c generator systems. Load sharing and loss of system capacity are determined by the sensitivity of the real and reactive LDC. The minimum value of reactive load division sensitivity is determined by steady-state gain requirements as defined by specifications for load sharing and loss of system capacity. To avoid sustained oscillations of circulating current,[1] the maximum permissible reactive load division sensitivity must be smaller than the synchronous reactance of the generators.

The problem of paralleling and synchronizing of generators has been analyzed and results of an analog computer simulation of two complete electric power systems are given in the literature.[2] The computer representation was very detailed but also complex, requiring large amounts of computer equipment. However, this study presented the fundamental background for today's knowledge of aircraft power system simulation and analysis.[2]

Load transfer oscillations are a major problem in parallel generator operation because small amounts of load transfer will be present in most parallel generator systems. Real and reactive LDC create additional multiple-feedback loops around the electric system and constant speed drive. Any loop can contribute to system instability, which results in load transfer oscillations. Therefore, each loop must have transfer functions of such a form as not to amplify these load transfer oscillations.

The problem of load transfer function differs from the other two problems mentioned, real or reactive LDC sensitivity and paralleling and synchronizing, inasmuch as the system exhibits sustained oscillations which do not fit into either one of the two categories, steady-state or transient. The investigation and analysis require therefore the simulation of all components of the system. However, since load transfer oscillations are symmetrical with respect to a properly chosen reference frame only one electric power system need to be simulated.

The Problem

Electrical and mechanical characteristics of the two generating systems are assumed to be identical. The generators are paralleled and are supplying a common, fixed load. Each machine supplies one half of the load. Terminal voltage V_t and load current i_L are therefore fixed. Fig. 1 shows a vector diagram of the two generators, neglecting for simplicity, armature resistance and saliency. When the rotors of the two generators are displaced by an angle δ_{12} with respect to each other, one being retarded, the other advanced, and terminal voltage and load remaining constant, machine 1 will deliver a current i_1 which is smaller than one half of the load current i_L and machine 2 will deliver a larger current i_2. The sum of both currents equals the load current

$$i_1+i_2=i_L \tag{1}$$

A current i_c will circulate among the paralleled generators. Its magnitude is given by[1]

$$i_c=1/2i_L-i_1=i_2-1/2i_L=(E_2-E_1)/2x_d \tag{2}$$

I_c is driven by the difference of the two internal electromotive forces (emf). This difference can be expressed in terms of the rotor displacement angle δ_{12}:

$$E_2-E_1=E_1\,2\sin\frac{\delta_{12}}{2} \tag{3}$$

The circulating current can then be expressed in terms of machine 1 quantities:

$$i_c=\frac{E_1}{2x_d}\,2\sin\frac{\delta_{12}}{2} \tag{4}$$

Equation 4 indicates that a circulating current i_c will exist as long as there is a rotor displacement δ_{12} between the two alternators. Rotor displacement is a sufficient but not necessary condition for circulating current. Equation 2 demonstrates that different excitation levels of both alternators will also result in circulating current. Under the conditions depicted in Fig. 1, the vector locus of circulating current is the line of symmetry between the two alternator rotors. Its relative position to the terminal voltage determines the magnitude of real and reactive load unbalance.

System conditions as described will persist if no corrective action is taken by the real and reactive LDC.

Effect of Reactive Load Division Circuit

The reactive LDC corrects the unbalance in reactive load by sensing the reactive component of circulating current. As a result of this corrective action, the excitation of one generator will be increased and that of the other will be decreased. Hence, assuming that the power to the two prime movers remain unchanged, the real component of each alternator current remains unchanged during the corrective action produced by the reactive LDC.

The system conditions are shown in the vector diagram of Fig. 2. The dashed-line vectors refer to the condition before the reactive LDC becomes effective; the solid lines and prime symbols refer to the condition thereafter. The action of the reactive LDC is to reduce the reactive component of circulating current to zero. (In practice, the reactive component will not be reduced to zero since the regulator uses proportional control, and the loop is therefore of type zero.) This reactive component will be called the imaginary component $Im(i_c)$, in agreement with mathematical notations and to avoid confusion between real and reactive

Paper 60-63, recommended by the AIEE Feedback Control Systems Committee and approved by the AIEE Technical Operations Department for presentation at the AIEE Winter General Meeting, New York, N.Y., January 31–February 5, 1960. Manuscript submitted September 29, 1959; made available for printing November 25, 1959.

H. A. KAHLE is with Jack & Heintz, Inc., Cleveland, Ohio

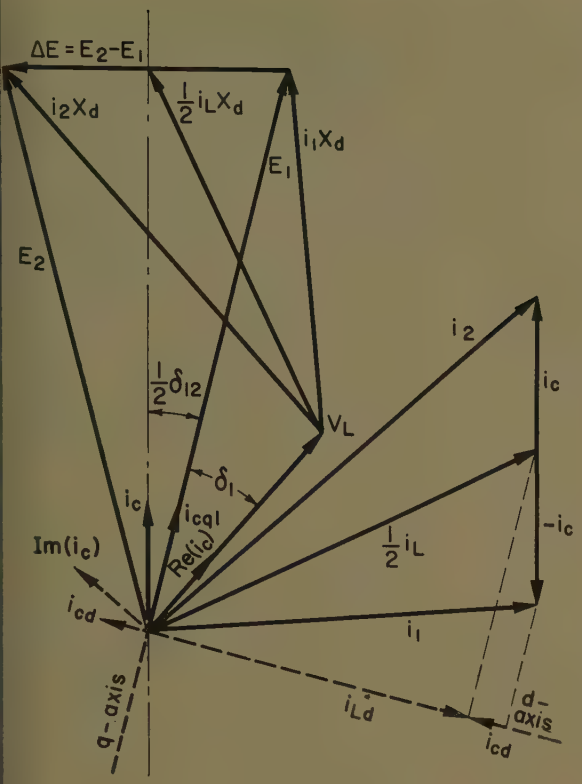

Fig. 1 (left). Vector diagram of two parallel generators

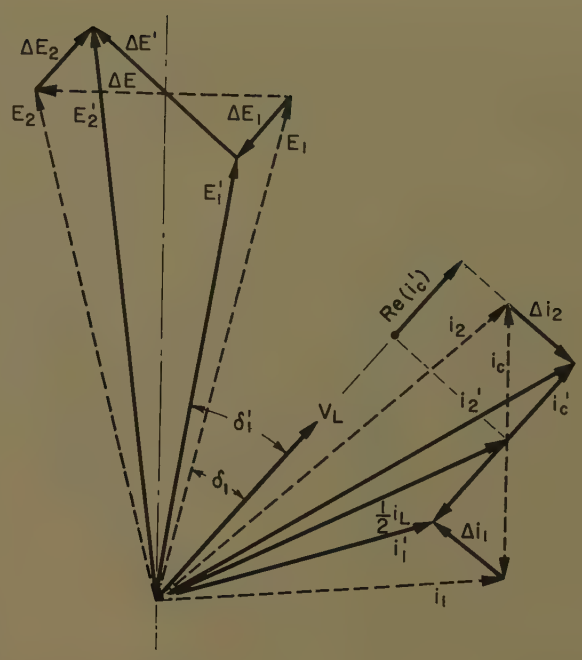

Fig. 2 (right). Vector diagram of two parallel generators, reactive load division circuit effective

components. The real component will be denoted as $Re(i_c)$.

The reactive LDC will provide a signal to the voltage regulators which will change the excitation of both alternators so that the circulating current will be in phase with the terminal voltage. The real power output of each alternator load current i_L and the terminal voltage V_L remain unchanged. It can easily be shown that the changes in excitation ΔE_1 and ΔE_2 are in phase with the terminal voltage, and that the input power to each alternator remained constant since, e.g., ϕ_1 decreased and δ_1 increased. The line A-A, connecting E_1' and E_2' is perpendicular to the terminal voltage V_L.

Effect of Real Load Division Circuit

The action of real LDC is shown in Fig. 3. Alternator 1 will be accelerated and alternator 2 decelerated until the circulating current is reactive. The voltage regulators will adjust the excitation so that $\Delta E = E_2' - E_1'$ is parallel to the terminal voltage. The reactive load delivered by each alternator is the same as it is without the real LDC. A rotor displacement δ_{12}' remains.

Figs. 2 and 3 show that the reactive or real LDC by themselves will not eliminate current circulating among the alternators. The combined action of real and reactive LDC is necessary to reduce circulating current to zero.

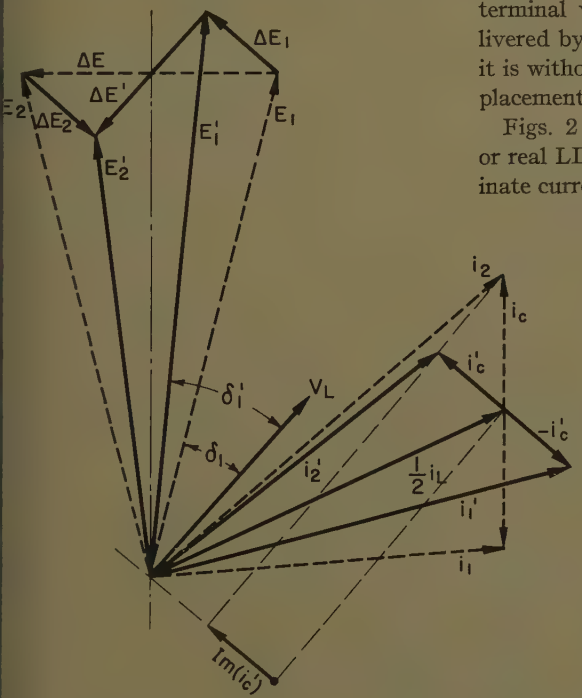

Fig. 3. Vector diagram of two parallel generators, real load division circuit effective

Analysis

A synchronous alternator connected to a power bus is capable of oscillations. The natural frequency of the oscillations is determined by electrical and mechanical characteristics of the alternator.[3] The oscillations between two alternators result in a periodic change of the rotor displacement angle δ_{12}. System analysis is possible by considering δ_{12} the independent variable, and expressing all quantities in terms of δ_{12}. System transfer functions can be defined in terms of the disturbance frequency u when we assume a sinusoidally varying angle

$$\delta_{12} = \delta_{12M} \sin ut \qquad (5)$$

Since a 2-generator system is symmetrical with respect to a line of symmetry, defined as the line dividing δ_{12} in half, performance calculations, simulation, and analysis of parallel generator systems can be reduced to the analysis of one system. This reduces considerably the complexity of the analysis and the simulation of a parallel generator system.

Analysis of the signal and power transfer properties of salient pole alternators requires decomposition of voltages and currents into direct- and quadrature-axis components.[3,4] Referred to machine 1, the d- and q-axis components of circulating currents are found from Fig. 1.

$$i_{cq1} = i_c \cos \frac{\delta_{12}}{2} = \frac{E_1}{2x_d} \sin \delta_{12}$$

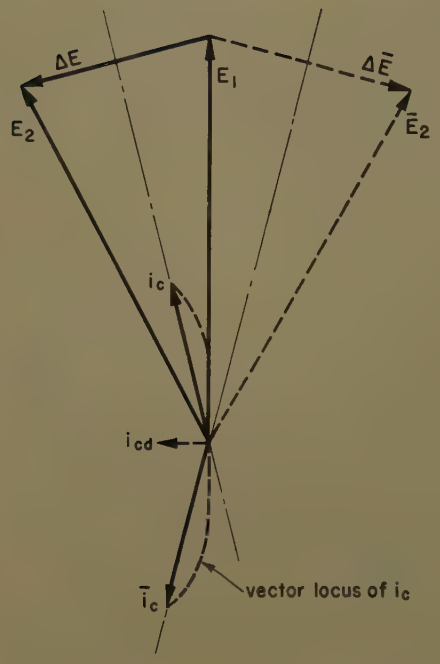

Fig. 4. Vector locus of current circulating among generators

$$i_{cd1}=i_c \sin\frac{\delta_{12}}{2}=\frac{E}{2x_d}(1-\cos\delta_{12}) \qquad (6)$$

The load current can be resolved into d- and q-axis components i_{Lq1} and i_{Ld1}, respectively. The current components in the generator are (Fig. 1)

$$i_{q1}=i_{Lq1}-i_{cq1}$$
$$i_{d1}=i_{Ld1}-i_{cd1} \qquad (7)$$

Real and reactive components of circulating current determine the corrective action of the real and reactive LDC. The real component of circulating current is

$$R_e(i_c)=i_{cq1}\cos\delta_1-i_{cd1}\sin\delta_1 \qquad (8)$$

and the reactive component is

$$I_m(i_c)=i_{cq1}\sin\delta_1+i_{cd1}\cos\delta_1 \qquad (9)$$

These components of currents shall now be expressed in terms of the independent variable δ_{12}, assuming sinusoidal oscillations according to equation 5. Inserting equation 5 into equation 6 yields

$$i_{cq1}=\frac{E}{2x_d}\sin(\delta_{12M}\sin ut) \qquad (10)$$

$$i_{cd1}=\frac{E}{x_d}\sin^2(1/2\delta_{12M}\sin ut) \qquad (11)$$

$$i_{cd1}=\frac{E}{2x_d}[1-\cos(\delta_{12M}\sin ut)] \qquad (12)$$

These equations lead to Bessel functions of the first kind; see the Appendix. One should also notice the presence of a second harmonic in equations 10 and 11 for the d- and q-axis component of circulating current. This second harmonic is more pronounced in i_{cd} than in i_{cq}. Second harmonics in load transfer oscillations have been observed in test.[5,6] They have usually been atrributed to saturation or other nonlinear machine characteristics but might, at least partially, be explained by this analysis. Equations 10 and 11 indicate also, that the magnitude of any second harmonic increases with increasing δ_{12M} in agreement with test results.[6]

The presence of a second harmonic in circulating current can also be shown by means of the vector diagram of Fig. 1. The circulating current of generator 1 will be observed. Thus, assuming the vector E_1 to be stationary and the vector E_2 oscillating about E_1 it is seen that the circulating current follows a vector locus as indicated in Fig. 4. Resolving this current into its direct axis component demonstrates that i_{cd1} always leads E_1 and never reverses polarity. The d-axis component of circulating current has twice the exciting frequency.

Block Diagram Representation

Synthesis of the foregoing equations with conventional system simulation techniques including dynamic system characteristics is shown in Fig. 5. This is a complete block diagram of one alternator system, simulating load transfer oscillations between two paralleled generators. The advantage of this analysis becomes apparent, since only one generator need to be simulated because of system symmetry in order to investigate load transfer oscillations among parallel generators. The alternator applies d- and q-axis voltages to the load.[4] The effect

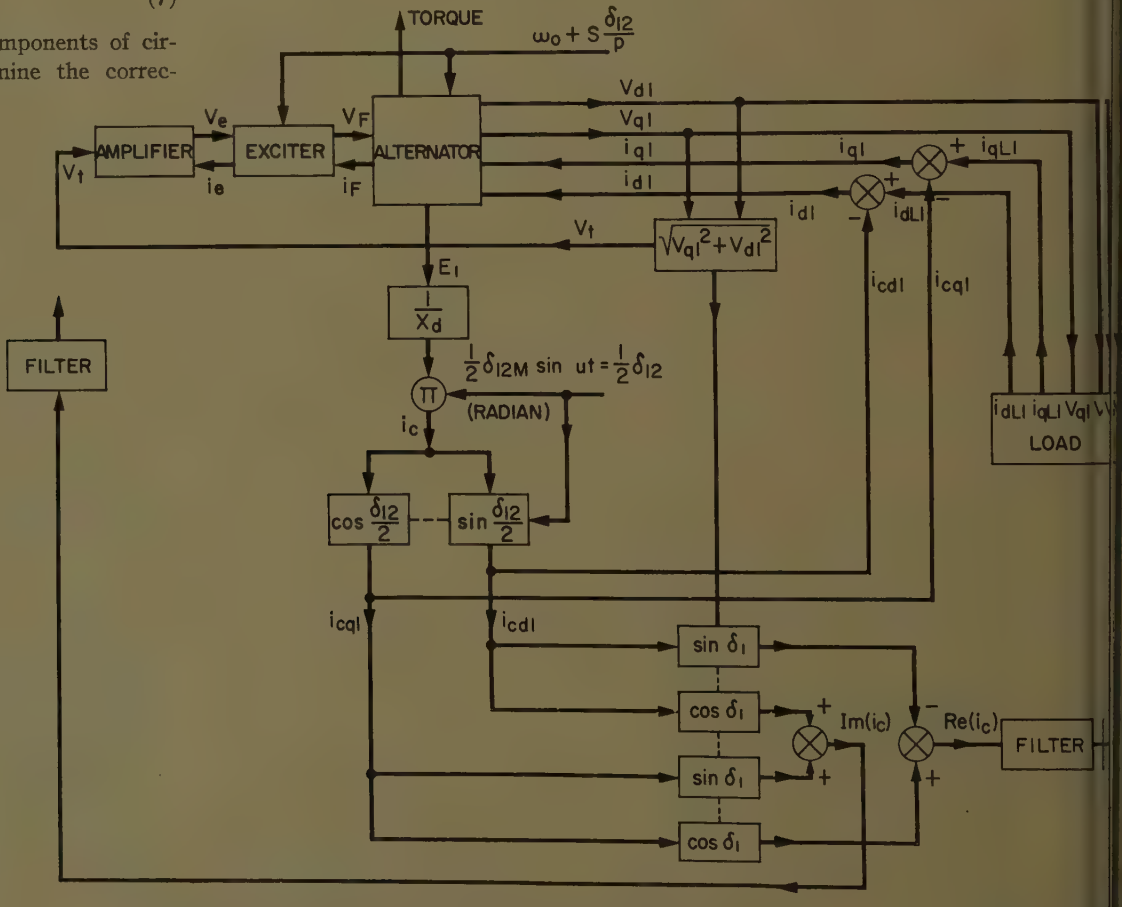

Fig. 5. Block diagram representation of a parallel generator system

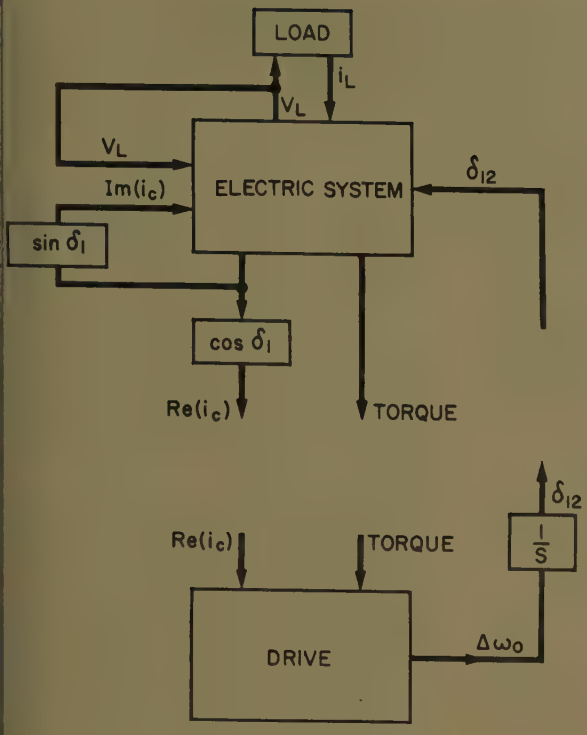

Fig. 6 (left). Block diagram representation of power system and drive in a parallel generator system

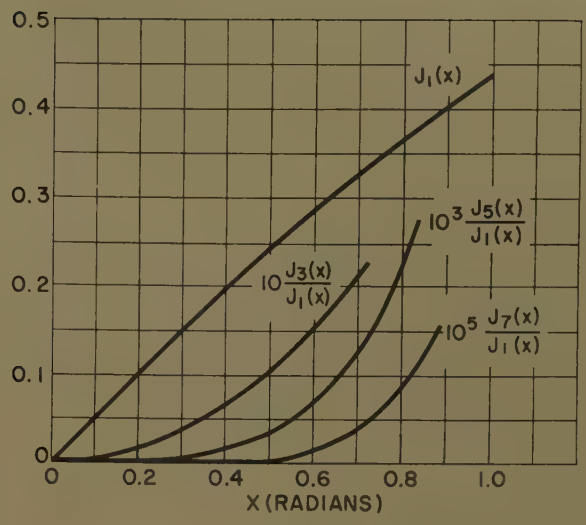

Fig. 7 (right). Magnitude fundamental and harmonic components in circulating current

of load on the alternator is indicated by load current components "fed back" to the alternator.

Circulating current is found according to equation 4 by dividing the internal alternator electromotive forces by x_d and multiplying it by the independent variable

$$\sin \frac{\delta_{12}}{2} \approx 1/2\delta_{12}$$

Since these angles are small, the error of using $1/2\ \delta_{12}$ instead of $\sin 1/2\ \delta_{12}$ will be negligible. Multiplication of the resulting circulating current by the cosine and sine of the same angle yields the d- and q-axis components of circulating current. Synthesis of these components according to equations 8 and 9 yields real and reactive components of circulating current. These provide signals to the corresponding real and reactive LDC for corrective action.

Periodic variations in δ_{12} will also cause modulation of the generator speed. Differentiation of δ_{12} with respect to time represents speed modulation, and when added to the base speed ω_0, gives the instantaneous speed of the generator as indicated on the block diagram of Fig. 5. (p equals the number of pole pairs). The air-gap torque T of the generator can also conveniently be obtained by the analog computer representation.[2,4]

System Simulation

Fig. 6 is a block diagram of one generator system. The interconnecting loops between generator and drive are broken. Each part of the system can therefore be investigated separately. This discussion deals with a properly defined open-loop system rather than a closed-loop system; thus, the complexity of analysis is reduced.

The electric system is considered with δ_{12} as independent disturbance. The resulting dependent variables are real and reactive component of circulating current and torque. These dependent variables of the electric system are then considered independent variables for the drive, and when applied to the drive will yield the dependent variable δ_{12}.

When the resulting dependent variable δ_{12}, obtained at the drive, equals the independent variable δ_{12} applied to the generator in magnitude and phase, no stability problem exists.

The system, simulated according to Fig. 5 and with a disturbance δ_{12} of given frequencies u applied, will yield several transfer functions determining operational characteristics of the parallel system. These transfer functions are: 1. reactive component, 2. real component, and 3. generator torque, as a function of disturbing frequency u.

Similar transfer functions can be obtained for the drive part of the electric power system. The form of these transfer functions indicates if the parallel generator system will exhibit sustained load transfer oscillations when the real and reactive LDC signals are connected to the corresponding regulators. Filters having proper transfer functions can be added into the real and reactive LDC loop to improve and to ensure stability.

Summary

The preceding analysis of load transfer oscillations among parallel generators leads to a relatively simple method for performance evaluation under certain symmetrical conditions. Though these conditions will not prevail throughout, they are nevertheless representative of most hunting problems. The method makes use of the inherent symmetry of parallel generator systems with respect to the voltage bus. It is therefore sufficient to simulate only one power system. This reduces considerably the complexity of the problem and the amount of simulation equipment required

The method is considered to be helpful to the engineer confronted with problems of sustained load transfer oscillations. In certain applictions, it will be desirable to include the constant speed drive into the simulation loop. This can be done with conventional techniques. Similar transfer functions can be defined in terms of drive speed or drive torque, thus giving access to more information for the system design engineer.

Appendix

Assuming sinusoidal variations in the rotor displacement angle δ_{12}, the circulating current is found from equations 4 and 5 as

$$i_c = \frac{E}{x_d} \sin (1/2\delta_{12M} \sin ut) \qquad (13)$$

This equation can be expressed in terms of the Bessel function $J_n(x)$ of the first kind of order n. The Bessel function determines the amplitude of the harmonics of circulating current. With the use of known formulas[7-10] equation 20 becomes

$$i_c=\frac{2E}{x_d}\,[J_1(1/2\delta_{12M})\sin ut+ J_3(1/2\delta_{12M})\sin 3ut+\dots] \quad (14)$$

or

$$i_c=\frac{2E}{x_d}J_1(1/2\delta_{12M})\times\left[\sin ut+\frac{J_3(1/2\delta_{12M})}{J_1(1/2\delta_{12M})}\sin 3ut+\dots\right]$$

Equation 14 indicates that i_c is not sinusoidal but contains higher harmonics of decreasing amplitude. Fig. 7 shows the relative amplitudes of the fundamental and the harmonics of circulating current. For small variations in δ_{12} the Bessel function of the first order can be approximated by a series.[10] Equation 14, when restricted to the fundamental, becomes

$$i_c=\frac{2E}{x_d}J_1(1/2\delta_{12M})1/2\sin ut$$

$$=\frac{E}{x_d}\,1/2\delta_{12M}\sin ut$$

in agreement with Fig. 5.

Expressions for d- and q-axis components of i_c can be found similarly from equations 10 and 12[7,8,9,10]. Eliminating intermediate results, the d-axis component is

$$i_{cd}=\frac{E}{2x_d}\,[1-J_0(\delta_{12M})]-\frac{E}{x_d}J_2(\delta_{12M})\times\left(\cos 2ut+\frac{J_4(\delta_{12M})}{J_2(\delta_{12M})}\cos 4ut+\dots\right) \quad (15)$$

and the q-axis component is

$$i_{cq}=\frac{E}{x_d}\,J_1(\delta_{12M})\times\left(\sin ut+\frac{J_3(\delta_{12M})}{J_1(\delta_{12M})}\sin 3ut+\dots\right) \quad (16)$$

The equations for i_{cq} and i_c are very similar except that the total angle δ_{12M} is used in one case and one half of the angle in the other case. Equation 22 for the d-component is different, inasmuch as a d-c component exists. This cannot persist for steady-state conditions and the power system will approach an equilibrium through the closed-loop control actions indicated in Fig. 5 so that there is no d-c component.

Nomenclature

E = electromotive force
i = current
$J(x)$ = Bessel function of first kind
p = number of pole pairs
s = Laplace operator
T = torque
u = frequency of disturbance
x_d = synchronous reactance
δ = rotor angle
δ_{12} = rotor diplacement angle between two generators in parallel
ϕ = power factor angle
ω_0 = base speed

Subscripts

1 = machine 1
2 = machine 2
c = circulating
d = direct-axis
L = load
q = quadrature-axis

References

1. Parallel Operation of Aircraft A-C Generators: Reactive Load Division and Selective Protection, **H. A. Kahle.** *AIEE Transactions*, pt. II (*Applications and Industry*), vol. 75, July 1956, pp. 175–81.

2. Analog Computer Representations of Aircraft Parallel Alternating Current Generating Systems, **L. V. Boffi, M. Riaz, P. E. Smith.** *WADC Technical Note 56-384*, Wright Air Development Center, Dayton, Ohio, Sept. 1956.

3. Electric Machinery, **M. Lischwitz, et.al.** D. Van Nostrand Company, Inc., Princeton, N. J., vol. II, 1946.

4. Analog Computer Representations of Synchronous Generators in Voltage-Regulation Studies, **M. Riaz.** *AIEE Transactions*, pt. III (*Power Apparatus and Systems*), vol. 75, Dec. 1956, pp. 1178–84.

5. Frequency Modulation and Load-Division Instability in 400-Cycle Aircraft Electric Systems, **Henry Oman.** *Ibid.*, pt. II (*Applications and Industry*), vol. 75, July 1956, pp. 181–88.

6. Discussion by **H. M. McConnell** of reference 5, pp. 185–86.

7. Ordinary Differential Equations (book), **E. L. Ince.** Dover Publications, Inc., New York, N. Y., 1944.

8. High Frequency Alternating Current (book), **K. McIlwain, J. A. Brainard.** John Wiley & Sons, Inc., New York, N.Y., 1939.

9. Bessel Functions for Engineers (book), **N. W., McLachlan.** Oxford University Press, London, England, 1934.

10. Abhandlungen der Akademie fuer Wissenschaften (book), **Bessel.** Berlin, Germany, 1824, p. 34.

Mechanical Rectifier Definitions

AIEE COMMITTEE REPORT

WORK ON mechanical rectifier standards was initiated by the Mechanical Rectifier Subcommittee in 1955. Because of the comparative newness and very rapid development of the mechanical rectifier, the work was slow and difficult. The first stumbling block, as in all standardization work, was encountered in the matter of definitions, since no uniform terminology had developed. The entire effort of the subcommittee was therefore concentrated on definitions.

Before the work on definitions was completed, it became obvious that production of mechanical rectifiers would soon come to an end because of the even more rapid development of semiconductor rectifiers with their economic and other advantages. The committee felt, however, that the work already in progress should be carried through, at least to the point of publishing a set of definitions and possibly a partial bibliography, which is appended to the definitions.

It is the opinion of the subcommittee that the present installed capacity of mechanical rectifiers, the existence of considerable literature, the possible rebirth of this rectifier at some future time, and the possible application in other fields of the many useful circuits and devices developed for the mechanical rectifier, all make it important to record and preserve the work already accomplished. Knowledge of mechanical rectifiers and their circuits is very poorly distributed. We have attempted to make the definitions educational in the areas peculiar to mechanical rectifiers, so as to serve as a starting point for any future investigations. As a consequence, some of these definitions tend to be wordy and sometimes clumsy.

Paper 60-35, recommended by the AIEE Industrial Power Rectifiers Committee and approved by the AIEE Technical Operations Department for presentation at the AIEE Winter General Meeting, New York, N. Y., January 31–February 5, 1960. Manuscript submitted October 29, 1959; made available for printing December 4, 1959.

The personnel of the AIEE Mechanical Rectifiers Subcommittee of the Industrial Power Rectifiers Committee are: I. K. Dortort, *chairman;* John Chaumlak, D. C. Hoffmann, D. W. Human, Otto Jensen, N. A. Koss, Kenneth McCaskill, and J. C. Trackman.

Standards for Mechanical Rectifiers

Section I. Definitions

1.000 Scope

Definitions given herein apply particularly to the type of mechanical rectifier in which groups of contacts are sequentially driven by a synchronous motor. The so-called magnetic rectifier in which contacts are individually operated by electromagnets without any mechanical linkages between contacts is not specifically covered in these definitions. Many of the terms, however, are applicable to both types.

Only the rectifier part of the rectifier unit is covered. For the most part

hese definitions have been made consistnt with the American Standard for pool athode mercury-arc power converters.[1]

Most of the symbols and circuits of *C-34* re applicable as they relate to general ectifier circuitry. Symbols for the exitation circuits and properties of mehanical rectifiers are so far from being tandardized that it was not considered easible to include them at this time.

.100 Equipment Terms

.101 *Mechanical Rectifier*

A mechanical rectifier is an operable ssembly of rectifier contacts and a recti-ier mechanism which drives the contacts n synchronism with the primary fre-uency, so that each contact completes a onductive circuit between an a-c and a l-c terminal during selected portions of ach cycle. It includes all auxiliaries nd control devices integrally housed or nounted between the a-c terminals of the ectifier and the d-c switchgear.

.102 *Mechanical Rectifier Unit*

A mechanical rectifier unit is an operative ssembly consisting of the mechanical ectifier(s), auxiliaries, commutating re-actors, the rectifier transformer, and ssential switchgear.

.103 *Section of a Mechanical Rectifier Unit*

A section of a mechanical rectifier unit is a part of a mechanical rectifier unit with ts auxiliaries which may be operated ndependently of other sections of the nit.

.104 *Contact Power Converter*

A contact power converter is an equip-ment which employs rectifier contacts for *ransforming* electric power.

.105 *Contact Power Rectifier*

A power rectifier is a rectifier unit in which the direction of average power flow s from the a-c circuit to the d-c circuit.

.106 *Contact Power Inverter*

A power inverter is a rectifier unit in which the direction of average power flow is from the d-c circuit to the a-c circuit.

.107 *Contact Frequency Changer*

A contact frequency changer is a contact power converter for changing the fre-quency of electric power.

1.200 Rectifier Parts and Auxiliaries

1.201 *Rectifier Contact*

A rectifier contact is a synchronously operated switch consisting of fixed and movable contacts, structural parts, insulating, and spring members, which opens and closes a main power circuit between an a-c terminal and a d-c terminal at selected intervals of each cycle to perform the functions of rectification or inversion. A rectifier contact may or may not be an integral assembly.

1.202 *Rectifier Mechanism*

A rectifier mechanism is the mechanical apparatus which actuates the rectifier contacts in synchronism and proper phase relationship with the alternating voltage and each other.

1.203 *Push Rod*

A push rod is the direct actuating member which opens and closes the contacts in rectifier mechanisms employing lineal motion.

1.204 *Commutating Reactor*

A commutating reactor is a saturable reactor connected in series with one or more rectifier contacts to provide a break and/or make step. The instantaneous magnetizing current must be small and substantially constant over a wide range of magnetization and speed of magnetization. It is generally equipped with control and bias windings.

1.205 *Contact Protector*

A contact protector is a high-speed switch used to bypass fault currents around the contacts of a mechanical rectifier.

1.206 *Overlap Regulator*

The overlap regulator is an assembly of components designed to maintain the break in its proper position in the break step by control of the mechanical overlap. It operates through the overlap adjusting means and/or the motor angle adjusting means.

1.207 *Contact Time Meter*

The contact time meter is an instrument and its circuitry designed to measure the dwell time, generally when the rectifier is not in service.

1.208 *Overlap Meter*

The overlap meter is an instrument and its circuitry designed to measure the angle of mechanical overlap, generally while the rectifier is in service.

1.209 *Break Margin Meter*

The break margin meter is an instrument and its circuitry designed to measure the overload margin or the load-dropping margin or to indicate position of the break within the break step.

1.210 *Temperature Regulating Equipment*

The temperature regulating equipment of a rectifier is any equipment used for cooling the rectifier, together with the devices for controlling and indicating its temperature.

1.211 *Cooling System*

The cooling system of a rectifier is the equipment, i.e., parts and their interconnections, used for cooling a rectifier. It includes all or some of the following: rectifier water jackets or tubes, water-cooled busses, cooling fins, heat exchangers, blowers, pump, expansion tank, piping, insulating tubing, etc.

1.212 *Natural-Air Cooling System (of a Rectifier)*

A natural-air cooling system is an air-cooling system in which heat is removed from the cooling surfaces of the rectifier only by the natural convection of the ambient air.

1.213 *Forced-Air Cooling System (of a Rectifier)*

A forced-air cooling system is an air-cooling system in which heat is removed from the cooling surface of the rectifier by means of a flow of air produced by a fan or blower.

1.214 *Direct Raw-Water Cooling System*

A direct raw-water cooling system of a rectifier is a cooling system in which water, received from a constantly available supply such as a well or water system, is passed directly over the cooling surfaces of the rectifier and discharged.

1.215 *Direct Raw-Water Recirculation Cooling System*

A direct raw-water cooling system with recirculation is a direct raw-water cooling system in which part of the water passing over the cooling surfaces of the rectifier is recirculated and raw water is added as needed to maintain the required temperature, the excess being discharged.

1.216 *Heat-Exchanger Cooling System*

A heat-exchanger cooling system of a rectifier is a cooling system in which the coolant, after passing over the cooling surfaces of the rectifier, is cooled in a heat exchanger and recirculated.

1.300 Rectifier Circuits

1.301 *Single-Way Rectifier*

A single-way rectifier is a rectifier in which the current between each terminal of the alternating voltage circuit and the rectifier contact (or contacts) conductively

connected to it flows only in one direction.

1.302 *Double-Way Rectifier*

A double-way rectifier is a rectifier in which the current between each terminal of the alternating voltage circuit and the rectifier contacts conductively connected to it flows in both directions.

Note: The terms single-way and double-way provide a means for describing the effect of the rectifier circuit on current flow in transformer windings connected to rectifiers. Most rectifier circuits may be classified into these two general types.

1.303 *Commutation*

Commutation in a contact power converter is the transfer of current between contacts which conduct in succession.

1.304 *Commutating Group*

A commutating group of a contact power converter is a group of contacts and the alternating voltage supply elements conductively connected to them in which the direct current of the group is commutated between individual contacts which conduct in succession.

1.305 *Set of Commutating Groups*

A set of commutating groups of a contact power converter consists of two or more commutating groups which have simultaneous commutation.

1.306 *Simple Rectifier*

A simple rectifier is a rectifier consisting of one commutating group if single-way, or two if double-way.

1.307 *Multiple Rectifier*

A multiple rectifier is a rectifier in which two or more similar simple rectifiers are connected in such a way that their direct currents add, but their commutations do not coincide.

1.308 *Cascade Rectifier*

A cascade rectifier is a rectifier in which two or more simple rectifiers are connected in such a way that their d-c voltages add but their commutations do not coincide.

Note: When two or more rectifiers operate so that their commutations coincide, they are said to be in parallel if the direct currents add, and in series if the d-c voltages add.

1.309 *Number of Rectifier Phases*

The number of rectifier phases in a rectifier circuit is equal to the total number of successive, nonsimultaneous commutations occurring within the rectifier circuit during each cycle when operating without phase control. It is also equal to the order of the principal harmonic in the d-c voltage waveshape.

Note: The number of rectifier phases influences both a-c and d-c circuit waveform. In a simple single-way rectifier the number of rectifier phases is equal to the number of rectifier contacts.

1.400 Excitation and Control Circuits and Functions

1.401 *Excitation Circuits*

Excitation circuits are low-power auxiliary and control circuits and components designed to provide the proper conditions at the instants of contact make and break to avoid excessive material transfer and contact erosion. Included in this general term are excitation bias circuits, straightener circuits, flux-resetting circuits, and contact bypass circuits and components.

1.402 *Excitation Bias Circuit*

The excitation bias circuit is a circuit which provides the required ampere-turns to the commutating reactor during the break and/or make steps to adjust the value of the current in the main winding to the desired level during the step. As in the normal usage of the term "bias," its value is held essentially constant, but may be varied manually or automatically to meet varying conditions.

Note: Since, for the specified purpose, the value of bias is of interest only during the step, direct, alternating, or pulse currents may be used. Other functions are often assigned to the same auxiliary windings and to the same circuits.

1.403 *Straightener Circuit*

A straightner circuit is the circuit and circuit elements used to correct for the variation of the magnetizing current of a commutating reactor during the break step.

1.404 *Contact Bypass Circuit*

A bypass circuit is a circuit connected to one or more rectifier contacts to provide a low-impedance path for the small residual current broken at the contact, together with the components required to prevent the flow of excessive current in the bypass circuit when the full inverse voltage or commutating voltage appears across the contact. It is essentially a spark-suppressor circuit, but sometimes performs other functions as well.

1.405 *Excitation Bypass Circuit*

An excitation bypass circuit is one which bypasses around the rectifier contact all or most of the excitation current required by the commutating reactor during the break step so that the contact opens at essentially zero voltage and current. It also acts as a spark-suppressor by providing a low-impedance path for any residual current flowing through the contact at the instant of break.

1.406 *Flux-Reset Circuits*

The flux-reset circuit impresses across the commutating reactors a voltage of proper magnitude, duration, and phasing to effect a predetermined change in its flux density after completion of the break step and before contact make.

Note: The balance of flux not reset by the flux-reset circuit prior to contact make is reset by the commutating voltage during the make step and determines the amount of magnetic phase control.

1.407 *Phase Control*

Phase control is the process of varying the point within the cycle at which conduction of power current through a rectifier contact is permitted to begin. By reducing the a-c voltage integrated into the average d-c voltage, the phase control regulates the d-c voltage of the rectifier.

The amount of phase control may be expressed in two ways: 1. the reduction in d-c voltage obtained by phase control, or 2. the total angle of phase retard (or advance).

1.408 *Mechanical-Phase Control*

Mechanical-phase control is the process of varying the mechanical-make point so as to control the point within the cycle at which conduction of power current through a rectifier contact is permitted to begin.

1.409 *Magnetic-Phase Control*

Magnetic-phase control is the process of varying by magnetic means the point within the cycle at which conduction of power current through a rectifier contact is permitted to begin after make.

1.410 *Ballast Load*

The ballast load is a small internally connected load sometimes required to preset the commutating reactor flux for the break step during periods of very light load.

1.500 Functional Terms

1.501 *Phase Transition*

Phase transition is the instant at which the commutating voltage between two commutating phases increases through

zero in the direction to effect commutation.

1.502 *Make*

Make is the point within the cycle at which the rectifier contacts close, measured from the phase transition.

1.503 *Break*

Break is the point within the cycle at which the rectifier contacts open, measured from the phase transition. (Commutating voltage decreasing in the sense to decrease power current in the opening contact.)

1.504 *Dwell Time*

Dwell time is the electrical angle in each cycle during which the rectifier contact is closed. It is equal to 360 degrees divided by the number of phases in the commutating group plus the mechanical overlap angle.

1.505 *Mechanical Overlap*

Mechanical overlap is the electrical angle during which the contacts of similar polarity of two commutating phases are simultaneously closed. It is equal to the dwell time less 360 degrees divided by the number of phases in the commutating group.

1.506 *Premake Step*

The premake step is the period just prior to the closing of the contact during which the flux of the commutating reactor is caused to change in a manner to reduce the voltage across the contact at the instant of closing.

1.507 *Make Step*

The make step is the period immediately following the closing of the contact during which the current through the contact is limited by the properties of the commutating reactor and associated circuits.

1.508 *Break Step*

The break step is the interval at the end of the conduction period during which the flux of the commutating reactor is reversed from saturation in the forward direction to a predetermined value in the reverse direction. The current in the contact is limited to a very low value by the properties of the commutating reactor and associated circuits. The contact is generally opened near the middle of this low-current interval.

1.509 *Rated-Step Length*

The rated-step length of a break and/or make commutating reactor is the time required at rated peak commutating voltage to swing the core through the full useful range of flux density (during which time the magnetizing current is essentially constant).

1.510 *Volt-Second Rating*

The volt-second rating of a commutating reactor is the product of the rated peak commutating voltage and the rated step length. The integrated product of voltage and time is a constant of the reactor design and is independent of the applied voltage.

Note:

$$\int_{t_1}^{t_2} e\,dt = A(B_2 - B_1)N \times 10^{-8}$$

where A is the iron cross section, B_1 and B_2 are the limits of useful flux density, and N the number of turns.

1.511 *Speed of Magnetization*

The speed of magnetization is the time rate of change of the flux density of a ferromagnetic core, specifically applied for the purpose of these standards, to the core of a commutating reactor. (It is equal at any instant to the voltage per-turn per-unit area times 10^8.)

1.512 *Step Current*

The step current of a commutating reactor is the uncorrected magnetizing current of the commutating reactor during the make-or-break step.

Note: It varies with speed of magnetization.

1.513 *Residual-Break Current*

The residual-break current is the modified contact current flowing in the contact immediately prior to the break.

1.514 *Make Margin*

The make margin is the time interval (expressed in electrical degrees) between the contact make and the end of the useful make step. If no premake step is used, the make margin is the minimum make step that can occur without changing fixed-circuit constants.

1.515 *Overload Margin*

Overload margin is the time interval between the beginning of the useful break step and the contact break. It is also a measure of a-c undervoltage margin.

1.516 *Load-Dropping Margin*

Load-dropping margin is the time interval between the contact break and the end of the useful break step. It is also a measure of the a-c overvoltage margin.

1.517 *Make Voltage*

The make voltage is the voltage across the contact immediately before the make.

1.518 *Make Current*

Make current is the current flowing through the contact immediately after the make and before the contact is firmly seated.

1.519 *Break Voltage*

The break voltage is the voltage across the contact immediately after the break.

1.520 *Break-Voltage Increase*

The break-voltage increase is the increase of the voltage across the opening contact from the break voltage to the end of the break step, and before the rapid increase to the inverse voltage.

1.521 *Recovery-Voltage Gap*

The recovery-voltage gap is the opening between the contact members at the end of the break step.

1.522 *Switching Speed*

The switching speed of a contact is the velocity of the moving contact just prior to make and immediately after break. These speeds are equal if the contact motion is essentially harmonic.

1.523 *Motor Angle*

The motor angle is the angle by which the motor rotor is shifted from the phase position in which the midpoint of the contact dwell time would coincide exactly with a point halfway between two successive phase transitions. It is equal to one-half the mechanical overlap angle if the contact motion is essentially harmonic.

1.524 *Mechanical Angle of Delay*

The mechanical angle of delay is the electrical angle by which the make point lags the phase transition.

1.525 *Magnetic Angle of Delay*

The magnetic angle of delay is the length of the make step in electrical degrees and is the angle by which the release of power-current flow lags the contact make.

1.526 *Total Angle of Delay*

The total angle of delay is the electrical angle by which the release of power-current flow is caused to lag the phase transition by the action of both mechanical and magnetic delay.

1.527 *Angle of Advance*

The angle of advance of a contact-power converter is the angle by which the beginning of power-current conduction leads the phase transition preceding the prin-

cipal power-conduction period of the incoming contact.

1.528 *Commutating Reactance*

Commutating reactance is the sum of all linear reactances between the d-c connection of the rectifier contact and the real or virtual neutral of the commutating group, including all reflected linear reactances.

Note: For convenience, the reactance from contact to neutral including the reflected a-c system reactance, or one half of the total linear reactance in the commutating circuit, is the value usually employed in computations and is the value designated as the commutating reactance.

1.529 *Air-Core Reactance*

The air-core reactance of a commutating reactor is considered to be the reactance of the series winding at primary frequency after the core is fully saturated. It is the value of the reactance of the winding with all core material removed.

1.530 *Reactor Saturation Drop*

The reactor saturation drop is the equivalent d-c voltage drop, caused by any additional flux change in ferromagnetic materials between the end of the useful make step and full saturation of the ferromagnetic materials involved.

1.531 *Power-Overlap Angle*

The power-overlap angle is the angle during which the power current is commutated between two rectifier contacts.

Note: In symmetrical circuits the instantaneous d-c output voltage of the commutating group during this interval is the instantaneous average of the phase voltages of the two commutating phases.

1.532 *Total Commutation Time*

Total commutation time is the time from the beginning of the premake step through the make step of the closing contact, the power overlap angle, and to the end of the break step of the opening contact.

Note: The phase-to-phase voltage of the two commutating contacts is essentially zero throughout the total commutation time.

1.533 *Mode of Operation*

The mode of operation of a rectifier circuit is the characteristic pattern of operation determined by the sequence and duration of commutation and conduction.

Note: Most rectifier circuits have several modes of operation which may be identified by the shape of the contact-current waves. The particular mode obtained at a given load depends upon the circuit constants.

1.534 *Transition Load*

A transition load is the load at which a rectifier changes from one mode of operation to another.

Note: A transition load of a rectifier shall be the load current corresponding to the intersection of extensions of successive portions of the d-c regulation curve at points where the curve changes shape or slope.

1.535 *Light Load, Transition*

The light transition load is the transition load which occurs at light load, usually at less than 5% of rated load.

Note: Light transition load is important where multiple rectifiers are used.

1.536 *Conducting Period*

The conducting period of a rectifier contact is that part of an alternating-voltage cycle during which power current flows through the contact.

1.537 *Inverse Period*

An inverse period of a rectifier contact is that part of an alternating-voltage cycle during which the flow of reverse power current is blocked by the open contact only.

Note: The make and break steps are excluded.

1.538 *Forward Nonconduction Period*

The forward nonconducting period of a rectifier contact is that part of an alternating-voltage cycle during which the flow of normal power current is blocked by the open contact only.

Note: The make step is excluded.

1.539 *Crest Working Voltage*

The crest working voltage is the maximum instantaneous voltage which occurs between given terminals in normal operation.

1.540 *Peak Inverse Voltage*

The peak inverse voltage of a rectifier contact is the maximum instantaneous voltage across the open contact during the inverse period.

1.541 *Peak Forward Voltage*

The peak forward voltage of a rectifier contact is the maximum instantaneous voltage across the open contact during the forward nonconducting period.

1.542 *Initial Inverse Voltage*

The initial inverse voltage of a rectifier contact is the crest value of the voltage which occurs across the open contact immediately after the end of the break step.

1.600 RATING

1.601 *Rating of a Rectifier Unit*

The rating of a rectifier unit is the kw-power output, voltages, currents, number of phases, frequency, amount of control angle, etc., assigned to it by the manufacturer.

1.602 *Continuous Rating of a Rectifier Unit*

The continuous rating of a rectifier unit is the rating that defines the maximum load which can be carried for an indefinitely long time.

1.603 *Short-Time Rating of a Rectifier Unit*

The short-time rating of a rectifier unit is a rating that defines the maximum load which can be carried for a short and definitely specified time.

Note: The short-time rating includes loads of 2 hours duration.

1.604 *Rated Load of a Rectifier Unit*

The rated load of a rectifier unit is the kw-power output which can be delivered continuously at the rated output voltage. It may also be designated as the 100% load or full-load rating of the unit.

Note: Where the rating of a rectifier unit does not designate a continuous load it is considered special.

1.605 *Rated Output Voltage of a Rectifier Unit*

The rated output voltage of a rectifier unit is the voltage specified as the basis of rating.

1.606 *Rated Output Current of a Rectifier Unit*

The rated output current of a rectifier unit is the current derived from the rated load and the rated output voltage.

1.607 *Basic A-C Voltage*

The basic a-c voltage of a power rectifier unit is the sustained sinusoidal voltage which must be impressed on the terminals of the a-c winding of the rectifier transformer, when set on the rated voltage tap, to give rated output voltage at rated load with designed minimum mechanical and magnetic angles of delay.

1.608 *Rated A-C Voltage*

The rated a-c voltage of a rectifier unit is the rms voltage between the a-c line

terminals which is specified as the basis for rating.

Note: When the a-c winding of the rectifier transformer is provided with taps, the rated voltage shall refer to a specified tap which is designated as the rated-voltage tap.

1.609 *Ceiling D-C Voltage*

The ceiling d-c voltage of a power rectifier unit is the average d-c voltage at rated output current with rated sinusoidal voltage applied to the terminals of the a-c winding of the rectifier transformer, when set on the rated-voltage tap, with designed minimum mechanical and magnetic angles of delay.

1.700 Rectifier Characteristics

1.701 *Power Factor*

The power factor of a rectifier is the ratio of the total active power, in watts, to the total apparent power, in rms volt-amperes, determined at the a-c line terminals of the rectifier unit.

Note: This definition includes the effect of harmonic components of current and voltage, the effect of phase displacement between the current and voltage, and the exciting current of the transformer.

1.702 *Displacement Power Factor*

The displacement power factor of a rectifier unit is the displacement component of power factor and is the ratio of the active power of the fundamental wave, in watts, to the apparent power of the fundamental wave, in rms volt-amperes (including the exciting current of the rectifier transformer).

1.703 *Voltage Regulation*

The voltage regulation of a rectifier unit is the change in output voltage, expressed in volts, which occurs when the load current is reduced from its rated value to the ballast or minimum load at which the rectifier is capable of operating, with constant sinusoidal voltage applied to the a-c line terminals.

1.704 *Inherent Voltage Regulation*

The inherent voltage regulation of a rectifier unit is the change in output voltage, expressed in volts, which occurs when the load current is reduced from its rated value to the ballast or minimum load at which the rectifier is capable of operating, with rated sinusoidal voltage applied to the a-c line terminals, excluding the effect of a-c system impedance, with the rectifier transformer on the rated tap, designed minimum mechanical and magnetic angles of delay.

1.705 *Total Voltage Regulation*

The total voltage regulation of a rectifier unit is the change in output voltage, expressed in volts, which occurs when the load current is reduced from its rated value to the ballast or minimum load at which the rectifier is capable of operating, with rated sinusoidal a-c voltage applied to the a-c line terminals, but including the effect of the specified a-c system impedance as if it were inserted between the line terminals and the transformer, with the rectifier transformer on the rated tap and with designed minimum mechanical and magnetic angles of delay.

1.706 *Efficiency*

The efficiency of a rectifier unit is the ratio of the power output to the total power input. It may also be expressed as the ratio of the power output to the sum of the output and the losses.

1.707 *Ripple Voltage or Current*

A ripple voltage or current is the alternating component whose instantaneous values are the difference between the average and instantaneous values of a pulsating unidirectional voltage or current.

1.708 *RMS Ripple*

The rms ripple is the effective value of the instantaneous difference between the average and instantaneous values of a pulsating unidirectional wave integrated over a complete cycle.

Note: The rms ripple is expressed in per cent or per unit referred to the average value of the wave.

1.709 *Ripple Amplitude*

The ripple amplitude is the maximum value of the instantaneous difference between the average and instantaneous values of a pulsating unidirectional wave.

Note: The amplitude is a useful measure of ripple magnitude when a single harmonic is dominant. Ripple amplitude is expressed in per cent or per unit referred to the average value of the wave.

1.800 Operating Faults

1.801 *Contact Erosion*

Contact erosion is the roughening of the surface and loss of contact material during normal operation. It is more or less uniformly distributed over most of the contact area and is generally caused by contact "make" phenomena. It may also be caused by mechanical impact.

1.802 *Material Transfer*

Material transfer is the transfer of contact material between movable and stationary contacts during normal operation. It is usually highly concentrated, producing matched hills and valleys in the mating contact surfaces. Material transfer is associated with "break" phenomena. Extreme cases may occur due to separation of contacts before the start of the break step.

1.803 *Backfire*

Backfire is the failure of a mechanical rectifier contact to prevent reversal of power current, resulting in an internal short circuit of the rectifier, exactly analogous to an arc-back in the mercury-arc rectifier.

Note: In a properly designed rectifier, backfire is caused by any mechanical malfunction or circuit condition which produces contact break after the break step, ionization in the contact gap at the end of the break step, or actual short circuiting of the contact. Some of the common causes are: 1. excessive residual break current, 2. presence of loose metallic particles in the contact area, 3. severe a-c voltage fluctuations, 4. severe load fluctuations beyond design limits, 5. motor lag due to a-c voltage dips, and 6. incorrect operation of overlap control.

1.804 *Arc-Through*

Arc-through is the failure of a contact to prevent flow of power current in the normal direction during a scheduled nonconducting period analogous to an arc-through in a mercury-arc rectifier. The causes, however, are exactly the same as for backfires in mechanical rectifiers.

Reference

1. Practices and Requirements for Pool Cathode Mercury-Arc Power Converters. *ASA C34.1-1958*, American Standards Association, New York, N. Y., 1958.

Bibliography

1. Synchronous-Mechanical Rectifier-Inverter, **Stanley S. Seyfert.** *AIEE Transactions* (*Electrical Engineering*), vol. 52, June 1933, pp. 397–408.

2. Der Kontaktumformer, **Floris Koppelmann.** *Elektrotechnische Zeitschrift*, Wuppertal-Elberfeld, Germany, vol. 62, 1941, pp. 3–20; also *Elektrotechnik und Maschinenbau*, Vienna, Austria, vol. 59, 1941, pp. 253–62, vol. 60, 1942, pp. 189–94, vol. 60, 1942, pp. 368–77.

3. Fortschritte auf dem Gebiete des Kontaktumformers, **Erich Rolf.** *Frequenz*, Berlin, Germany, vol. 1, 1947, pp. 2–15.

4. A Mechanical Rectifier, **Otto Jensen,** *Transactions*, Electrochemical Society, Baltimore, Md., vol. 90, 1946, pp. 93–109.

5. A New Design of the Contact Converter (in German), **F. Koppelmann.** *Elektrotechnik*, Berlin, Germany, vol. 2, 1948, pp. 329–32.

6. Plant Scale Process for Production of Rectangular Hysteresis Loop Material, **E. Both.** *Technical Memo M-1091*, Signal Corps Engineering Laboratory, Fort Monmouth, N. J., 1947.

7. Der Kontaktumformer mit Schaltdrosseln (book), **Alexander Goldstein.** Leeman, Zurich, Switzerland, 1948.

8. Das Schutzproblem des Kontaktumformers, **Emil Kittl.** *Elektrotechnik und Maschinenbau*, vol. 67, 1950, issues 3 and 4, 15 pp.

9. The Contact Rectifier—Its Construction, Connection, and Performance, **H. Blatter.** *The Brown Boveri Review*, Baden, Switzerland, vol. 37, no. 12, Dec. 1950, pp. 468–77.

10. Contact Rectifier Switching Problems, **A. Goldstein.** *Ibid.*, pp. 478–88.

11. The Erection of Contact Rectifier Plants, **E. Gerber, E. Zantop.** *Ibid.*, pp. 499–501.

12. The Determination of Contact Rectifier Efficiencies, **A. Goldstein, H. Blatter.** *Ibid.*, pp. 493–96.

13. The Protection of Contact Rectifiers, **E. Kern.** *Ibid.*, pp. 496–99.

14. The Large Contact Rectifier (in German), **F. Koppelmann.** *AEG Mitteilungen*, Berlin-Grunewald, Germany, issue 9/10, 1951, pp. 3–18.

15. Mechanical Rectifier Completes Year's Operation, **Otto Jensen.** *Iron and Steel Engineer*, Pittsburgh, Pa., vol. 27, no. 4, Apr. 1950, pp. 69–75.

16. Commutating Reactor Control for Mechanical Rectifier, **E. J. Diebold.** *AIEE Transactions*, vol. 70. pt. I, 1951, pp. 1062–65.

17. Further Development in the Field of the Large Contact Converter (in German), **Hans Joachim Kleinvogel.** *Siemens-Zeitschrift*, Erlangen, Germany, vol. 26, issue 3, 1952.

18. Operating Experience with a Mechanical Rectifier, **J. Chamulak, W. C. McCullough, J. W. Tracht.** *AIEE Transactions*, pt. II (*Applications and Industry*), vol. 74, Nov. 1955, pp. 290–94.

19. Application of a Mechanical Rectifier to a Cyclotron, **Jack Warren.** *Ibid.*, vol. 76, Nov. 1957, pp. 273–77.

20. Superposition Applied to Mechanical Rectifier Contacts, **I. K. Dortort.** *Ibid.*, vol. 77, July 1958, pp. 167–72.

Virginian Railway Motor-Generator Electric Locomotive Maintenance Costs

T. F. PERKINSON
MEMBER AIEE

AN OUTSTANDING advantage of electric traction for heavy mainline ilroading is the lower maintenance sts realized with electric locomotives comparison with other forms of motive ower such as the steam locomotive or e diesel-electric. This attribute is rtually self-evident when it is considered at the electric locomotive is essentially converter of energy, and is not burdened ith power generators as are the self-con-ined types of motive power.

Despite this self-evident favorable fac-r, and because of the relative scarcity statistics covering electric-locomotive aintenance, few realize the magnitude the differences which exist in compara-ve motive power repair costs in favor the so-called "straight-electric" loco-otive.

An outstanding example of the low aintenance costs realizable with elec-ic motive power is available in statistics pplying to the operation of a fleet of 1,000-volt 25-cycle single-phase motor-enerator locomotives which have been in ervice on the electrified zone of the irginian Railway during the past 9 ears.

Four double-unit locomotives[1] (Fig. 1) ith the dimensional and rating character-tics listed in Table I, were furnished to ne Virginian Railway by General Elec-ic in 1948 for heavy-drag coal haulage ver the Alleghenies on the profile dia-rammed in Fig. 2.

It is to be noted that the "input-to-he-generators" rating of 8,000 hp (horse-ower) corresponds to a rating equivalent o that of five 1,600-hp diesel-electric ocomotives.

These locomotives are operated in astward tonnage movements of 3,000 ons per locomotive from Elmore to Clark's Gap against a ruling grade of .07%; a fill-out to 9,000 tons at Clark's Gap, and completion of the total 132-mile un with 9,000 tons per locomotive from Clark's Gap to Roanoke against a ruling grade of 0.6%. The return trip is made with a trailing load of approximately 3,600 tons, consisting largely of empty coal cars.

Because of their superior operating characteristics these locomotives are given preference in assigning available tonnage with the result that substantial mileage is accumulated in the course of a given period. During the 9-year period (1948–56, inclusive) the locomotives each have averaged 84,595 miles per year, with the greatest average annual mileage of 106,-986 occurring in 1956 coincident with an augmented movement of export coal to the Eastern Seaboard at Norfolk, Va. The average annual mileage operated per locomotive is shown for the 9-year period in Fig. 3. The maximum average monthly mileage recorded during this time was 9,775 for the month of August 1956.

Contributing to the high mileage performance are the high availability and reliability of these locomotives. So high is the reliability the practice of "calling" the locomotives for the west-bound return trip before they arrive at Roanoke in east-bound movements has come into being as standard operating procedure.

An analysis of the operating statistics for the year 1956, yields the performance factors in Table II, in terms of average per locomotive.

The railway has kept detailed maintenance records on the four locomotives and an analysis of these statistics reveals an uncommonly low repair cost for the character of the service performed.

Curve A in Fig. 4 illustrates the average annual repair costs per locomotive as actually incurred, without adjustment for dollar variation. No classified repairs were involved during the first 6 years of operation, but moderate classified expenses were incurred in 1954, and heavier repairs were introduced in 1955. Relatively light class repairs were made during the first 2 months of 1956.

Curve C in Fig. 4 depicts the maintenance-cost history adjusted for dollar-value variations in accordance with the Association of American Railroads' index of average unit prices of railway material and supplies, and wage rates, with 1947–49 rates as 100.

The influence of mileage on the over-all costs is apparent in Figs. 3 and 4, particularly during the early years of the period covered. There has been a steadily increasing trend in annual mileage accumulations throughout the period with actual decreases under previous years occurring only in 1953–54, when available tonnage presented for movement decreased below the tonnages of preceding years.

The adjusted or "constant-dollar" cumulative cost to the end of 1956—23.2 cents per mile—represents a figure of 3.41 cents per 1,000 rated rail-hp miles, a value approximately 1/4 to 1/3 of comparable diesel-electric locomotive maintenance costs for the same type of service performed. While the same ton-miles performance in similar service would ordinarily be secured with diesel-electrics of lesser total horsepower, the equivalent ton-miles per train-hour would necessi-

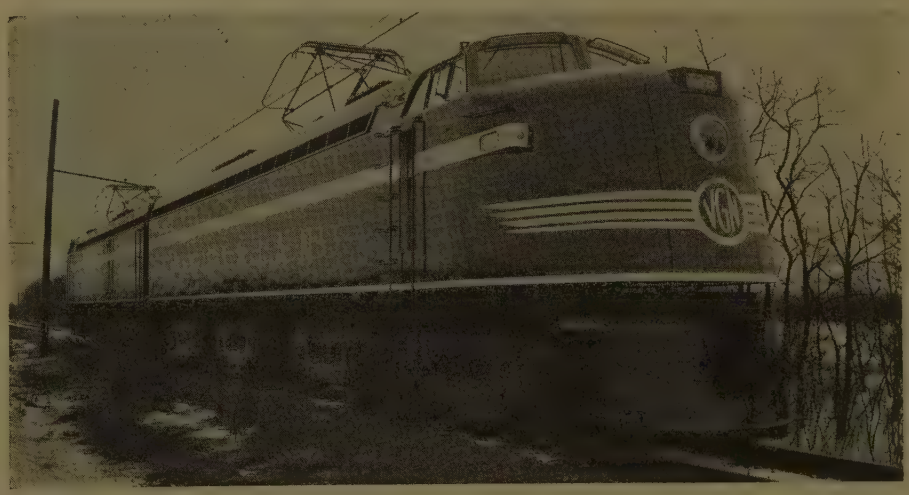

Fig. 1. Double-unit motor-generator locomotive rated 11,000 volts, 25 cycles, 8,000-hp input to generators

aper 60-50, recommended by the AIEE Land ransportation Committee and approved by the IEE Technical Operations Department for resentation at the AIEE Winter General Meeting, ew York, N. Y., January 31–February 5, 1960. anuscript submitted December 11, 1958; made vailable for printing December 1, 1959.

. F. PERKINSON is with the General Electric ompany, Schenectady, N. Y.

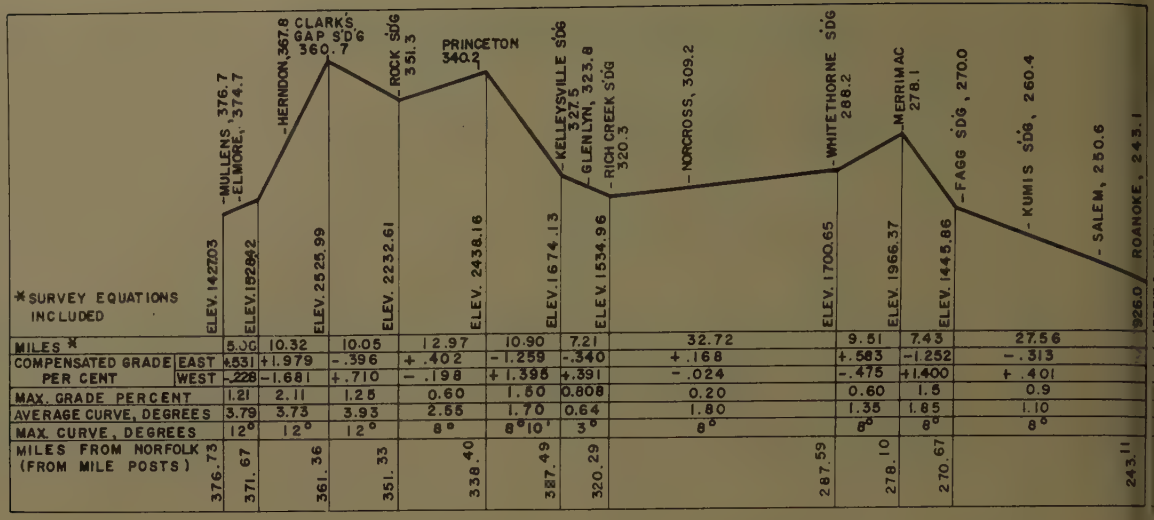

*SURVEY EQUATIONS INCLUDED												
MILES *		5.00	10.32	10.05	12.97	10.90	7.21	32.72	9.51	7.43	27.56	
COMPENSATED GRADE PER CENT	EAST	+.531	+1.979	-.396	+.402	-1.259	-.340	+.168	+.583	-1.252	-.313	
	WEST	-.228	-1.681	+.710	-.198	+1.395	+.391	-.024	-.475	+1.400	+.401	
MAX. GRADE PERCENT		1.21	2.11	1.25	0.60	1.50	0.808	0.20	0.60	1.5	0.9	
AVERAGE CURVE, DEGREES		3.79	3.73	3.93	2.55	1.70	0.64	1.80	1.35	1.85	1.10	
MAX. CURVE, DEGREES		12°	12°	12°	8°	8°10'	3°	8°	8°	8°	8°	
MILES FROM NORFOLK (FROM MILE POSTS)		376.73	371.67	361.36	351.33	338.40	387.49	320.29	287.59	278.10	270.67	243.11

Fig. 2. Profile of the electrified section of The Virginian Railway

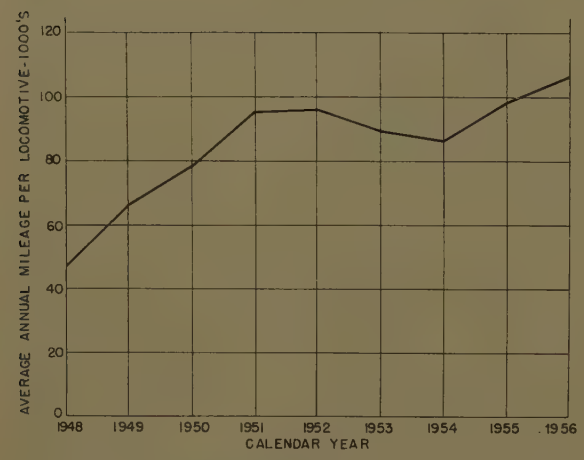

Fig. 3. Motor-generator locomotive average annual miles run

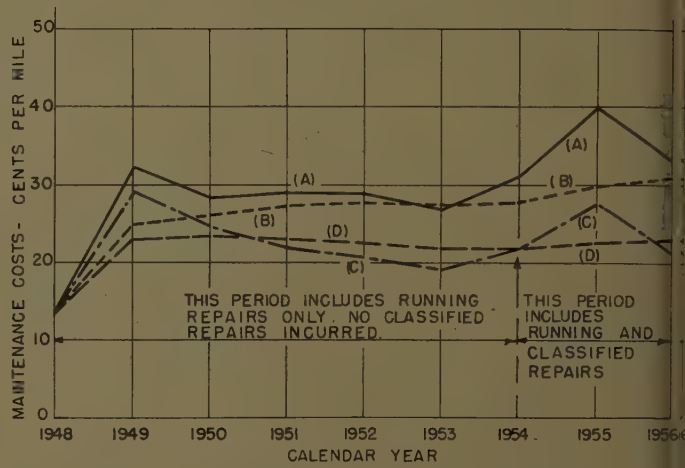

Fig. 4. Motor-generator locomotive maintenance costs

A—Costs as incurred, average annual
B—Cumulative cost, average, in current money values
C—Adjusted costs, average annual, with 1947–49 labor and materials costs = 100%
D—Cumulative cost, average, adjusted

tate as great or slightly more rail hp in the diesel-electric motive power because of the higher ratio of locomotive weight to total train weight that would be involved with the self-contained motive power.

Each of the four locomotives handles approximately 1,600,000 GTM (gross-ton-mile) trailing in the course of a round trip over the 132 miles between Elmore and Roanoke, and for the 9 years covered by the statistics averaged a total of 2,890 round trips, with a total average of 4,624,000 MGTM (thousand GTM) per locomotive.

The total average maintenance expenditure actually incurred for the period amounted to $232,340 per locomotive, which represents a maintenance cost of approximately 5 cents per MGTM handled.

The average repair cost for the first 10 months of 1957 has amounted to 41.6 cents per mile (1957 dollars), approximately 26.5 cents per mile in terms of the 1947–49 dollar value.

It is to be expected that as the locomotives age, the cost of maintenance will increase somewhat, but the data available currently are insufficient to predict the expected rate of rise with any semblance of accuracy.

In any comparison of the motor-generator locomotive with nonregenerating motive power, some credit of at least a qualitative nature should be accorded to the former, since these perform during part of their on-the-road time as power generators when in regenerative braking action. It would be practically impossible to rationalize this feature in terms of reduced costs assessable as haulage units.

In fairness to self-contained motive power with which these electric loco-

Table I. Dimensional and Rating Characteristics of Double-Unit Locomotives

Wheel arrangement	2 (B−B+B−B)
Total weight (all on drivers), pounds	1,033,832
Number of driving axles	16
Weight per driving axle, pounds	64,614
Length over couplers	150 feet 8 inches
Rigid wheel base	9 feet 0 inches
Height over-all	16 feet 3 inches
Driving-wheel diameter	42 inches
Horsepower input to generators	8,000
Continuous horsepower at rail	6,800
Continuous tractive effort, pounds	162,000
Speed at cont. rating, miles per hour	15.75
Maximum safe speed, miles per hour	50
Adhesion at cont. rating, %	15.8

Table II. Performance Factors

Annual mileage	106,98
Monthly mileage	8,91
Greatest monthly mileage	9,77
Round trips per day	1.11
Miles per day	29
Trailing GTM/hour—eastbound	203,00
Trailing GTM/hour—westbound	95,00

otive maintenance costs might be compared, the necessity of considering in an over-all motive-power system comparison, the costs of maintenance of the power supply facilities required by the electric locomotive should not be overlooked. Unless these cost elements are included as part of the power costs, they are directly assessable to the cost of maintenance of the electric locomotive.

Reference

1. Motor-Generator Locomotives, Their Design and Operating Characteristics, J. C. Fox, J. F. N. Gaynor, F. D. Gowans. *ASME Transactions*, American Society of Mechanical Engineers, New York, N. Y., vol. 72, Feb. 1950, pp. 153–64.

A Statistical Method for Determining Heat Losses in Electrically Heated Residences

E. E. LINDEN
MEMBER AIEE

N MOST CASES, heating facilities to be installed in a particular residence and other structures) must be sized before the house is built and prior to any actual experience knowledge of the heating requirements. This makes necessary the introduction of calculations, which wise practice indicates should provide an unquestionably ample heating system. Overdesign is common and not of substantial consequence, so long as fuel-fired systems are involved, since the fuel is usually readily stored in the basement, garage, or gas holder awaiting uses. Overdesign in electric heating installation may be necessary to a certain degree to provide for quick pick-up; however, any surplus represents an instantaneous liability on utility system capacity at the time of system peak load, since kilowatt-hours (kw-hr) cannot readily be stored as such. Surplus capacity should be minimized to assure a low cost to serve ratio.

Present standards for heat loss calculations have their origin in fuel-fired systems; and indications are that these methods do not wholly apply to calculation for electric comfort heating. Extensive tests on relatively few residences have indicated this discrepancy, however records should be kept on many more test residences to form a good average basis for altering or accepting present methods of calculation. This paper presents a method of recording and obtaining an actual heat-loss check on electrically heated residences by a statistical analysis of monthly or bimonthly kw-hr billing figures, eliminating the need for costly test metering facilities. The paper deals with resistance-type electric heating units and does not include heat-pump equipments, however the findings discussed should be useful in sizing either type system.

Paper 60-28, recommended by the AIEE Domestic and Commercial Applications Committee and approved by the AIEE Technical Operations Department for presentation at the AIEE Winter General Meeting, New York, N. Y., January 31–February 5, 1960. Manuscript submitted October 6, 1959; made available for printing December 3, 1959.

E. E. Linden is with the Narragansett Electric Company, Providence, R. I.

Heat Loss Calculations

The heat-loss calculation is essentially a heat transfer problem and generally accepted procedures are outlined in the ASHAE (American Society of Heating and Air Conditioning Engineers) Guide.[1] The calculation involves two considerations: the transfer of heat through the building wall, i.e., the warm side to the cold side; and the heat lost through infiltration, i.e., the warm air that leaks out through cracks and is replaced by cold air (which must be heated) leaking in. While the guide presents very precise constants, judgment, which must be exercised in their application, can result in widely different final results. Reference 2 is an example where estimates varied from 12.3–22 kw. If the design criterion were "an unquestionably ample heating system," then a plant capable of 22 kw should have been selected. While in practice it was found that a 12.3-kw system included sufficient reserve.

Heat Loss Measurements

In the case of the electrically heated house, all of the heating electricity is converted and used within the structure, no arbitrary amount is lost through infiltration of air for combustion or gas by-products. The results of tests conducted on a residence designed to gather data on electric heating is described in reference 3. The special metering provided was extensive, resulting in a measured heat-loss figure of 9.7 kw (compared with estimates of from 12.3–22. An earlier study[4] substantiates this discrepancy in a comparison of electric versus gas or oil heat in a different geographical area.

Calculated Versus Measured Heat Losses

That a wide discrepancy can exist between calculated and measured heat losses indicates the need for further study, geographically area by area. A study procedure need not be an expensive one, since it can be accomplished using meter-reader route books and weather bureau temperature sheets. For each monthly or bimonthly period total residence kw-hr use and degree-hour (deg-hr) temperature experience can be plotted for each test residences, where:

y = total (domestic + heating) kw-hr use for a period.
x = total deg-hr temperature experience of the residence for the same period.

These data when correlated linearly (preferably by the mathematical process) take thefamiliar form of a straight-line equation:

$$y = mx + b$$

Figs. 1(A)–(C) are plotted for data periods of 1 week, 1 month, and 2 months (bimonthly). In each case the y-axis intercept in kw-hr represents the energy con-

Table I

	From Data Gathered for		
	Weekly Periods	Monthly Periods	Bimonthly Periods
m, kw/deg.....	0.1345..	0.1502..	0.1509
Heat loss (70), kw.....	9.4	.. 10.5	.. 10.6
Residential use, kw-hr....	315	..971	..2,192

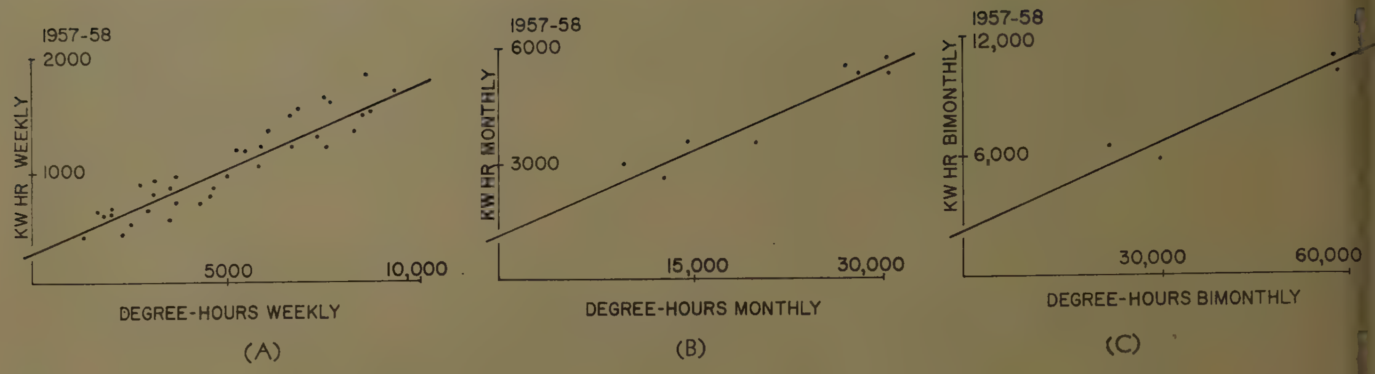

Fig. 1. Multiple correlation

A—Kw-hr weekly versus deg-hr weekly
Kw-hr = 0.1345 deg-hr + 315
Kw/deg = 0.1345
Loss at 70 F = 9.4 kw

B—Kw-hr monthly versus deg-hr monthly
Kw-hr = 0.1502 deg-hr + 971
Kw/deg = 0.1502
Loss at 70 F = 10.5 kw
Residential = 971 kw-hr/month

C—Kw-hr bimonthly versus deg-hr bimonthly
Kw-hr = 0.1509 deg-hr + 2,191
Kw/deg = 0.1509
Loss at 70 F = 10.6 kw
Residential = 2,192 kw-hr/bimonthly

sumed by domestic appliances, excluding heating. Since the x-axis is in terms of deg-hr, the slope of the line is equal to the ratio of heating kw-hr to deg-hr or simply, for any hour, kw/per deg of difference between outdoor and indoor temperature. In the formula $y = mx + b$, m is this ratio, and in order to determine the actual heat loss of a residence it is only necessary to multiply m by the maximum or design temperature difference (indoors minus outdoor). For the residence under consideration this analysis renders the summary in Table I.

These test results would substantiate (reference 2) the lowest estimate (12.3 kw) allowing a surplus capacity of 15%. In practice the heating capacity of the residence has been reduced to 12.3 kw for test and the plant operated satisfactorily through the 1957–58 heating season. Temperatures outdoors dropped as low as −10 F (degrees Farenheit) during this period, proving the surplus capacity adequate for temperatures at least 10 deg below the design figure.

Conclusions

Substantial reason has been developed to question the validity of converting the ASHAE Guide procedures and recommendations to the case of electric heating. The surpluses apparent here can be resolved by the correlation of data gathered from many electrically heated homes. The method advanced in this paper is:

1. Gather all basic information on each test residence as suggested in Fig. 2, area by area.

2. Transfer kw-hr billing records (usually monthly or bimonthly) and degree-hour temperature experience (for the same period) to graph paper, perform the mathematical linear correlation, and plot the

TOWN ______ STREET ______
NAME ______
DATE FROM ______ TO ______
RESIDENTS TO AGE 16 ______ 16 – 65 ______ OVER 65 ______

FLOOR LEVEL	HEATED AREA	HEATED VOLUME	UNHEATED AREA	UNHEATED VOLUME
BASEMENT				
FIRST				
SECOND				
THIRD				
ATTIC				
TOTAL				

NEMA HEAT LOST ESTIMATE ______ KW.
ΔT = 70°F ______ BTU/HR.
EST. KWHR. USE ______ COST ______
HEATING CAP. INSTALLED AT 240V. ______ KW.
HEAT PUMP ______ KW. I^2R ______ KW.
DEMAND, USE, & LOSS EST. BY ______
INFILTRATION CHANGES PER HOUR ______
INSULATION ______ X ______ X ______
WINDOWS/DOORS SINGLE/DOUBLE
AVE. THERMOSTAT ______
NORMAL 65°F DDD ______

DIVERSIFIED DEMAND (NAT. EL. CODE EST.) ______ KW.
SIZE SERVICE ENTRANCE ______ AMPS
SIZE SECONDARIES ______ WIRE
SIZE TRANSFORMER ______ KVA.
NO. OTHER CUSTOMERS ON CRIB ______
NO. OTHER HTNG. CUSTS. ON CRIB ______

APPLIANCES
RANGE ______ WATER HTR. ______
REFRIG. ______ INCINER. ______
FREEZER ______ DRYER ______
DISPOSAL ______ IRONER ______
DISHW. ______

TOTAL RESIDENCE KILOWATT-HOURS, DEGREE-HOURS, & KILOWATT DEMAND

YEAR				YEAR				YEAR			
MO.	KWHR.	°-HRS(70°F)	KW.	MO.	KWHR.	°-HRS(70°F)	KW.	MO.	KWHR.	°-HRS(70°F)	KW.
SEP.				SEP.				SEP.			
OCT.*				OCT.*				OCT.*			
NOV.*				NOV.*				NOV.*			
DEC.*				DEC.*				DEC.*			
JAN.*				JAN.*				JAN.*			
FEB.*				FEB.*				FEB.*			
MAR.*				MAR.*				MAR.*			
APR.*				APR.*				APR.*			
MAY*				MAY*				MAY*			
JUN.				JUN.				JUN.			
JUL.				JUL.				JUL.			
AUG.				AUG.				AUG.			
SEP.				SEP.				SEP.			
TOT.*				TOT.*				TOT.*			

AVE. MO. DOMESTIC KWHR ______	AVE. MO. DOMESTIC KWHR ______	AVE. MO. DOMESTIC KWHR ______
MAX. OCT.-MAY DEMAND ______ KW.	MAX. OCT.-MAY DEMAND ______ KW.	MAX. OCT.-MAY DEMAND ______ KW.
HEATLOSS ______ KW.	HEATLOSS ______ KW.	HEATLOSS ______ KW.
ΔT = 70°F ______ BTU/HR.	ΔT = 70°F ______ BTU/HR.	ΔT = 70°F ______ BTU/HR.
ACTUAL COST ______	ACTUAL COST ______	ACTUAL COST ______
ACTUAL DDD (65°F)	ACTUAL DDD (65°F)	ACTUAL DDD (65°F)

Fig. 2. Sheet for data accumulation

esulting line against the plotted points as a isible check of agreement.

The resulting comparison of measured ersus calculated heat losses, for an adequate sample, will form a basis of acceptnce for, or alteration of, present practices used in the calculation procedure.

References

1. American Heating and Air Conditioning Engineers Guide (book). American Society of Heating and Air Conditioning Engineers, New York, N. Y., 1958.

2. Heat Pump and Heating Cables Installed in the Same Residence for Data Purposes, C. W. Jones, E. E. Linden. *AIEE Transactions*, pt. II (*Applications and Industry*), vol. 76, Nov. 1957, pp. 307–14.

3. Heat-Pump and Heating Cables Installed in the Same Residence: First Year of Comparative Operation, C. W. Jones, E. E. Linden. *Ibid.*, vol. 77, Mar. 1958, pp. 43–8.

4. Residential Heating: Electric versus Gas or Oil, G. S. Smith. *Ibid.*, vol. 77, 1958 (Jan. 1959 section), pp. 524–29.

Voltage Temperature Life Testing of Fluorescent Ballast Insulation Systems

C. A. HOWLETT
MEMBER AIEE

FLUORESCENT lamp ballasts were first introduced by the General Electric Company in 1939 as a necessary auxiliary for a new lighting source, the fluorescent lamp. From the time of the introduction of this new product up through World War II, standard 105 C (degrees centigrade) (class *A*) insulation materials were used and little was done about improving this aspect of the product. Primary development activity was concerned with reducing size and improving circuitry of the units.

Along with the postwar housing construction boom and further expansion of industry and with wider acceptance of fluorescent lighting, the sale of fluorescent lamp ballasts has increased tremendously. At the same time, competition increased. It soon became apparent that to provide a quality product at a continually improved price, it would be necessary to take advantage of the many new materials and processes being introduced. With the need for determining the acceptable performance of these new materials and their satisfactory interaction with wire enamels, treatment, adhesive tapes, paper, case-filling materials (such as asphalt) and their decomposition products, it became apparent that a means of evaluating the life of the product was needed.

The need for assurance of a quality product for fluorescent ballasts lies primarily with the number of units produced. It is estimated that some 27 to 28 million fluorescent ballasts are sold each year in this country. These are installed in widely dispersed locations. Unnecessary replacement expense can be nearly double the initial cost of each unit.

Life of fluorescent lamp ballasts still requires definition. The majority of the installations currently in service are still too new to determine accurately the average life of insulation systems now in use. It is felt that a large part of the market is subject to redecoration of offices or rearrangement of facilities which leads to new lighting installations perhaps every 10 years. It is still felt, however, that a 12-year average life is desirable. Based upon a two-shift operation, 6 days of the week for 52 weeks of the year, it is estimated conservatively that life of approximately 55,000 to 60,000 hours at coil temperatures of 105 C is needed. The Appendix shows details of this estimate. Some ballast designs that avoid abnormal higher temperature conditions or have shorter duty cycles may be satisfactory with shorter life.

Ballast and System Characteristics

A fluorescent ballast is, primarily, a transformer designed to provide the necessary starting voltage for the lamp. Secondly, it introduces inductive reactance or a combination of capacitive and inductive reactances to limit the flow of current through the lamp to prevent its own self-destruction. Principal physical differences of ballasts from other small dry-type transformers are found in length and a shallow height used in order to adapt them to fixture design. This results in slightly increased volts-per-layer stresses because of longer coils. Typical ballasts are shown in Fig. 1.

Minimum cost has become an essential requirement for fluorescent lamp ballasts due to the competitive nature of the market in which they are sold and to the fact that ballasts represent a substantial part of fixture material costs.

Fixtures can be assembled against ceilings of flammable materials. Industry standards, therefore, specify that ballast case temperatures shall not exceed 90 C and winding temperatures during normal operation shall not exceed 105 C. It has become industry practice to permit a temporary abnormal condition to raise the winding temperature to as high as 135 C. In instances where a burned-out lamp is left in the circuit, this condition persists until the lamp is replaced.

As a result of these factors, only the lowest cost 105 C (class *A*) materials have been used. Materials used throughout the industry have generally consisted of oleoresinous, polyvinyl formal or polyamide wire enamels, low-cost kraft paper layer insulations, kraft paper and some acetate laminate ground insulations, and varnish or asphaltic treatments of the core and coils. The usual construction consists of several coils on a core and a capacitor, when used, assembled in a steel case filled with hot asphalt.

Since fluorescent lamp ballasts utilize inductance to control the current to the lamp, switching produces its special problems. With fast-acting switches, such as vacuum or mercury switches, considerable transient voltages can be developed.

Such transient voltages can become many times normal line voltages. Since these can be amplified by the step-up ratio of the transformer, ballasts are required to withstand greater impulses than any other types of equipment, e.g., motors.[1] Switching transient voltages, therefore, can be a factor in the life of ballasts.

Ballast Accelerated-Life Test

In 1953 the General Electric Company decided to undertake a program of laboratory life-testing ballasts. Test facilities were obtained and the first tests were started late that year. The primary consideration for a factory or laboratory accelerated-life test was that it include as many as possible of the factors which would affect the life of the core and coil portion of ballasts in normal applications.

Paper 60-24, recommended by the AIEE Production and Application of Light Committee and approved by the AIEE Technical Operations Department for presentation at the AIEE Winter General Meeting, New York, N. Y., January 31–February 5, 1960. Manuscript submitted June 20, 1958; made available for printing October 21, 1959.

C. A. Howlett, deceased, was with the General Electric Company, Danville, Ill.

Fig. 1 (left). Typical large and small fluorescent lamp ballasts

Fig. 2 (right). Reactor, or core and coil-type ballast

Fig. 3 (left). Reactor-type ballast in steel case ready for asphalt filling

Fig. 4 (right). Solenoid - operated rack of household mercury switches

Capacitor life, because of the need to evaluate it under more restrictive conditions, is excluded from this discussion.

Test Sample and Cycle

A small reactor-type ballast was selected as the test sample. This unit, shown in Fig. 2, is a single-coil reactor containing 0.0113-inch no. *29* American wire gage magnet wire and paper-layer insulation, is wound on a spiral-wrapped paper spool and is assembled on a double *E* core. At approximately 100 volts this coil carries between 0.4 and 0.5 ampere and has an internal coil temperature rise of about 40 C. Oven ambient temperatures of 100, 120, and 140 C, with this coil rise, provide coil temperatures of about 140, 160, and 180 C. Voltage stress, occurring at the end of and between two layers of winding, amounts to about 17 volts and occurs across the wire enamel films and 0.002 inch of paper-layer insulation.

This particular ballast is a typical high production item (this is the unit that may be supplying your bathroom or kitchen lights if you have fluorescent lamps) and so is an inexpensive, readily available, test sample. Insulations on wire, paper between layers of winding, ground insulation, spacings, and treatment materials can be changed as desired. To evaluate case-filling materials, this same core and coil also can be assembled in a steel case as shown in Fig. 3.

Ten units as described were run in each of the three ovens at 100, 120, and 140 C for each insulation system tested. The voltage applied to each coil was supplied through a 2-ampere cartridge fuse and a household-type mercury switch. Each group of 30 units in any oven was supplied from a variable transformer with a panel-type voltmeter for voltage indication. The mercury switches were assembled on racks and were operated with a solenoid from a timer circuit as shown in Fig. 4. Ballasts were switched off for about 20 seconds every 5 minutes, just long enough to produce the switching transient across the coil.

This switching assures at least two high-voltage transients per day through random occurrence of the switching at times when the energy stored in the ballast is near the maximum. The mercury switch appears to give approximately three times higher pulse voltages than the more commonly used circuit breaker. Table I shows relative transient voltages across the line leads to a ballast, measured with several types of switches.

The number of ballasts on one switch also affects the switching transient voltage generated across the line leads to the ballast. Table II shows that the measured voltage diminishes as the number of ballasts operated from the same household mercury switch is increased.

Both these tables indicate introduction in the test cycle of more severe overvoltages than usually will be found in service. This was considered desirable in a laboratory or factory life test.

With the exception of the short time off for switching, units operated continuously, 7 days a week. Coil temperatures were checked by the resistance method at the start of the test. This temperature was used in plotting the failure pattern. Since some impedance variation occurs, a spread of current and coil temperatures results.

To determine the effect of humidity on the ballast life some units were removed from test and placed in a humidity cabinet over week ends. Time at temperature only was used in plotting the failure patterns for these groups. Units were checked daily and failed units were removed and torn down to locate, as far as possible, the point of failure. Hours to failure were determined to within 72 hours (length of a usual week end).

Comparison of Ballast Life Test with AIEE No. 1E

In retrospect, most of the principles of AIEE No. *1E*[2] were considered in setting up the described test cycle. Following are comments on the differences:

1. Thermal aging. The above cycle

Table I

Type of Switch	Maximum Transient Voltage Peak Volts,* %
Relay contacts	100
Circuit breaker	117
Spring-loaded household	217
Household mercury	383
Vacuum	650

* Values are maximum obtained in approximately 100 random switch operations.

utilizes a combination of the two types of heating, oven and self-heating, discussed in AIEE No. *1E*, and to some extent enjoys the advantages of both. Variation hour to hour and day to day is minimized with the close control possible with ovens. Temperature gradients within the coils are not abnormally high as in self-heating alone, but approach that normally found in service.

2. Humidification. The initial choice to omit humidity exposure from the ballast life test was based on the fact that the majority of units rarely face excessive moisture when in operation. The use of humidification was tried as a tool for searching out dielectric faults and, as described later in this paper, appears to upset the normally expected life pattern due to thermal degradation with systems containing paper encapsulated in asphalt and tested with continuous voltage.

3. Associated materials. To minimize the effect of associated materials and their decomposition products, forced air convection ovens were used for these tests.

4. Mechanical stress. Since ballasts normally are not subject to vibration as in rotating or moving equipment, it was felt that the mechanical stress resulting from exciting the core and the extra stress caused by starting the units once every minutes were sufficient.

5. Dielectric stress. Voltages higher than normal were applied during this test but were obtained by switching the inductive loads to produce high transient voltages. This has the advantage of not only stressing the insulation to ground but also the turn-to-turn and layer-to-layer insulations.

6. Method of cooling. Cooling of the ballast samples was omitted in this test procedure. Normal ballast applications once installed cool only to normal room temperature and the significance of this change is still an open question.

7. Length of test cycle. Rather than calculate the life in cycles, the number of hours at operating temperature were used.

8. Failure criteria. The failure of a 3-ampere cartridge fuse was accepted as an indication of ballast failure.

9. Mathematical treatment of thermal aging data. The regression line, or average life line, and the 95% confidence limits for the data were calculated in accordance with the method presented in AIEE Standard no. *510.*[3]

Results

The insulation systems shown in Table III have been evaluated on this life-test cycle.

A typical failure pattern obtained from the units of the standard ballast system is shown in Fig. 5(A). The average life, or best regression line, and the 95% confidence limits are drawn in on this plot. Comparison of the estimated 60,000 hours average life needed for ballasts at winding temperatures of 105 C with the indicated minimum average life of 83,000 hours obtained from these test data, shows the standard ballast system to be more than adequate.

The standard ballast insulation system is compared with motor life tests[4] and motor-type insulation systems tested on the ballast life-test in Fig. 5(B). While not exactly the same materials are used in this core and coil-type ballast as are used in the motor system, it does include windings without paper-layer insulation and the same wire enamel. An oil-modified phenolic type of varnish treatment was used. In spite of some material differences, there is some evidence here that the ballast life-test cycle is more severe, or produces shorter life in terms of absolute hours of operation at temperature, than the motor tests. Also shown in Fig. 5(B) is the comparatively longer life of the standard ballast insulation system. This in part can be attributed to the paper-layer insulation and in part to the asphalt case filling which protects against effects of atmosphere.

A comparison of the standard ballast with a varnish treated core and coil type of ballast is shown in Fig. 5(C). The standard system and the core and coil-type system, whose data are shown in the bottom curve, are identical except for the oil modified phenolic varnish treatment in the case of the core and coil type and the asphalt treatment and the asphalt case-filling material in the standard system.

Table II

Number of Ballasts on Switch	Maximum Transient Voltage Peak Volts,* %
1	240
2	160
3	135
4	100
5	100
10	100

* Values are maximum obtained in approximately 100 random switch operations.

Comparison of the two wire enamels on the core and coil type of ballast represents the significant differences that can be achieved by choice of wire enamels. In terms of the old style of classification, both are rated as 105 C, or class *A*, wire enamels. In this system, however, there apparently should be a differentiation.

The radical change in slope of the average life lines in Fig. 5(D) shows the effect of combining three factors: humidity exposure, continuous application of voltage, and thermal aging. The standard ballast insulation system was tested without humidity in the life-test cycle and is compared with the same system exposed to 90% relative humidity at 90 F (degrees Fahrenheit) humidity over the week ends throughout the test. This suggests that the thermal degradation is no longer the predominant factor being measured in a system such as this where the test is conducted with all three factors included in the test cycle. Failure instead may be attributed to moisture penetration into the paper insulation in sufficient quantity to cause electrical failure. With the relatively good moisture seal of asphalt, entrance of moisture is slow. Internal heating of the coils may concentrate this moisture in the cooler portions of the coil such as at the end turns of each layer. When the moisture concentration is sufficient, conduction between layers of the coil or from coil to core may occur, particularly due to switching overvoltages, and ballast failure results.

It would appear unwise to extrapolate such data to lower temperatures based on the thermal degradation theory[5] when such other effects as these appear so strongly. Indication that the humidity exposure in the test cycle does measure the effect of the potting material is shown

Table III. Insulation Systems Evaluated

Designation of Insulation System	Type of Winding	Wire	Treatment	Case-Filling Material
Standard ballast	paper-layer insulation	enamel B	asphalt	asphalt
Motor type	random	enamel B	varnish	none
Core and coil	paper-layer insulation	enamel A	varnish	none
Core and coil	paper-layer insulation	enamel B	varnish	none

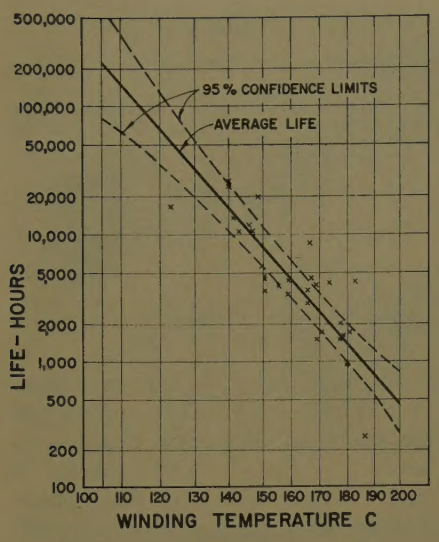

(A)

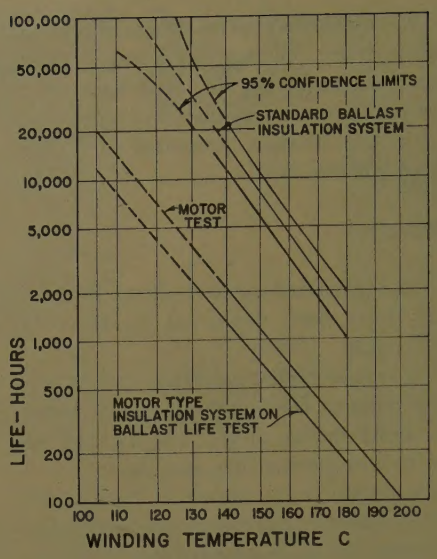

(B)

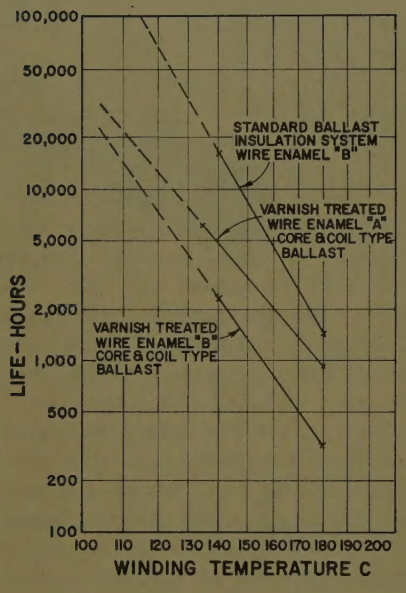

(C)

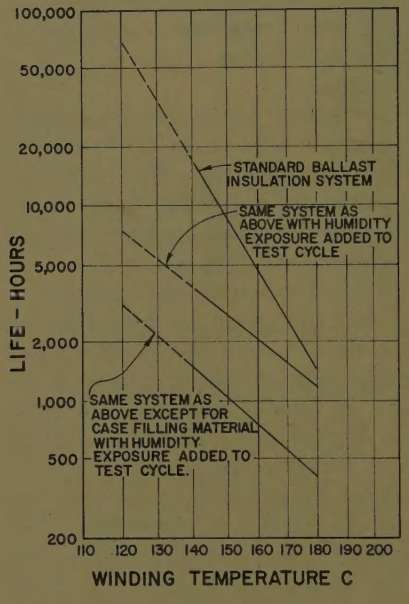

(D)

Fig. 5. Average life versus winding temperature, reciprocal absolute temperature scale

A—For standard ballast insulation system showing individual failure point
B—For motor-type system and standard ballast insulation system compared with motor life
C—Comparing two wire enamels in core and coil-type ballast with standard ballast insulation system
D—Effect of adding humidification on two insulation systems with ballast life-test cycle

in the lower line of Fig. 5(D). This is the average life of a similar insulation system except with a different case-filling material.

Conclusions

Use of this life-test cycle for comparison of ballast insulation systems had been successful in permitting design improvements. Changes in wire enamel and ground insulation have been adopted based on verification from this test method. Furthermore, the opportunity is now available to better match all of the insulation materials to achieve lower costs while still providing the desired product life.

Evaluation of the data obtained from this ballast life test, which may also be applicable to other dry types of transformers and especially to potted dry-type transformers, leads to the following conclusions:

1. Utilization of switching takes advantage of the natural inductance of the ballast to produce overvoltage testing of the insulation in a manner similar to, yet more severe than, service conditions.

2. The ballast life-test cycle appears to be more severe than the motor life tests, presumably as a result of the overvoltages generated by switching.

3. The potted, or asphalt-filled, construction appears to give a far longer life than open types of core and coil or motor-type constructions with these 105 C class *A* materials.

4. The test cycle developed permits comparisons of different insulation systems and demonstrates appreciable differences in life between them.

5. With continuous voltage applied, as in this test, the addition of humidification masks the thermal aging characteristics of the paper-insulated asphalt-filled ballast and prevents extrapolation of the data to normal operating temperatures as is desired of accelerated testing.

Appendix. Estimate of Ballast Life Needed

The following assumptions may be made:

1. Average service life, 12 years.

2. Average installations operate: (*a*) 16 hours per day; (*b*) 12 hours per day at 105 C coil temperatures; (*c*) 6 days per week; (*d*) 52 weeks per year; (*e*) approximately 5,000 hours per year; (*f*) approximately 3,750 hours per year at temperature.

3. Average lamp life, 7,500 hours or $1^1/_2$ years.

4. Lamp failure causes 1 month 130 C abnormal temperature.

5. Insulation life halves with 10 C increase.

If these assumptions are true, then:
Ballast normal operation = 12 years × 3,750 hours per year = 45,000 hours.
Ballast abnormal operation at 130 C:

$$\frac{12 \text{ years life}}{1^1/_2 \text{ years per lamp}} = 7 \text{ lamp failures}$$

7 lamp failures × 1 month = 7 months at 130 C.

This is equivalent to $3^1/_2$ years at 105 C × 3,750 hours = 13,125 hours. Estimated total ballast life needed: 58,125 hours, or 55,000 to 60,000 hours.

References

1. Overvoltages Resulting from the Disconnection of High-Voltage Motors, P. Baltensperger, H. Meyer. *The Brown Boveri Review*, Baden, Switzerland, vol. 40, no. 9, Sept. 1953, Tables I and II, and pp. 343–44.

2. Guide for the Preparation of Test Procedures for the Thermal Evaluation of Insulation Systems for Electric Equipment. *AIEE No. 1E*, June 1957, pp. 5–7.

3. Test Procedure for Evaluation of Systems of Insulating Materials for Random-Wound Electric Machinery. *AIEE Standard no. 510*, Nov. 1956, pp. 16–17.

4. Heat-Resistant Insulation Systems for Motors, C. J. Herman, K. N. Mathes. *AIEE Transactions*, pt. I (*Communication and Electronics*), vol. 74, Sept. 1955, pp. 561–65.

5. Electrical Insulation Deterioration Treated as a Chemical Rate Phenomenon, Thomas W. Dakin. *Ibid.*, vol. 67, pt. I, 1948, pp. 113–22.

Power Apparatus and Systems—February 1960

Conference Paper Open for Discussion

The conference paper listed below has been accepted for AIEE Transactions and is now open for written discussion until April 29. Duplicate double-spaced typewritten copies for each discussion should be sent to Edward C. Day, Assistant Secretary for Technical Papers, American Institute of Electrical Engineers, 33 West 39th Street, New York 18, N. Y., on or before April 29.

Preprints may be purchased at 40¢ each to members; 80¢ each to nonmembers if accompanied by remittance or coupons. Please order by number and send remittance to:

AIEE Order Department
33 West 39th Street
New York 18, N. Y.

59-1296 Optimization of the Adaptive Function by Z-Transform Method . . . . . Chang

AIEE PUBLICATIONS

	Member Prices	Nonmember Prices: Basic Prices*†	Nonmember Prices: Extra Postage for Foreign Subscriptions†
Electrical Engineering			
Official monthly publication containing articles of broad interest, technical papers, digests, and news sections: Institute Activities, Current Interest, New Products, Industrial Notes, and Trade Literature. Automatically sent to all members and enrolled students in consideration of payment of dues. (Members may not reduce the amount of their dues payment by reason of nonsubscription.) Additional subscriptions are available at the nonmember rates.		annually $12* Single copies $1.50*	$1.00
Bimonthly Publications			
Containing all officially approved technical papers collated with discussion (if any) in three broad fields of subject matter as follows:	annually	annually	
Communication and Electronics	$5.00	$8.00*	$0.75
Applications and Industry	$5.00	$8.00*	$0.75
Power Apparatus and Systems	$5.00	$8.00*	$0.75
Each member may subscribe to any one, two, or all three bimonthly publications at the rate of $5.00 each per year. A second subscription to any or all of the bimonthly publications may be obtained at the nonmember rate of $8.00 each per year.			
Single copies may be obtained when available.	$1.50 each	$1.50* each	
AIEE Transactions			
An annual volume in three parts containing all officially approved technical papers with discussions corresponding to six issues of the bimonthly publication of the same name bound in cloth with a stiff cover.	annually	annually	
Part I Communication and Electronics	$4.00	$8.00*	$0.75
Part II Applications and Industry	$4.00	$8.00*	$0.75
Part III Power Apparatus and Systems	$4.00	$8.00*	$0.75
Annual subscription to all three parts (beginning with vol. 77 for 1958).	$10.00	$20.00*	$2.25
Annual subscription to any two parts.		$15.00*	$1.50
AIEE Standards			
Listing of Standards, test codes, and reports with prices furnished on request.			
Special Publications			
Committee reports on special subjects, bibliographies, surveys, and papers and discussions of some specialized technical conferences, as announced in ELECTRICAL ENGINEERING.			

*Discount 25% of basic nonmember prices to college and public libraries. Publishers and subscription agencies 15% of basic nonmember prices. For available discounts on Standards and special publications, obtain price lists from Order Department at Headquarters.

†Foreign prices payable in New York exchange

Send all orders to:

Order Department
American Institute of Electrical Engineers
33 West 39th Street, New York 18, N. Y.